1-1-2005

Pax3 expression in cutaneous malignant melanoma

Judith A. Blake
Edith Cowan University

Edith Cowan University

Copyright Warning

USE OF THESIS

The Use of Thesis statement is not included in this version of the thesis.

Pax3 Expression in Cutaneous Malignant Melanoma

Judith Anne Blake
BNurs.

This thesis is submitted for the degree of
Master of Science
of Edith Cowan University
2005

Faculty of Computing, Health and Science
Edith Cowan University

COPYRIGHT AND ACCESS DECLARATION

This copy is the property of Edith Cowan University. However the literary rights of the author must also be respected. If any passage from this thesis is quoted or closely paraphrased in a paper or written work prepared by the user, the source of the passage must be acknowledged in the work. If the user desires to publish a paper or written work containing passages copied or closely paraphrased from this thesis, which passages would in total constitute an infringing copy for the purpose of the Copyright Act, he or she must first obtain the written permission of the author to do so.

DECLARATION BY CANDIDATE

I certify that this thesis does not, to the best of my knowledge, and belief:

i. incorporate without acknowledgement any material previously submitted for degree or diploma in any institute of higher education;

ii. contain any material previously published or written by another person except where due reference is made in the text; or

iii. contain any defamatory material.

ACKNOWLEDGMENTS

I would like to take this opportunity to gratefully acknowledge and thank the following persons without whom this research would not have been possible:

- *Tom Barber and Johns Hopkins University, for Pax3 antibodies;*
- *Clinical Professor Dominic Spagnolo, for human CMM biopsies;*
- *Dr. Adrian Charles, Dr. Lawrence Yu, Dr. Fiona Wood and Dr. Peter Heenan, for consultations;*
- *Carmel and the Sequencing Centre at Royal Perth Hospital, for consultations and sequencing work;*
- *Mick, Lauren, Tina, Meg, Chris, Andrea, Angus, Cheryl, Rebecca, Michael, Karen, Margaret, Doreen and Hugh for guidance and assistance in the Centre for Human Genetics, ECU;*
- *Mel Ziman, for editing, supervision, guidance and constant support;*
- *Richard Brightwell, for guidance;*
- *All the staff of King Edward Memorial Hospital Theatre Department, for patience and support;*
- *John, for patience, guidance, support and always a listening ear.*

ABSTRACT

This research investigated the repercussions of aberrant *PAX3* re-expression in cutaneous malignant melanoma (CMM). The transcription factor encoded by *PAX3* is amongst the first expressed in the embryo, with a principal role in the development of the melanocytic lineage. We theorised that abnormal re-expression of *PAX3*, consistently observed in CMM as compared to normal melanocytes, is linked to progression of CMM. Previous studies have stated that expression profiles of *PAX3* in CMM demonstrate predominant generation of a protein encoded by exons 1-9 (*PAX3D*) utilising cryptic splice sites in post-transcriptional pre-mRNA splicing. By contrast, normal human skin demonstrates low level generation of *PAX3C* (encoded by exons 1-8). Using RT-PCR based techniques and immunohistochemistry, we present original evidence of *Pax3c, Pax3d* mRNA and protein expression in normal murine embryogenesis and melanogenesis, identifying a conserved role for the *Pax3d* protein in transcriptional regulation of the murine melanoblast. Furthermore, to identify a role for Pax3 in adult skin, we used a reliable time-scale for the strict coupling of melanogenesis to active hair regrowth; *Pax3c* and *Pax3d* expression profiles were assessed during depilation experiments which induced murine melanocytic stem cells to proliferate, migrate into the hair cortex and differentiate in order to produce melanin for new hair. Results indicate that strict temporal expression of *Pax3d* may be linked to either melanoblast proliferation or migration in early melanogenesis thus supporting a possible role for *PAX3D* in the tumourigenesis of CMM.

Differences in the structure of the C-terminal region of the transcription factors PAX3C and PAX3D influence transcriptional activation of downstream target genes via protein-protein interactions. As PAX3 is known to up-regulate the gene encoding micropthalmia-associated transcription factor (*MITF*), we sought to establish a possible link between

aberrant *PAX3* expression and regulation of *MITF* in CMM by comparison of *Pax3c*, *Pax3d* and *Mitf-m* mRNA expression in murine embryogenesis and melanogenesis. Results indicate that while *Mitf-m* expression may be reliant on *Pax3c* expression, *Pax3c* expression is not solely linked to *Mitf-m* upregulation. Moreover, no apparent correlation appears between *Mitf-m* and *Pax3d* expression as random inverse and overlapping expression of these genes was observed during murine embryogenesis and adult hair regrowth. Finally, a link between Pax3 and c-Kit was sought. Knowing that loss of the c-Kit tyrosine kinase receptor occurs in CMM and that PAX3 functions as a gene repressor, we analysed mRNA profiles of *Pax3c*, *Pax3d* and *c-Kit* in depilation experiments to investigate possible inverse correlations in gene expression. Although the *c-Kit* promotor sequence reveals potential binding sites for *Pax3*, our results indicate that loss of *c-KIT* expression in CMM is not potentially linked to aberrant *PAX3* expression.

TABLE OF CONTENTS

DEFINITION OF ABBREVIATIONS

Table 1. Terms and abbreviations.

Terminology	**Definition**
PAX3	Gene encoding the human transcription factor PAX3
PAX3	Human PAX3 transcription factor
Pax3	Gene encoding the murine transcription factor Pax3
Pax3	Murine Pax3 transcription factor
CMM	Cutaneous malignant melanoma
MITF-M	Gene encoding human micropthalmia-associated transcription factor (melanocyte specific)
Mitf-m	Murine micropthalmia-associated transcription factor (melanocyte specific)
Mitf-m	Gene encoding murine Mitf-m
SCF	Stem cell growth factor
c-KIT	Human receptor tyrosine kinase for SCF
c-Kit	Murine receptor tyrosine kinase for SCF
c-KIT	Gene encoding human c-KIT
c-Kit	Gene encoding murine c-Kit

LIST OF FIGURES

LIST OF TABLES

1

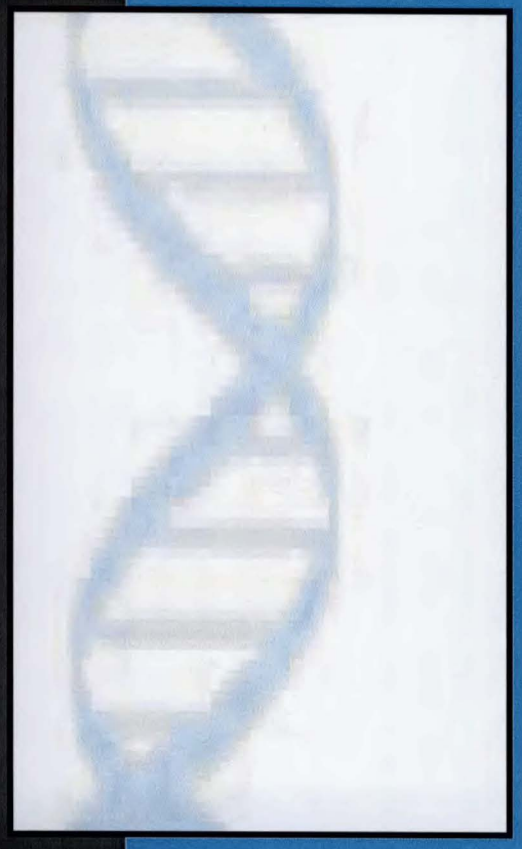

INTRODUCTION

1.1 INTRODUCTION

As far back as 1910, cancer was suspected to be primarily a genetic disease; undeniably, the past century has witnessed the unravelling of numerous genetic events involved in the pathogenesis of the neoplastic cell. The basis of this research lies in the supposition that gene transcription factors that function to regulate development within the embryo are often re-expressed in tumourigenesis and therefore able to be selectively utilised by neoplastic cells for cancer progression. In line with this supposition, CMM arises within cells of neural crest origin, a lineage in which *PAX3* is a principal regulator of progenitor cell migration and differentiation. This, combined with the observation that *PAX3* is over-expressed in CMM (in contrast to virtually no expression in normal skin or benign naevi) led to the hypothesis that the developmental role of *PAX3* may be re-activated in CMM and thus contribute to neoplastic progression of melanocytes. The aims of this research therefore became to investigate normal *Pax3* expression profiles during key stages of melanocytic development in order to more clearly hypothesise possible repercussions of aberrant re-expression in CMM. Correlations were sought between *Pax3* expression and the expression of *c-Kit* or *Mitf*, two potential downstream targets of Pax3 to examine the consequences of aberrant *PAX3* expression in CMM.

2

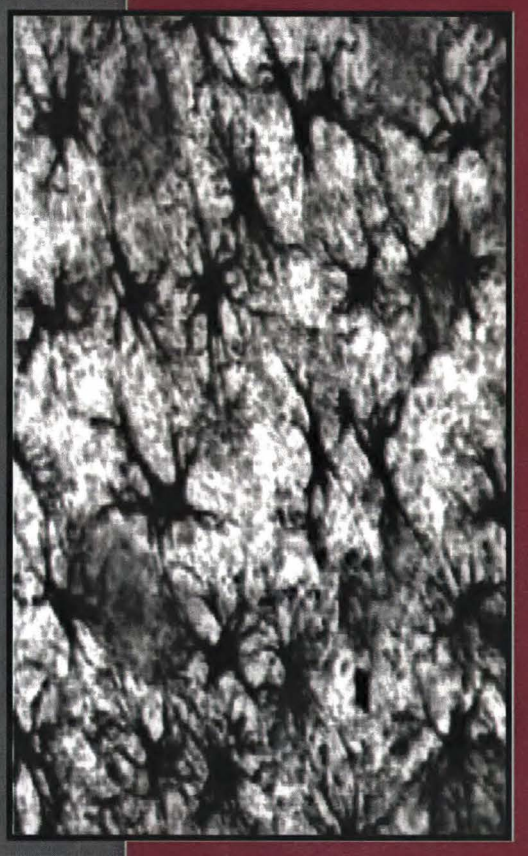

LITERATURE REVIEW

In an effort to understand the implications of increased *PAX3* expression in CMM, this literature review focuses on development of melanocytic cells from the neural crest, melanocytic function following differentiation and pigment production, aetiologies and pathogenesis of CMM, *PAX3/Pax3* involvement in embryogenesis and finally, key proteins thought to be activated by *PAX3* and implicated in the progression of CMM. The scope of the review is wide-ranging; it has led to a publication (Blake & Ziman, 2003) which generated international interest and formed the foundation on which the discussion is based.

2.1 MELANOCYTIC CELLS

Melanocytes are specialised pigment producing cells located primarily in the epidermis, hair follicle, cochlea and choroid of the eyes. Production of melanin pigment within each subpopulation of melanocyte is associated with varying function according to the tissue. For example, in the stria vascularis (the lateral wall of the cochlear duct), melanin pigment is thought to play a role in hearing (Mou *et al.,* 1997; Takeuchi & Ando, 1997; Masuda *et al.*, 1994) while in the choroid of the eye, melanin is essential for the maintenance of vision (Hu *et al.*, 2002). This review, however, focuses on epidermal (cutaneous) and hair follicle (follicular) melanocytic cells, from their specifications as melanoblasts (melanocytic stem cell) to their differentiation into melanocytes (cells capable of melanin production). In order to unravel possible repercussions of the aberrant expression of *PAX3* in CMM, review of the literature initially focused on the normal development of melanocytes.

2.1.1. Melanocytic Development

Due to lack of human embryonic tissues or models for study of

melanocytic development, much of what is known about the migration and differentiation of melanocytic cells has been studied in a murine animal model. Throughout the review, reference will be made to melanocytic development in mice, although it differs slightly from human melanocyte development. Where necessary, key differences are noted.

In mice, neural crest cells become committed to the melanoblast lineage at around embryonic day 8.5 (E8.5) and begin migration dorsolaterally toward the ventral midline and into the dermis at around day E10.5 (Mayer, 1973). An early study by Mintz (1967), used groups of coloured mice, containing two alternatively pigmented melanocytic *genotypes* to reveal that all melanocytes in murine coats are clonally derived from a fixed, small number of primordial melanoblasts that proliferate and migrate to prospective regions of the dermis in a specific pattern, as described by Mintz:

> "The animals are dramatically striped, with a series of broad transverse bands of alternating colors extending down the full length of head, body, and tail. The sharp mid-dorsal separation indicates that the two sides are established autonomously, without physical contiguity, so that a left and a right member are actually present. Each cell appears to proliferate laterally, and to a lesser extent longitudinally, to fill the available space between epidermis and dermis, bounded on each side by neighboring clones. There are 17 successive bands down each side of an animal. The head has three per side. On each side, there are 6 bands on the body, and 8 on the tail. The simplest explanation for these bands, consistent with all known facts of pigmentary ontogeny, is that each is a clone of melanoblasts, descended mitotically from a single cell." (Mintz, 1967)

That melanocytes of the murine coat are descended from a small number of primordial melanoblasts whose progeny proliferate, migrate and regionalise within specific regions of the body, may be analogous to human melanocytic proliferation and migration; this will be further discussed in

relation to germline pathogenesis of human melanocytes such as is seen in giant congenital naevus (see page 29).

Following regionalisation of melanoblasts in the murine dermis, during a specific window of time at around E12.5-13.5, melanoblasts enter the epidermis synchronously and proliferate extensively (Yoshida *et al.*, 1996). Subsequently, at around E15, a subpopulation migrates toward the developing hair germ (Hirobe, 1984). Here, a fraction of melanoblasts remain within the follicle as stem cells, while others begin to terminally differentiate at around E14, with pigmentation induced around 2 days later (Hirobe, 1984). After birth, most epidermal melanocytes, except those of hairless areas such as the ears and tail, undergo apoptosis (Hirobe, 1984) leaving only melanoblasts and melanocytes of the hair follicles to produce pigmentation of the coat in mice.

In human melanocytic development, melanoblasts are found in the epidermis at 9-11 weeks of gestation, prior to the development of the hair germs (Hashimoto, 1991). Most of the primary hair germs over the skin surface develop at around four months of gestation (Hashimoto, 1970). At this point, a subpopulation of epidermal melanoblasts migrates into developing hair matrices before maturation into melanin producing cells; it is currently unknown, however, whether a fraction of these melanoblasts remain in the human follicle as stem cells such as is seen in mice. In contrast to murine melanocytes, both populations of human follicular and epidermal melanocytes remain active throughout postnatal life in the pigmentation process, although activity diminishes with aging.

2.1.2 Normal melanocyte morphology and histology

Visualised by bright light microscopy, normal melanocytes have a rounded cell body with characteristically clear cytoplasm and small round nucleus (Figure 2.1); their primary function is to produce and distribute melanin pigments to adjacent keratinocytes. Visualised by electron

microscopy, long, fine cytoplasmic dendrites can be seen extending from the soma of the melanocyte (Figure 2.2).

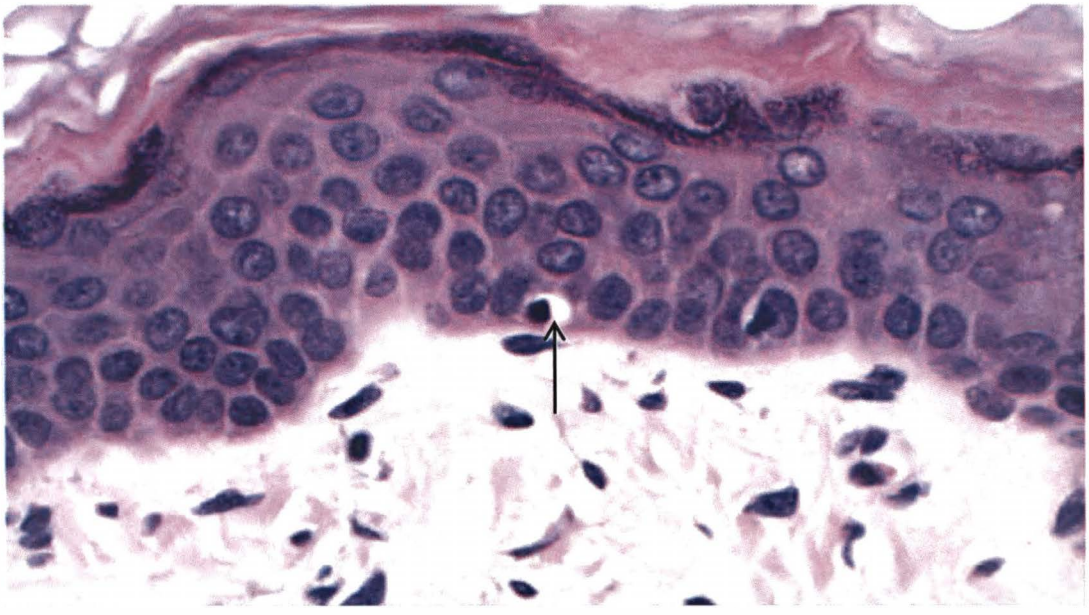

Figure 2.1. **Human Epidermis.**
Light microscopy showing normal epidermal melanocyte (indicated by arrow) situated at the dermal/epidermal border. Note the characteristic round cell body, round nucleus and clear cytoplasm.

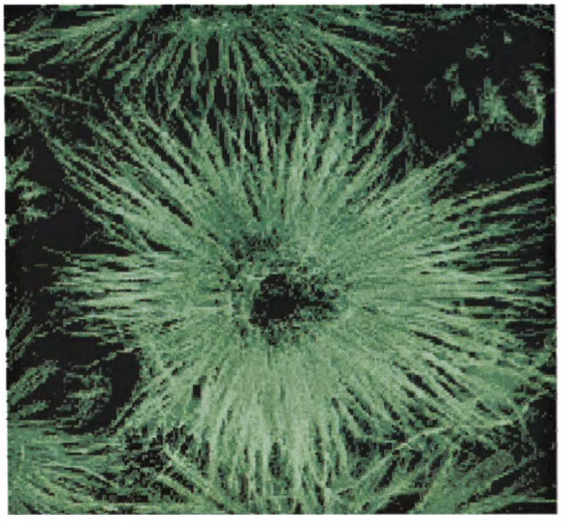

Figure 2.2. **Melanocyte.**
Electron microscopy showing melanocyte with fine dendritic processes.

In human skin, there is an orderly ratio of one melanocyte per several keratinocytes, called the epidermal-melanin unit. Once transferred from the melanocyte, melanin pigment accumulates above the nuclei of keratinocytes within the unit (Figure 2.3). Proliferating and the least mature post-mitotic keratinocytes are in the basal layer of the epidermis, adjacent to the dermis. Here, melanin is thought to protect mitotic cells from the ionising effects of UV irradiation.

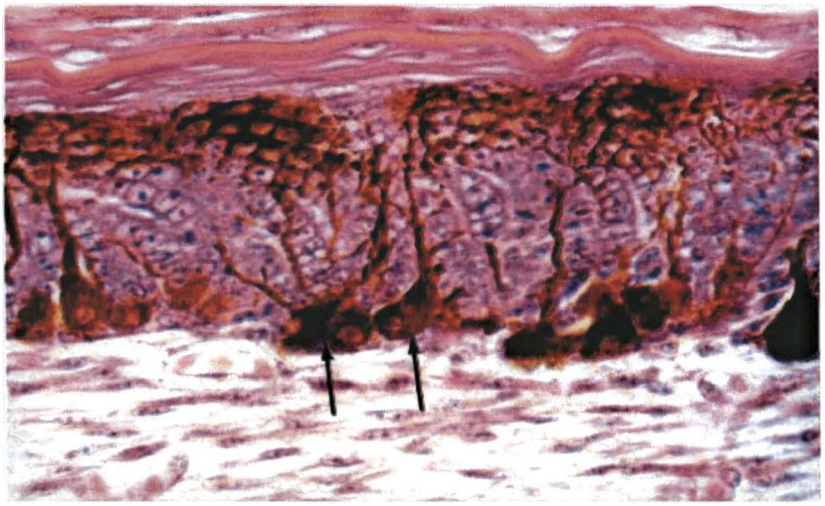

Figure 2.3. **Epidermal-melanin unit.**
Melanocytes distributing melanin among adjacent keratinocytes of epidermal-melanin unit. Arrows indicate cell bodies of the melanocytes.

2.1.3 Melanogenesis in the Hair Follicle

Melanogenesis refers to the complex process leading to the production of pheo- and eumelanin pigments within melanocytic cells. An intensely studied form of melanogenesis occurs in conjunction with the growth of new hair (both in humans and in mice). As the hair follicle cycles through stages of active growth (anagen), regression (catagen), resting (telogen), and shedding (exogen), pigment cells also cycle through periods of proliferation, migration, differentiation and apoptosis (Müller-Röver *et al.*, 2001) (Figure 2.4).

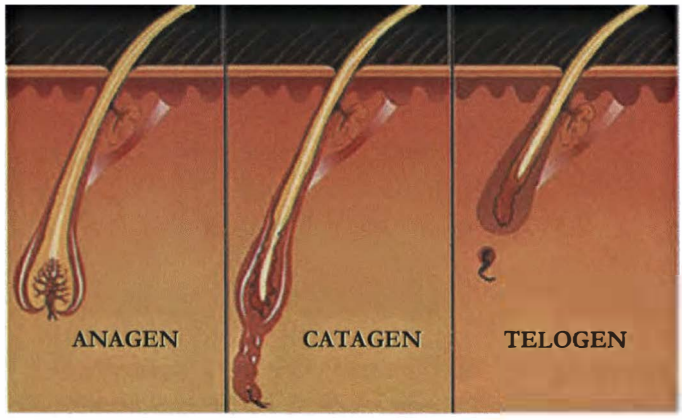

Figure 2.4. **Hair Follicle Cycling.**
Diagram depicting hair cycling through stages of anagen (active growth), catagen (regression) and telogen (resting).

In mice, the hair follicle contains at least two distinct populations of melanocytes and melanoblasts; one melanogenic, the other not, respectively (Tobin *et al.*, 1995; Tobin & Bystryn 1996; Nishimura *et al.*, 2002). Melanogenically active melanocytes are located in the hair cortex where they are distributed in close contact with the basal lamina, separating the cortex and the dermal papilla (Figure 2.5). These cells express tyrosinase mRNA and actively produce pigment during late anagen (Slominski *et al.* 1991; Ortonne & Prota 1993); in murine hair, pigment is passed from melanocytes to follicular kerytinocytes via dendritic processes (Staricco, 1962; Morrelli *et al.*, 1991). In the stages of follicular catagen or exogen, cortex melanocytes have been seen to retract dendritic extensions before undergoing apoptosis (Tobin *et al.*, 1998). In mice, replacement of these lost cortex melanocytes occurs by proliferation of a distinct, small population of melanoblasts that remain in an undifferentiated state, as a stem cell population, within an area known as a "niche" (Nishimura *et al.*, 2002). This niche is located in the outer root sheath of the lower permanent portion of the hair follicle, just below the bulge area where the arector pili muscle is attached (Nishimura *et al.*, 2002). Melanoblasts do not produce melanin or melanosomes and are always maintained in this bulge area (Nishimura *et al.*, 2002). Furthermore, *in vitro* studies demonstrate

that amelanotic melanoblasts in anagen have extensive proliferative potential. By contrast, cortex melanocytes are not cultured successfully, suggesting that these cells are more terminally differentiated (Tobin *et al.* 1995; Tobin & Bystryn 1996).

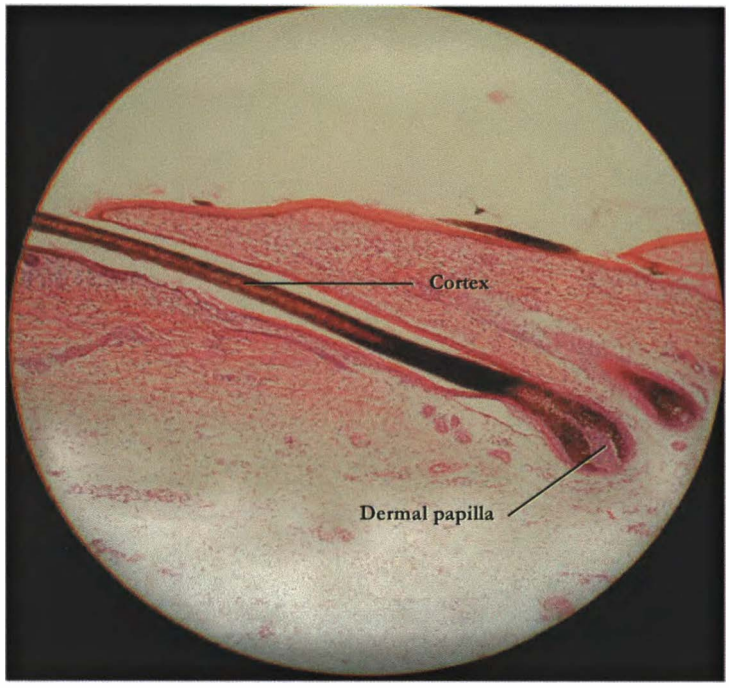

Figure 2.5. **Hair Follicle.**
Within the hair follicle, fully differentiated melanocytes capable of melanin production are located within the cortex, above the dermal papilla.

As the hair follicle undergoes transition from telogen to anagen, melanoblasts migrate out of the stem cell niche to proliferate. At least one of the daughter stem cells remain in the bulge area while the other migrates into the developing hair germ where it eventually localises in the cortex, further proliferates and differentiates into a melanocyte. The reserve of melanocytic stem cells within the niche is thought responsible for the continued proliferation of both follicular and cutaneous melanocytes in the mouse (Nishimura *et al.,* 2002). In this research, proliferation of murine melanocytic stem cells from the follicular niche was induced by depilation of normal murine skin in order to assess *Pax3* mRNA expression profiles during proliferation and migration of melanoblasts.

2.1.4 Melanogenesis in the Skin

In human skin, cutaneous melanocytes are located in the epidermis within the basal layer (adjacent to the basement membrane) where they adjoin to epidermal keratinocytes via dendritic extensions in order to pass cytoplasmic melanosomes. It has been estimated that the ratio of melanocyte to keratinocyte is 1:40, although this ratio varies according to the area of the body. Melanisation patterns of human skin reveal that some areas with concentrated pigmentation are not exposed to UV; this is linked to an alternate function for melanin as an antimicrobial for skin (Mackintosh, 2001).

In transgenic mice bred to retain functional cutaneous melanocytes, analysis of induced proliferation has shown that following apoptosis of cutaneous melanocytes, melanocytic stem cells migrate out of neighboring hair follicles to proliferate. These cells then migrate further along routes connecting the follicular outer root sheath and epidermis toward their final destination within an epidermal-melanin unit (Lei *et al.,* 2002; Nishimura *et al.,* 2002). Similarly, human studies have shown that following treatment of skin in disorders such as vitiligo (a condition in which skin lacks pigmentation due to loss of functional melanocytes), re-pigmentation follows a pattern where pigmented spots first appear in concentric rings surrounding the hair follicle. With time, these rings enlarge and eventually fuse to recolour the skin (Nishimura *et al.,* 2002). These two studies imply that follicular melanocytic stem cells are associated with a continued renewal of lost cutaneous melanocytes, although research has not demonstrated evidence of a stem cell population in the human hair follicle to date.

2.1.5 Human Melanogenesis with UV Exposure

Melanin plays an important role in the protection of keratinocytic cellular DNA by forming a protective envelope around the cell nucleus (Valverde *et al.,* 1995). It absorbs free radicals generated in the cytoplasm and

shields the nucleus from various types of ionizing radiation, including ultra-violet (UV) light. In the event of extreme or repeated exposure to UV irradiation, increased synthesis of melanin is evidenced by "tanned" skin. Exposure of melanocytes to UV irradiation results in a highly complex process of DNA repair (Eller *et al.,* 1994; Barker *et al.,* 1995; Winter *et al.,* 2001), upregulation of autocrine and paracrine cytokines (Abdel-Malek *et al.,* 1995; Imokawa *et al.,* 1996) and induction of mitosis (Kawaguchi *et al.,* 2001). Signalling between UV exposed keratinocytes, melanocytes and fibroblasts results in an increase in the number, size and dendricity of melanocytes (Halaban *et al.,* 1988; Grichnik *et al.,* 1998). Studies have shown that the skin has precise mechanisms in place both for the prevention of uncontrolled UV induced melanocytic apoptosis (Allsopp *et al.,* 1993) and uncontrolled proliferation within the epidermis (Bacharach-Buhles, 1999).

Controversy has existed as to whether increased numbers of melanocytes following UV exposure is due to an increase of mitotic activity of cutaneous melanocytes or due to induction of melanoblasts from a stem cell population. Rosdahl & Szabo (1978) reported that cell division of established cutaneous melanocytes is responsible for a 4-6 fold increase in melanocyte numbers during irradiation. However, only 65-80% of their increased population were from labelled precursors; they had no explanation for the origin of the further 20-35% neo-melanocytes.

Using transgenic mice in which cutaneous melanocytes function postnatally, murine studies have shown that a high percentage of cutaneous melanocytes undergo apoptosis in response to intense UV exposure. This, along with cytokine signaling via epidermal keratinocytes in response to irradiation, promotes migration of melanoblasts from the outer root sheath of hair follicles (Kawaguchi *et al.,* 2001; Lei *et al.,* 2002). Increases of melanoblasts (not yet capable of melanin production) have been seen in the epidermis on the first day following UV exposure. Around the fifth day following exposure,

differentiation of the melanoblasts was evident and resulted in four times as many melanin producing cells as compared to normal control skin (Kawaguchi *et al.*, 2001). These studies indicate that *intense* UV exposure may overwhelm normal mitotic capabilities of cutaneous melanocytes leading to apoptosis and further recruitment of stem cells from the niche in order to replace lost cells.

Undeniably, primary causes for transformation of the melanocytic cell to neoplasia are numerous and are continuously being investigated. While many theorise that mutagenic disturbances following intense UV exposure occur within melanin-producing melanocytes, this study supports the possibility of UV mutagenesis within mitotic stem cells or post-mitotic melanoblasts and discusses possible repercussions of this occurance.

2.2 PRECURSORS OF CMM

Although exposure to UV is a principle factor involved in the acquisition of CMM from benign melanocytic naevus, several studies detail neoplasia arising due to occurrence of giant congenital melanocytic naevus and dysplastic naevus syndrome.

2.2.1 Benign melanocytic naevus

A large percentage of CMMs are known to arise from cutaneous melanocytes within normal skin (Barnhill & Mihm, 1993), however, 40-50% of CMMs are thought to develop from benign melanocytic naevi (Lopansri & Mihm, 1979). A benign melanocytic naevus is thought to arise as a consequence of excessive ultraviolet exposure leading to mutagenesis and mitogenesis of cutaneous melanocytes. UV mutagenesis of melanocytic cells can lead to loss of tumour suppressor genes, low-level microsatellite instability and a reduction in expression of mismatch repair proteins (Alvino *et al.*, 2002; Hussein *et al.*, 2002; Hussein & Wood, 2003). In any event, these atypical melanocytes are referred to as naevus cells and they usually develop between the first and thirty-fifth year of life, undergo specific stages of maturation and finally senesce (Lund & Stobbe, 1949).

In contrast to normal melanocytes, naevus cells are oval or cuboidal with large, often vesicular nuclei and clearly outlined cytoplasm; although they are capable of melanin production, they follow a divergent path of differentiation eventually expressing proteins similar to those of Schwann cells (Reed *et al.*, 1999). Within the skin, collections of naevus cells aggregate to form nests at rete ridges (where the epidermis invaginates toward the dermis) (Figure 2.6).

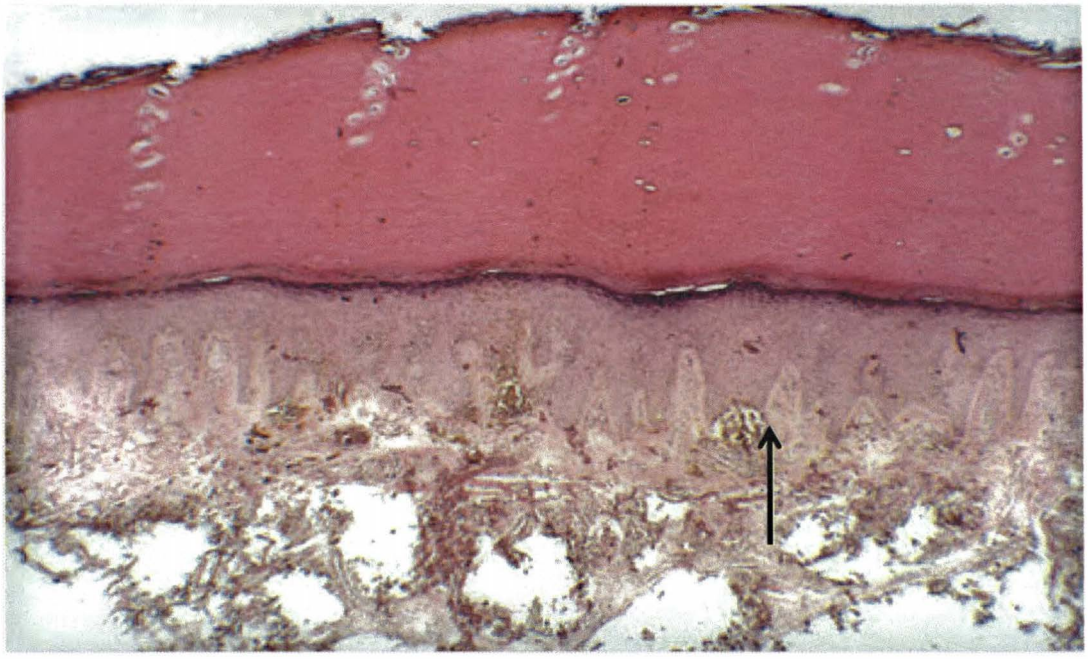

Figure 2.6. **Nest of melanocytic naevus cells. H&E staining. X400**
Arrow indicates nest of atypical naevus cells located at the rete ridges of the epidermis.

At this stage, a benign melanocytic naevus is classified as a 'junctional naevus'; typically, naevus cells do not extend into the dermis. However, as naevus cells continue to proliferate and differentiate, post-mitotic cells acquire the ability to migrate into the dermis. At this stage a benign melanocytic naevus is classified as 'compound' with naevus cells spanning both the epidermis and dermis. From this stage, naevus cells become separated from the epidermis by connective tissue, cease to proliferate and eventually senesce (Reed *et al.*, 1999).

It is hypothesised that CMM may arise from nests of benign melanocytic naevi, either from a naevus cell or from melanocytes adjacent to or within nests of naevi. Fortunately, most benign melanocytic naevus cells undergo transition from proliferative to non-proliferative, rendering them harmless to the carrier. An important phenotypic characteristic of benign naevus cells is loss of telomerase activity during their transition from

proliferative to non-proliferative (telomerase activity is necessary during cell proliferation to prevent telomere attrition). This is in stark phenotypic contrast to CMM, where neoplastic cells retain the ability to proliferate due to *increased* telomerase activity (Rudolph *et al.,* 2000).

This begs the question, do benign naevus cells diverge from the benign differentiation pathway to become CMM; for example, is each cell able to change from one pathway to the other? While this theory is feasible, an alternate explanation for phenotypic differences between benign melanocytic naevi and CMM may be that mutagenesis of mitotic or post-mitotic cells results in cellular differentiation down one pathway *or* the other, both being mutually exclusive and randomly occurring within the cell.

2.2.2 Congenital Naevi

Another precursor of CMM is thought to be a congenital naevus, present at birth and affecting 1-2% of neonates (Walton *et al.,* 1976). A congenital naevus appears as a brown or black round or oval plaque, often associated with overgrowth of hair (Figure 2.7). The naevus may be small (15mm), medium (15-199mm) or giant (>200mm) and comprised of the following cell types in any combination: melanocytic naevi, neuroid naevi (naevus cells expressing nerve sheath proteins), blue naevi, and/or cellular blue naevi.

While a small congenital naevus is associated with a 3% risk of transformation, a giant congenital naevus has a 15% risk of developing into CMM before the age of pubescence (Dellon *et al.,* 1976). Furthermore, statistics have shown that 40% of CMM cases seen in children arise from giant congenital naevus (Dellon *et al.,* 1976; Quaba & Walllace, 1986). Although there is no known genetic contribution to date, it has been suggested that a number of cases of congenital naevus may be determined by an autosomal dominant gene of variable expressivity (Goodman *et al.*, 1971).

As melanocytes of human skin are thought to be clonally derived from a small population of primordial melanocytic stem cells which migrate in a standard pattern such as the murine melanocytes seen in Mintz' work (see pg. 17), mutagenesis of mitotic stem cells or post-mitotic primordial melanoblasts may be a plausible explanation for development of giant congenital naevi (Figure 2.7).

Figure 2.7. **Congenital melanocytic naevus.**
Infants with giant congenital naevus. Removal of the naevus requires several extensive surgeries.

2.2.3 Dysplastic naevus syndrome

10% of CMM cases are familial and suggest an inherited predisposition (Fountain *et al.*, 1990). One such predisposition may be dysplastic naevus syndrome, an autosomal dominant inherited disposition in which affected individuals develop 10-100 large naevi following puberty (Haley *et al.*, 2000)(Figure 2.8).

In comparison to benign melanocytic naevus cells, cells of a dysplastic naevus are increasingly atypical relative to normal melanocytes. Following a progression of developmental stages similar to benign naevus cells, the dysplastic naevus cells divert at migration into the dermis. Here cells continue to proliferate, synonymous with increasing atypia, hyperplasia, hypertrophy and dysplasia. Histological criteria for diagnosis of dysplastic naevus syndrome are lamellar and concentric dermal fibroplasia, presence of dermal lymphocytic infiltrate and elongation of rete ridges (Elder *et al.*, 1982; Kraemer

& Greene, 1985). Furthermore, dysplastic naevus cells have significantly larger nuclei, consistant with a hyperdiploid or tetradiploid DNA content.

Figure 2.8. **Dysplastic Naevus Syndrome.**
Note the number of naevi present on the trapezoidal region of the back. Arrows indicate suspect melanomas. Circled naevi are examined for growth and color changes over time. Persons with this syndrome are considered highly susceptible to development of CMM.

Dysplastic naevus is known to be a precursor of many cases of CMM; in fact persons inheriting dysplastic naevus syndrome are highly susceptible to CMM (Greene *et al.*, 1985; Bale *et al.*, 1986). Two principal loci known to be associated with dysplastic naevus syndrome are at 1p (the gene locus called *CMM1*) and 9p (the gene locus called *CMM2*). Through multipoint linkage analysis, Bale *et al.* (1989) mapped *CMM1* to 1p36. Patients carrying a mutation at this locus have distinctive characteristics of the skin, closely resembling xeroderma pigmentosum (a syndrome in which individuals possess a defect in DNA-repair mechanisms). It has recently been shown that reduced DNA-repair ability combined with presence of dysplastic naevi syndrome is strongly associated with risk of CMM and may contribute to susceptibility to

sunlight-induced CMM (Landi *et al.*, 2002).

The *CMM2* locus at 9p21 contains several candidate genes for CMM (Puig *et al.*, 1995). Chromosome region 9p21 is involved in homozygous deletions in more than half of all melanoma cell lines (Kamb *et al.*, 1994). The region was found to contain the gene *CDKN2A* which encodes an inhibitor of cyclin-dependent kinase-4 (CDK4) (Serrano *et al.*, 1993; Kamb *et al.*, 1994). Complexes formed between CDK4 and cyclins are involved in the control of cell proliferation during the G1 phase. In familial melanomas it has been established that a mutation in the *CDKN2A* gene leads to a marked increased risk for CMM, although a number of 9p21-linked kindred lack germline coding mutations in *CDKN2A* (Loo *et al.*, 2003).

In summary, deficiency in mutation excision repair systems is strongly linked to development of CMM, particularly when an affected individual is subjected to extreme UV exposure. CMM arise from normal skin or an existing benign melanocytic naevus; persons possessing either congenital naevus or dysplastic naevus are at an increased risk. In the case of congenital naevus, risk of developing CMM has not been linked to a particular mutation. By contrast, in dysplastic naevus syndrome, mutations in *CMM1* at 1p36 or *CMM2* at 9p21 have been identified; however, many persons with dysplastic naevus syndrome do not possess either mutation and yet develop CMM while many persons with dysplastic naevus syndrome harbouring a known mutation in either 1p36 or 9p21 do not develop CMM. Although mutations in *PAX* genes are associated with many forms of cancer (Bennicelli *et al.*, 1996; Iida *et al.*, 1996; Kroll *et al.*, 2000), these studies have demonstrated that causative *mutations* in CMM are not associated with PAX3.

2.3 CUTANEOUS MALIGNANT MELANOMA

CMM tumours are classified into five histologic types: lentigo maligna melanoma, superficial spreading melanoma, nodular melanoma, acral-lentiginous melanoma and desmoplastic melanoma. As the desmoplastic variety of tumour is very rare (McGovern & Murad, 1985), discussion will focus on the four most common types of CMM.

2.3.1 Lentigo Maligna Melanoma

Lentigo maligna melanoma arises from a noninvasive malignant lesion (also known as Hutchinson's freckle). Lentigo maligna develops as a tan or brown macule with uneven, superficial black spots on sun-exposed areas of the body such as the face (Figure 2.9). Lentigo maligna melanoma occurs with an incidence of approximately 7% of CMMs (Davis, 1982, pg. 72). The condition is diagnosed most often in the elderly, as lentigo maligna usually arises in the fourth decade of life or later; there is a slow, insidious development of malignancy over a period of rarely less than 20 years (Davis, 1982, pg. 72). A notable increase in size, darkening and/or bleeding of a lentigo maligna lesion heralds the change from noninvasive to invasive growth.

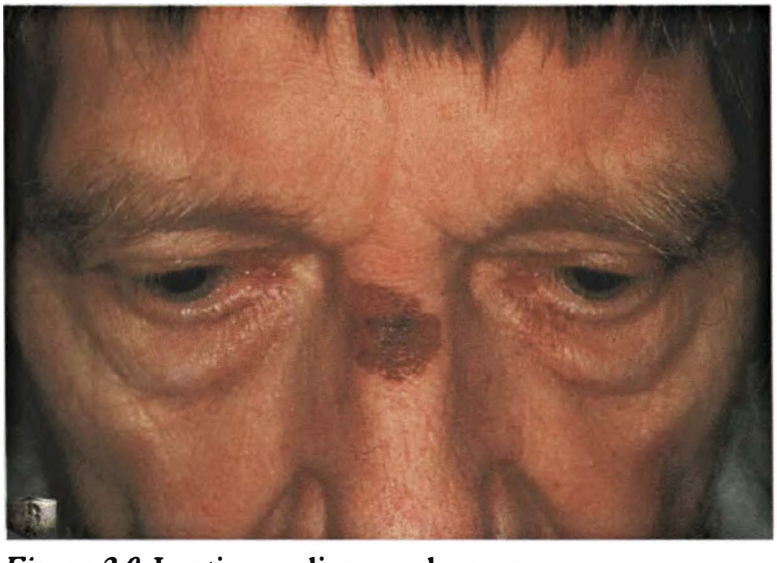

Figure 2.9. **Lentigo maligna melanoma.**
Note the irregular border and dark brown areas which are characteristic of the lesions.

2.3.2 Superficial Spreading Melanoma

Superficial spreading melanoma is the most common form of CMM, estimated to account for 55-75% of all of CMMs (Davis, 1982, pg. 72). Superficial spreading melanoma can be diagnosed at any age; however it usually begins in middle age. Although these lesions can occur anywhere on the body, they most commonly appear on the lower legs of women and torsos of men. Lesions are irregular, raised plaques, multicoloured with white, red, blue or black areas and blue-black nodules (Figure 2.10). Horizontal growth may continue for several years (as lentigo maligna does for decades) before invasive vertical growth into the dermis.

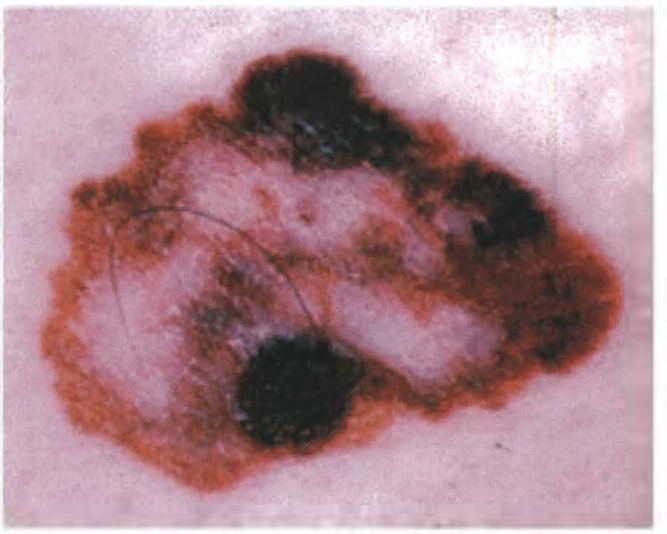

Figure 2.10. **Superficial spreading melanoma.** The multi-coloured appearance is characteristic of the lesion.

2.3.3 Acral-Lentiginous Melanoma

Acral-lentiginous melanoma arises on the palmar, plantar and subungual tissues, notably the distal phalanges of the fingers and toes (Figure 2.11). It is the least common type of CMM, accounting for approximately 1% of CMMs (Davis, 1982, pg. 74). Acral-lentiginous melanoma initially manifests as an irregular brown or black macule on the sole, palm, digit or nail-bed and is often mistaken for a haematoma or fungal infection.

Histologically, acral-lentiginous melanoma resembles lentigo maligna melanoma and shares a similar lengthy stage of non-invasiveness. Subungual acral-lentiginous melanoma cannot be staged using thickness criteria, as invasive growth is noted histologically by nail erosion, scaling, furrowing or elevation. Eventually the subungual acral-lentiginous melanoma ulcerates to push the nail aside. Although acral-lentiginous melanoma is the least common of the four types of CMM, it is the most common melanoma of non-white persons (Davis, 1982, pg. 74).

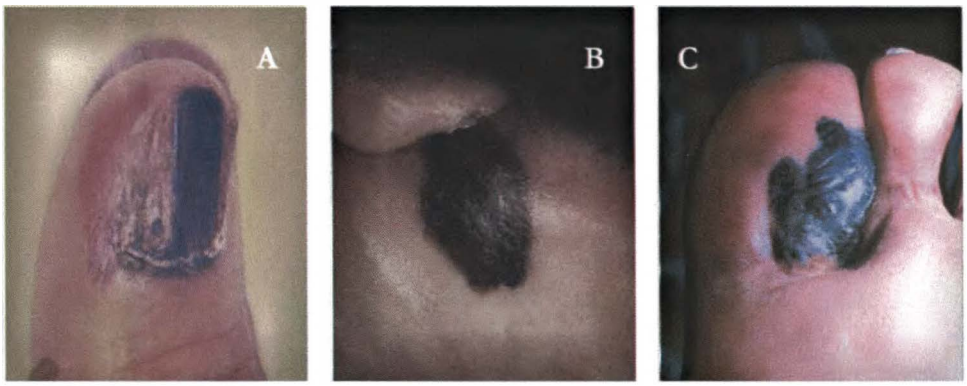

Figure 2.11. **Acral-lentiginous melanoma.**
Lesions located in the nail-bed of thumb (A) and plantar surfaces (B, C) of the foot.

2.3.4 Nodular Melanoma

Nodular melanoma (Figure 2.12) is the second most common type of CMM (15-30%) with a very high risk of metastasis due to aggressive, invasive vertical growth of the nodule (Davis, 1982, pg. 72). An increase in lesion pigmentation usually precedes nodular enlargement; eventual ulceration and bleeding are late signs of malignancy. Nodular melanoma is histologically characterised from other types of CMM by its nodules of large, epithelioid melanocytes expanding exclusively in a vertical manner into the dermis (Davis, 1982, pg. 72).

Figure 2.12. **Nodular melanoma.**

2.3.5 Histopathology of CMM

Transformation of the normal melanocyte to neoplasia leads to a relatively uniform progression of cellular pathology. Morphologically, CMMs may contain cell types that are epithelioid (rounded) or lentiginous (spindle) shaped. Tumours with predominantly epithelioid shaped cells tend to organise atypical cells into "nests" whereas tumours with spindle shaped cells organise into irregularly branched formations. The histopathological features in the early stages of CMM show an accumulation of neoplastic cells in the epidermis above the basement membrane; at this stage the lamina may or may not be intact, however the tumour is thought to have no metastatic potential due to inaccessibility of blood vessels and lymphatics situated below the basement membrane.

As the neoplasm continues to develop, cells penetrate the papillary dermis (fingerlike projections of the dermis between the rete ridges of the

epidermis). In the earliest portion of this stage, only single neoplastic cells invade the papillary dermis; therefore, the metastatic potential of the lesion is still considered to be zero. Following invasion of the papillary dermis, tumour cells acquire the ability to proliferate in the cellular and stromal environment of the dermis. Proliferating intra-dermal tumour cells aggregate into multi-celled populations that continue to expand to the level of the reticular dermis. At this stage, an initial, slight risk of metastasis exists, gradually increasing as the tumour invades deeper into the dermis. Once CMM invades the reticular dermis and eventually the subcutaneous fat, the risk of metastasis is great and visceral metastases are likely to occur.

2.3.6 Diagnosis/Staging of CMM

There are currently two systems employed to grade or stage CMM. The Breslow system (Breslow, 1975) is based on the total thickness of the tumour as measured from the outermost layer of the stratum granulosum to the deepest point of tumour invasion into the dermis during the vertical growth stage. This measurement has a strong predictive value in the prognosis of patients with non-metastatic melanomas (Table 2). The Clark system (Clark *et al.,* 1975) grades a tumour according to depth of invasion of atypical cells or inflammatory infiltrates in relation to cutaneous histologic structures and correlates prognosis to the anatomic level of involvement (Table 3).

Table 2. The Breslow system of tumour grading/prognosis (Breslow, 1975).

Total thickness of tumour	Five Year Survival Rate
0.00-0.76mm	98-99%
0.76-1.49mm	85%
1.50-2.49mm	84%
4.00mm	44%

Table 3. The Clark system of tumour grading/prognosis (Clark *et al.*, 1975).

Clark System	Five Year Survival Rate
Level I-Tumour is confined to the epidermis and is above the basement membrane	**100-98%**
Level II- Invasive cells are present solely in the papillary dermis	**96-72%**
Level III- Tumour cells are seen throughout the papillary dermis with impingement on the reticular dermis	**90-46%**
Level IV- Tumour cells are seen between collagen bundles of the reticular dermis	**67-31%**
Level V- Tumour cells are seen in the subcutaneous fat	**48-12%**

Following diagnosis of CMM, subsequent measures attempt to discern whether the cancer remains localised or has metastasised. The presence of metastases leads to a particularly unfavorable prognosis for the patient as CMM proves resistant to many conventional therapies. CMM progression has been the focus of much study and a review of these studies in its entirety would be insurmountable; therefore, this review is focused on events of progression thought potentially related to *PAX3* expression.

2.4 *PAX3/ Pax3* EXPRESSION

Nine members of the *PAX* family of genes derive their name from a 384 bp DNA paired box sequence that encodes a highly conserved DNA binding domain termed the paired domain (Burri *et al.*, 1989; Krauss *et al.*, 1991). *PAX* genes are further classified into groups (I-IV) according to possession of a full or partial homeodomain, another important DNA binding domain. (Figure 2.20). The *PAX3* gene, located at 2q35 (Ishikiriyama, 1993), encodes a class III PAX protein transcription factor.

2.4.1 Pax3 in Embryogenesis

Pax3 is amongst the earliest transcription factors functioning during embryogenesis (Goulding *et al.*, 1991). Within the neural tube, it is expressed in cells that specify dorsal neurons (Goulding *et al.*, 1991) and plays a role in neural tube closure (Li *et al.*, 1999).

Pax3 expression is also required for survival and migration of myogenic precursor cells. In mice, *Pax3* is expressed in early somites as segmentation of the paraxial mesoderm occurs (Goulding *et al.*, 1991; Maroto *et al.*, 1997; Heanue *et al.*, 1999). Expression in cells of the medial lateral edge of somites denotes early stages of myogenic cell specification and cells arising from the hypaxial portion of the dermamyotome (medial lateral portion of the somite) migrate laterally to enter limb bud regions where they become limb musculature (Goulding *et al.*, 1991; Williams & Ordahl, 1994; Tremblay *et al.*, 1998; Henderson *et al.*, 1999; Lamey *et al.*, 2004).

Finally, *Pax3* functions in specification and migration of neural crest derived cells fated to become enteric ganglia (Lang *et al.*, 2000), heart septum (Li *et al.*, 1999), Schwann cells (Kioussi *et al.*, 1995) and melanocytes of the skin and hair follicles (Galibert *et al.*, 1999). As stated previously, melanoblasts are derived from the neural crest where *Pax3* is expressed in melanoblast precursor cells prior to their migration from the neural crest (Galibert *et al.*,

1999). *PAX3/Pax3* is thought to function in both proliferation of melanoblasts (Hornyak *et al.*, 2001) and differentiation of melanocytes through regulation of gene expression involved in melanin production (Galibert *et al.*, 1999).

2.4.2 *Pax3* Mutations

The role of *Pax3* has been largely determined by studies in *Pax3* mutant *Splotch* mice (Figure 2.13). The name *'Splotch'* refers to melanocytic defects resulting in splotchy pigmentation abnormalities of the fur. Homozygous *Splotch* mice ($Pax3^{-/-}$) die at embryonic day 14 due to neural tube defects in the lumbosacral region leading to spina bifida and exencephaly (Fleming & Copp, 1998; Moase & Trasler, 1992). In a study done in 1999, *Splotch* mice with transgenic *Pax3* expression in the neural tube and neural crest demonstrated rescue of neural tube closure and these mice did not have exencephaly (Li *et al.*, 1999).

In the *Splotch* mouse, mutations in *Pax3* affect myogenesis due to a failure of myoblasts to migrate into the limb buds (Bober *et al.*, 1994; Franz *et al.*, 1993). In transgenic mice with inhibited *Pax3* expression in the somites, pups reveal absence of diaphragm, supraspinatus, infraspinatus, subscapularis, terres minor and all distal limb muscles, consistent with the finding that hypaxial muscles arise from $Pax3^{+}$ cells of the lateral somites (Li *et al.*, 1999).

Mutations in *Pax3* also lead to a number of neurocristopathies. Lang *et al.* (2000) compared development of *Splotch* mice to transgenic mice in which *Pax3* expression was restored to the neural tube and neural crest. Analysis of these pups demonstrated that where *Pax3* expression was restored, embryos showed enteric ganglion formation. Furthermore, *Splotch* mice have cardiac defects due to failure of septation in the truncus arteriosus (Epstein *et al.*, 1996; Franz *et al.*, 1989). Li *et al.* (1999) demonstrated that transgenic Splotch mice with re-expression of *Pax3* in the neural crest restored cardiac flow

septation and promoted survival until birth.

Finally, *Pax3* mutations result in hearing, craniofacial and pigmentation anomalies which demonstrate variability in penetrance and expressivity. Asher *et al.* (1996) stated that a minimum of two genes, one of these being either X-linked or sex-influenced and the other autosomal, interact with the *Splotch Pax3* mutation to influence the craniofacial features of *Splotch* mice and concluded that further studies may lead to identification of genes that interact in order to modify the expression of human *PAX3* mutations in Waardenburg syndrome.

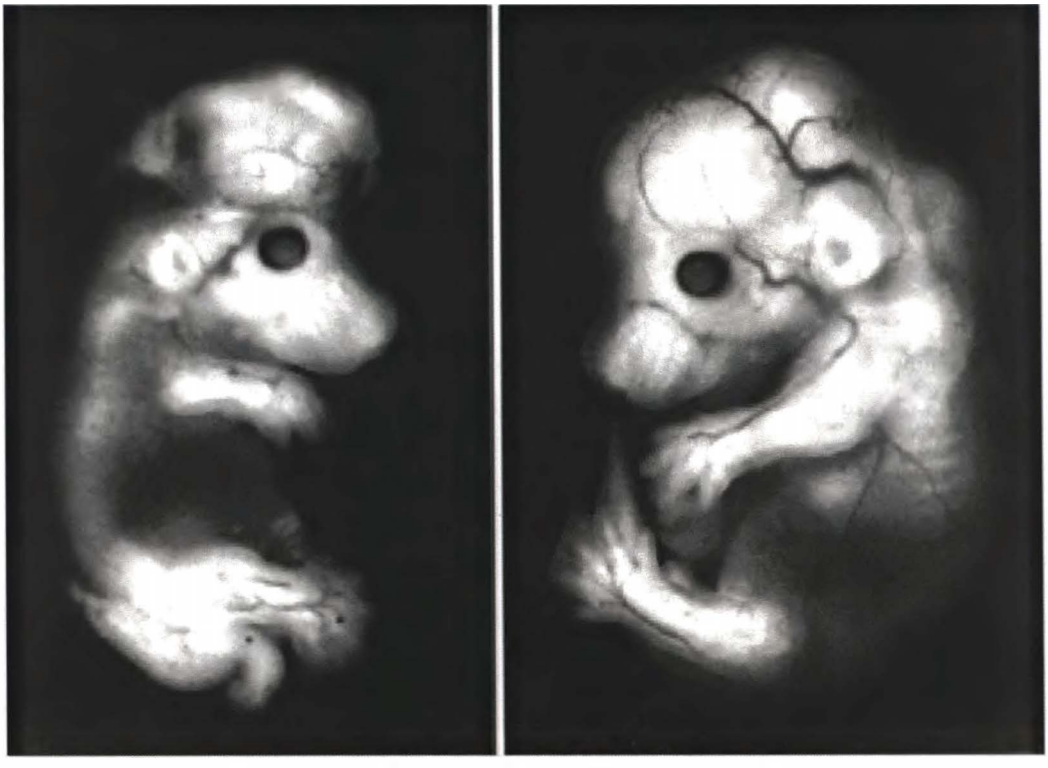

Figure 2.13. **Photomicrograph of a Splotch Murine Embryo.**
The mouse embryo on the left is a *Pax3* mutant "Splotch" mouse. Note the defects in the area of the neural tube, neural crest derived cranial facial structures and limb bud formation as compared to the wild type mouse on the right.

2.4.3 *PAX3* Mutations

Mutations in human *PAX3* are associated with Waardenburg syndrome Type 1, an autosomal dominant condition that presents with deafness and pigmentary disturbances due to dysfunction in the proliferation of neural crest derived cells (Tassabehji *et al.*, 1993). Mutations in *PAX3* encode abnormal transcription factors that are unable to regulate transcription of micropthalmia-associated transcription factor (*MITF*). *MITF* functions in survival of melanoblasts and synthesis of enzymes involved in melanogenesis; therefore, loss of *MITF* results in the absence of functioning melanocytes in the stria vascularis and hair follicles (Figure 2.14) (Bentley *et al.*, 1994; Ganss *et al.*, 1994; Yasumoto *et al.*, 1994; Tachibana *et al.*, 1996).

Figure 2.14. **Children affected by Waardenburg Syndrome I.**
The white forelock is a pigmentation defect in the hair follicles due to absence of melanocytes.

It can be seen from mutation studies that *PAX3*/*Pax3* plays an important role in the early development of particular lineages, most likely being associated with cellular proliferation, migration and/or regulation of the migratory phenotype of *Pax3* expressing cells. In CMM, *PAX3* mutations do not occur; rather, aberrant expression of a particular isoform is demonstrated. Knowing this led to the hypothesis that the developmental role of *PAX3* may be re-activated in CMM and thus contribute to neoplastic progression.

2.4.4 Alternative *PAX3* Transcripts

Functional diversity of *PAX3/Pax3 in vivo* is linked to its ability to produce alternatively spliced gene products which alter the structure and consequently the binding activity of the paired and homeodomain regions (Tsukamoto *et al.*, 1994; Underhill & Gros, 1997; Seo *et al.*, 1998). Originally *PAX3* was thought to contain only eight exons. Recent studies show that *PAX3/Pax3* may be alternately spliced at exons 4, 5, 8, and 9 to produce many different transcripts including transcripts that lack an entire homeobox (Parker *et al.*, 2004; Pritchard *et al.*, 2003; Barber *et al.*, 1999; Tsukamoto *et al.*, 1994) (Figure 2.15).

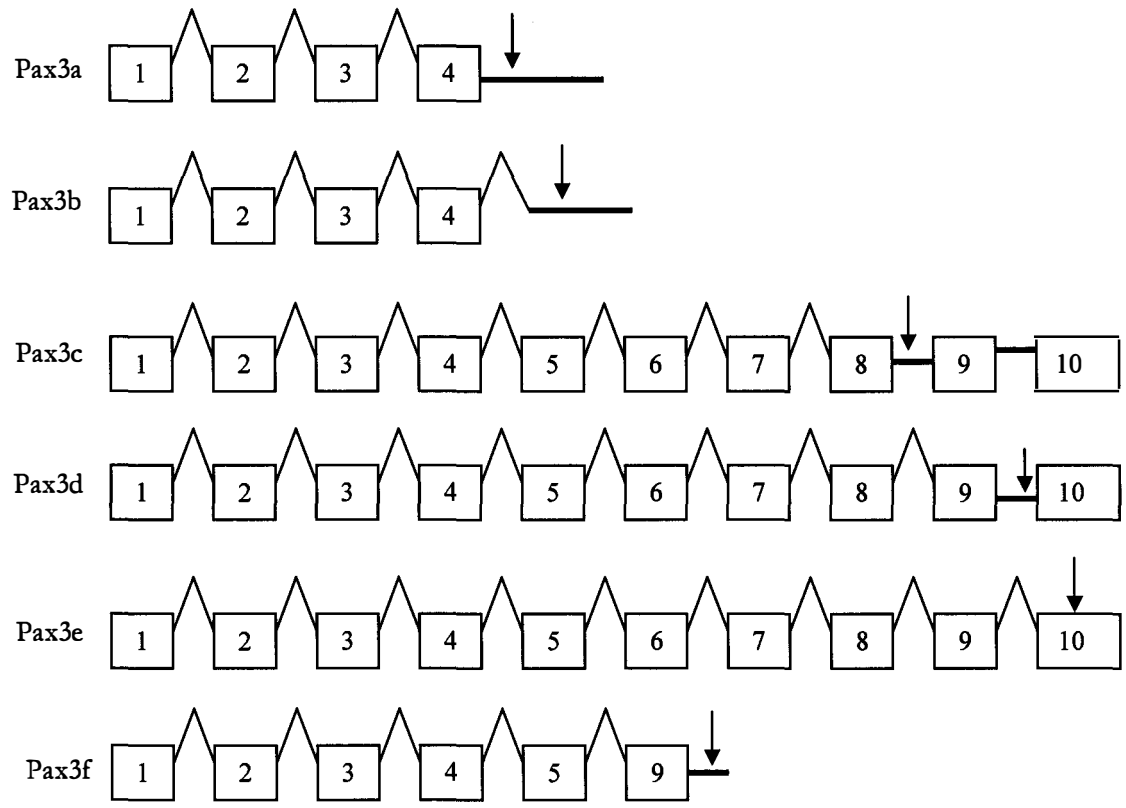

Figure 2.15. **Alternate transcripts of *PAX3* produced by alternate splicing.**

An arrow for each transcript indicates the predicted locations of translation termination. ***Pax3a and Pax3b)*** These transcripts lack the entire homeobox and 3' end (Tsukamoto et al., 1994). ***Pax3c)*** Transcript containing 8 exons and a stop codon 5 bp into intron 8 (Goulding et al., 1991). ***Pax3d)*** Transcript contains exon 9 spliced directly onto 3' end of exon 8 (Barber et al., 1999). ***Paxe)*** transcript containing 10 exons Barber et al., 1999). ***Pax3f)*** transcript found in murine cDNA that contains exon 9 directly spliced to the 3' end of exon 5 Barber et al., 1999).

Alternate transcripts are likely to encode proteins with different binding and transactivation activities therefore having an important effect on the functional role of the gene (Underhill & Gros, 1997; Fortin *et al.*, 1998) Generation of differing transcripts of *PAX3/Pax3* is accomplished by post-transcriptional pre-mRNA splicing and central to this research was the identification and analysis of constitutive and cryptic splice sites that generate alternate *PAX3/Pax3* transcripts found expressed in various tissues. Therefore, an intricate understanding of splice site consensus sequences, splice site selection and splicing machinery involved in pre-mRNA processing was essential to understand the observed *PAX3/Pax3* transcript expression profiles in CMM, murine embryogenesis and specifically melanogenesis.

2.4.5 Generation of Alternate *PAX3* Transcripts

RNA splicing is dependent on the existence of consensus sequences located at exon/intron boundaries and within the intron itself. Small nuclear ribonucleoproteins (snurps) and splicing factors bind to consensus sequences leading to assembly of the splicing machinery (sliceosome). Briefly, base pairing of the U1 snurp occurs at the 5' splice site consensus sequence GUA/GU located at the exon/intron border and this signals subsequent events (Mount *et al.*, 1983; Black *et al.*, 1985; Watakabe *et al.*, 1992). The U2 snurp then binds to the branchpoint sequence CTA/GAC/T within the intron causing the adenosine residue to bulge out, forming a lariat structure (Pikielny *et al.*, 1986; Cheng & Abelson, 1987; Konarski & Sharp, 1987; Zhuang *et al.*, 1989). Further splicing factors bind to a polypyrimidine tract (PPT) located within the intron (Green *et al.*, 1991). Finally, snurps U4, U5 and U6 bind to the 3' consensus sequence YAG (Y is a pyrimidine) located at the intron/exon border (Pikielny *et al.*, 1986; Konarski & Sharp, 1987; Cheng & Abelson, 1987) (Figure 2.16A).

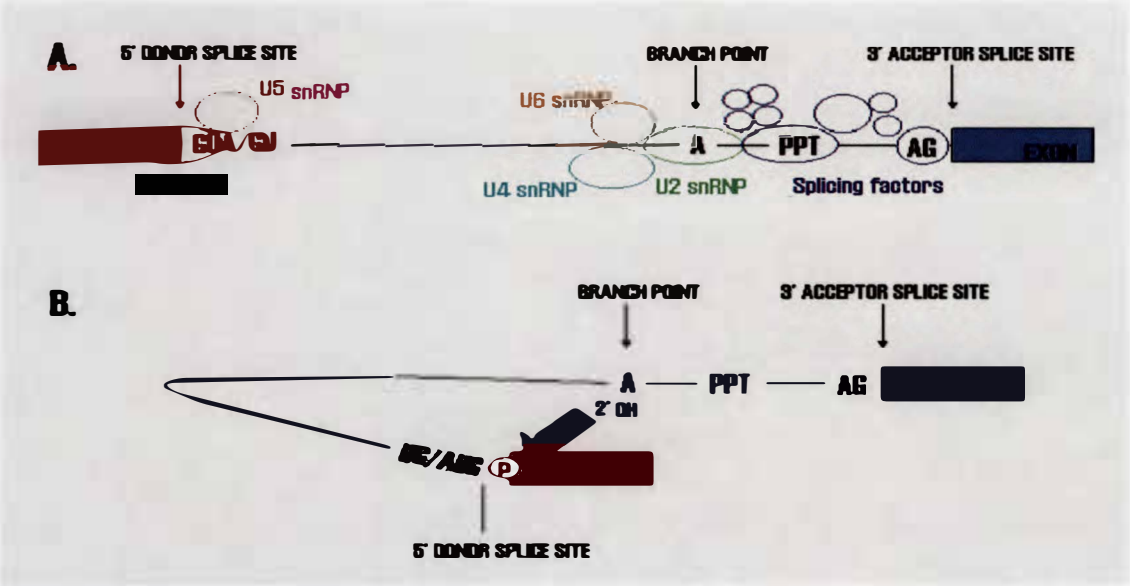

Figure 2.16 **Initial pre-mRNA splicing.**

A.) Assembly of the spliceosome. Exons denoted by boxes, intron indicated as a solid line; consensus sequences are letters along line; snurps and splicing factors are coloured circles.

B.) Step one of intron excision. Assembly of the spliceosome causes conformational change of the gene such that the 2' OH of the bulged out branchpoint adenosine is able to disrupt the phosphodiester bond (P in circle) at the 5' splice site (blue arrow indicates disruption of phosphodiester bond)

The excision process occurs in two steps. Step one occurs as assembly of the spliceosome causes conformational change of the pre-mRNA such that the 2' OH of the branchpoint adenosine is able to disrupt the phosphodiester bond at the 5' splice site, releasing the upstream exon and forming the lariat intron intermediate (Figure 2.16B). Step two proceeds as the hydroxyl group of the cleaved upstream exon attacks the phosphodiester bond at the 3' splice site (Figure 2.16C) resulting in displacement of the lariat intron and ligation of the two exons (Figure 2.16D).

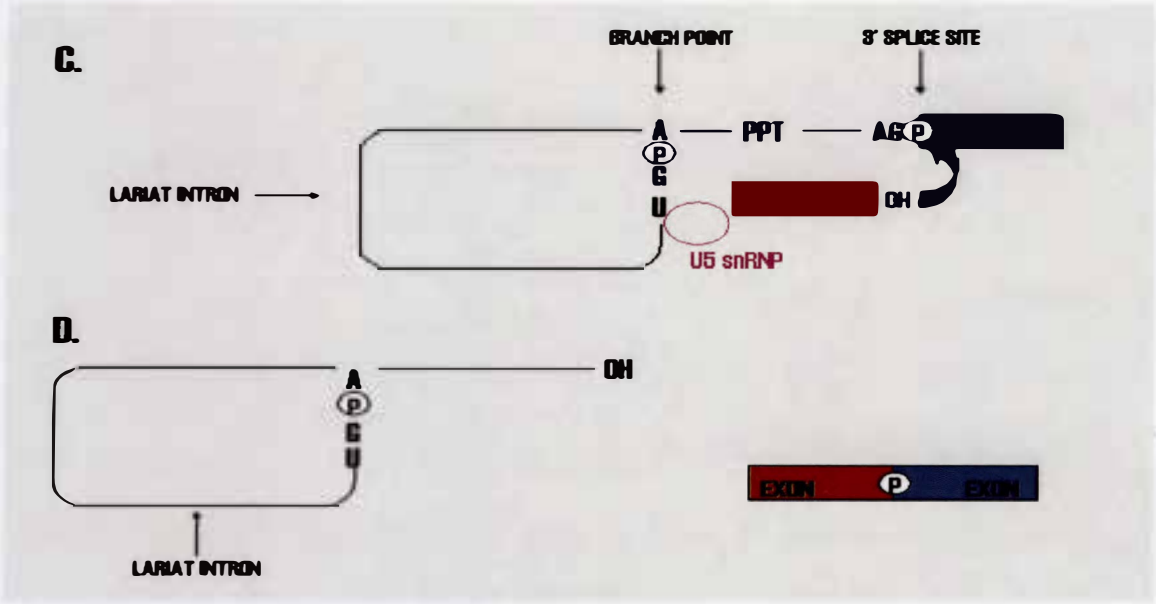

Figure 2.16 (cont). **Final pre-mRNA Splicing.**

C.) Diagram depicting release of upstream exon (red box), formation of lariat intron (loop on left), and disruption of 3' phosphodiester bond (P in circle); blue arrow indicates proximity of OH of cleaved upstream exon to 3' bond. Step two proceeds as the hydroxyl group of the cleaved upstream exon attacks the phosphodiester bond at the 3' splice site resulting in displacement of the lariat intron and ligation of the two exons.

D.) Diagram depicting release of lariat intron (on left) and ligation of exons (coloured boxes).

Normally, RNA processing guarantees that the 5' donor site pairs with the closest 3' acceptor site. Many genes, such as *PAX3,* however, have sequences which are ambiguous, therefore the spliceosome may search for additional splice site choices up or downstream from ambiguous sequences. The function of gene splice site selection is thought linked to production of tissue specific transcripts, although mechanisms for splice site selection are presently unknown.

2.4.6 *PAX3C* and *PAX3D* Transcripts

PAX3C mRNA is transcribed from exons 1-8. The sequence for the 3' end (beginning at exon 8) is shown below and is generated using the stop codon and polyadenylation signals located within intron 8 (Figure 2.17).

AGGTAATGGG ACTCCTGACC AACCACGGTG GGGTACCTCA TCAGCCCCAG ACTGATTACG
CGCTCTCCCC TCTCACCGGG GGTCTGGAAC CTACCACCAC GGTGTCGGCC AGCTGCAGTC
AGAGACTAGA CCATATGAAG AGCTTGGACA GTCTGCCAAC ATCTCAGTCC TACTGTCCAC
CCACCTATAG CACCACAGGC TACAGTATGG ACCCTGTCAC AGGCTACCAA TATGGGCAGT
ATGGACAAAg taagccttgg acttttagg gggcaatttc tcctggaagg gagataaact
caactcttcc ttaagaaagg tgaattagag gcaagattaa gccacacatg ccggtatcaa
ttttttttt tgcaaagcca gctgactgtt ccagcagggg cttccttgtg taattatttt
cttaactgat gtcaacaaca tcttgcggtt attaattgtt gagacgtgaa acctgattgc
cactaggtaa aacacaaggg ttggccaaaa tgaaataatc cctgacatta gaaacacatg
ttcttaatga ggtcagctcc aggatcatat gggggataat cccagggaca caaagttgtg
tcaaacttgt ctcaggaata aaaatattag tctcaagcct ttgatagcac ggtattaaat
atgacattgt cagcctgtag ctgatcttgc ccctgactgt gaattgtccc agcatgacct
aaaaagctgc gtgtgtttcc ttacagGTGC CTTTCATTAT CTCAAGCCAG ATATCGCGTA
AGTGAACTGT CCACTTGGAG CTAAAACTGG CCCTGTTTCT GGTCTTCGCA GCCTAGATAT
GAAGAATCTG CTCTGAAAAC AAAAAAAAAT TACCCTTTTG TTGGGGGGGG TGGGGCAGTG
GTCCCAATAG GAGACAAAGG AGAGTGATTG ATTTTCTTCC TCCAATAGTT GGTTTCAAAT
CCTTTTGAAC ACGTTCGACA AAAGCAGTGG AGAAGAGGAA GACCTGGAGC AATAAA

Figure 2.17. **Differing generation of the *PAX3C* and *PAX3D* transcripts.**

Shown is the genomic sequence of *PAX3*, from exon 8. Exons 8 and 9 are denoted by large case letters while the intronic region is denoted by small case. In generation of the *PAX3C* pre-mRNA, splicing machinery recognises a signal for cleavage and adenylation located within the intronic region (indicated in red). In generation of the *PAX3D* pre-mRNA transcript, splicing machinery ignores the first signal for cleavage and polyadenylation used for *PAX3C* (in red) and continues transcription until the signal for cleavage and adenylation at the sequences indicated by pink lettering. This longer pre-mRNA will then be spliced at 5' and 3' consensus donor/acceptor sites (indicated in blue) utilising the branchpoint sequence and polypyrimidine tract indicated by green and orange lettering, respectively.

PAX3D mRNA is transcribed from exons 1-9 and has been found highly expressed in CMM, yet not expressed in normal skin (Barr *et al.*, 1999; Scholl *et al.*, 2000). The donor site for intron 8 is located 11 nucleotides upstream of the *PAX3*C stop codon with intron 8 branchpoint, polypyrimidine tract and acceptor site located downstream. In generation of the *PAX3D* transcript, splicing machinery ignores the first signal for cleavage and polyadenylation used for *PAX3C* and instead continues transcription producing a longer pre-mRNA that will be spliced at alternative donor/acceptor sites. It is interesting to note that the *PAX3D* splice sites are

considered weak due to poor matching of the 5' sequence (Nelson & Green, 1990; Zamore *et al.,* 1992) and a polypyrimidine tract that extends only 7 nucleotides (Smith *et al.*, 1993). Normally, weak splice elements such as these are ignored by the splicing machinery, however they may be used over stronger elements in the presence of an exon splice enhancer (ESE) (Lam & Hertel, 2002). Exon nine of *PAX3*, however, is not purine rich and cannot be considered as having an ESE. *PAX3C* and *PAX3D* splice variants were therefore further investigated in this study.

The encoded PAX3C and PAX3D transcriptional proteins vary only in the length and composition of their transactivation domains present within the alternate C' ends of the proteins. The amino acid encoded by the PAX3C C-termini is KPWTF while the amino acid encoded by the PAX3D C-terminal is AFHYLKPDIA (Figure 2.18 and Figure 2.19).

```
  1 mttlagavpr mmrpgpgqny prsgfplevs tplgqgrvnq lggvfingrp lpnhirhkiv
 61 emahhgirpc visrqlrvsh gcvskilcry qetgsirpga iggskpkqvt tpdvekkiee
121 ykrenpgmfs weirdkllkd avcdrntvps vssisrilrs kfgkgeeeea dlerkeaees
181 ekkakhsidg ilserasapq sdegsdidse pdlplkrkqr rsrttftaeq leelerafer
241 thypdiytre elaqraklte arvqvwfsnr rarwrkqaga nqlmafnhli pggfpptamp
301 tlptyqlset syqptsipqa vsdpsstvhr pqplppstvh qstipsnpds ssayclpstr
361 hgfssytdsf vppsgpsnpm nptignglsp qvmglltnhg gvphqpqtdy alspltggle
421 ptttvsascs qrldhmksld slptsqsycp ptysttgysm dpvtgyqygq ygqskpwtf
```

Figure 2.18. **The PAX3C Protein.**

Shown is amino acid sequence of the PAX3C protein with the alternate C' end indicated in red.

```
  1 mttlagavpr mmrpgpgqny prsgfplevs tplgqgrvnq lggvfingrp lpnhirhkiv
 61 emahhgirpc visrqlrvsh gcvskilcry qetgsirpga iggskpkqvt tpdvekkiee
121 ykrenpgmfs weirdkllkd avcdrntvps vssisrilrs kfgkgeeeea dlerkeaees
181 ekkakhsidg ilserasapq sdegsdidse pdlplkrkqr rsrttftaeq leelerafer
241 thypdiytre elaqraklte arvqvwfsnr rarwrkqaga nqlmafnhli pggfpptamp
301 tlptyqlset syqptsipqa vsdpsstvhr pqplppstvh qstipsnpds ssayclpstr
361 hgfssytdsf vppsgpsnpm nptignglsp qvmglltnhg gvphqpqtdy alspltggle
421 ptttvsascs qrldhmksld slptsqsycp ptysttgysm dpvtgyqygq ygqsafhylk
481 pdia
```

Figure 2.19. **The PAX3D Protein.**

Shown is amino acid sequence of the PAX3D protein with the alternate C' end indicated in red.

Analysis of the generation of varying PAX3/Pax3 isoforms was a focal point of this study as the predominant isoform expressed in CMM is the PAX3D isoform (Barr *et al.,* 1999). This being the case, it was thought curious that mRNA transcription in CMM utilises the weaker splice elements continuously over the constitutive splice sites. Therefore, the expression of *Pax3d* has been examined during stages of murine embryogenesis and melanogenesis to understand its possible significance in CMM.

2.4.7 *PAX3* and CMM

Results from previous studies have raised the possibility that *PAX3* regulated developmental programs may be at work in CMM cells and that neoplastic melanocytic cells may be functioning in a manner similar to pluripotent embryonic neural crest cells. The first indication that *PAX3* regulated developmental programs may be involved in the progression of CMM is the strong expression of *PAX3* in CMM cells, whereas little or no expression is observed in normal adult melanocytes (Scholl *et al.,* 2001). Although mutations in *PAX* genes are associated with many forms of cancer (Bennicelli *et al.*, 1996; Iida *et al.*, 1996; Kroll *et al.*, 2000), this is not the case in CMM, where causative mutations are at gene loci other than those of the *PAX* gene family. However, of note is the increased expression and aberrant expression profile of *PAX3* transcripts in CMM.

Aberrant expression of *PAX3* in CMM was first detected by Barr *et al.* (1999), who reasoned that expression of *PAX* genes in neural crest progenitors might be repeated in tumour cells arising from the same lineage. Using RNAse protection assays to quantify *PAX3* expression in both cell lines and tumour tissue from CMM, they found that levels of *PAX3* were "notably high". They also observed the predominant transcript found expressed in CMM was the *PAX3D* transcript, although *PAX3C* is also

expressed. These findings raised the possibility that the phenotype of CMM may be related to increased aberrant expression of *PAX3D*.

No published studies (to date) have identified expression of *PAX3D/Pax3d* or their encoded proteins in normal melanocytic tissues; therefore, it is not yet known whether this protein has a particular role in transcriptional regulation of the melanoblast. Differences in the structure of the C-terminal region of PAX3/Pax3 isoforms influence protein-protein interactions of transactivational domains and thus transcriptional activation of downstream targets bound by PAX3/Pax3 via its paired DNA binding domain. Therefore, a primary aim of this research was to investigate *PAX3C/PAX3D* and *Pax3c/Pax3d* expression profiles in CMM and murine tissues hoping to gain insight into a possible role for PAX3C/Pax3c and PAX3D/Pax3d proteins.

2.4.8 PAX3 Mediated Transcriptional Activation

Transcription factors such as PAX3/Pax3 require two functional domains within their protein structure to assist in transcription of target genes into RNA. Firstly, a DNA binding domain must recognise and bind specific regulatory sequences within promotor/enhancer regions of the target gene DNA; secondly, the transactivating domain of the transcription factor protein associates with basal transcriptional machinery and influences gene expression. Furthermore, the transactivation domain functions to recruit components of the pre-initiation complex, other transcription factors or transcriptional machinery to the area of the gene promotor, facilitating the formation of the protein-DNA complex which signals RNA polymerase to begin initiation and transcription of the gene (Ptashne, 1988; Mitchell & Tijan, 1989). The PAX3C/PAX3D and Pax3c/Pax3d isoforms analysed in this study vary only in the length and composition of their transactivation domains. The alternate C' end may confer different transcriptional ability to PAX3 binding domains or they may be associated with varying DNA target selection.

2.4.9 PAX3 DNA Binding Domains

PAX3/Pax3 has two DNA binding domains within its structure, a paired domain (PD) and a paired type homeodomain (HD) (Figure 2.20).

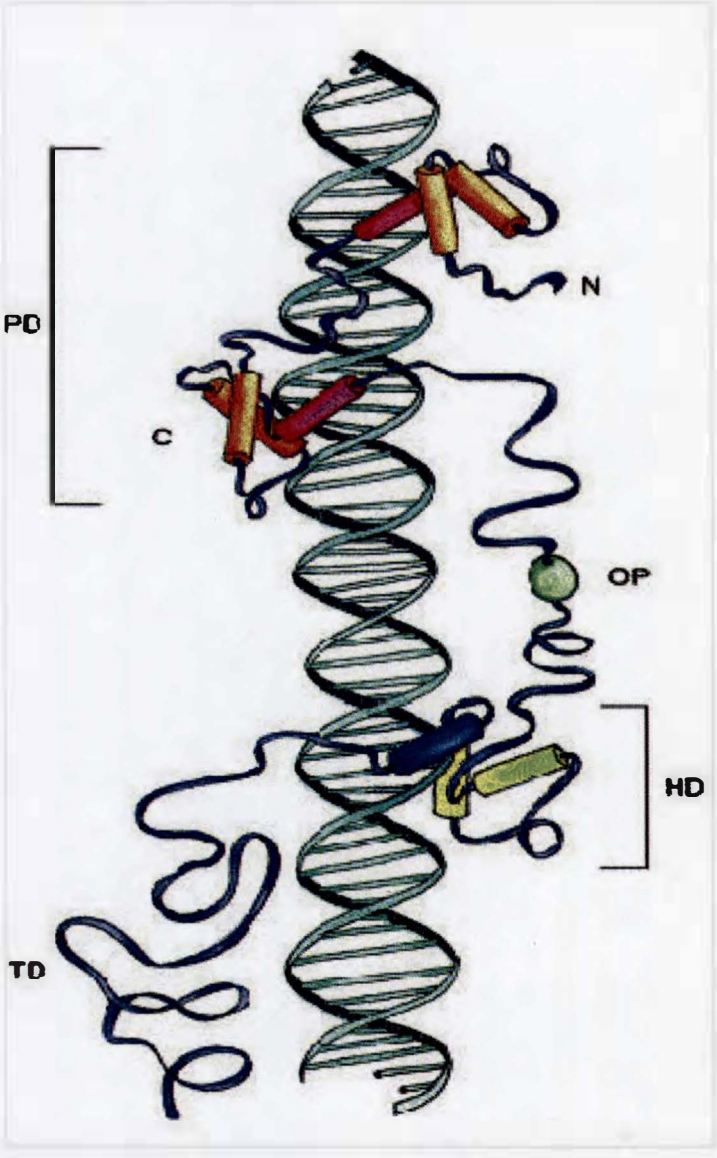

Figure 2.20. **Molecular structure of the Pax3 protein.**
Pax3 protein contains a paired domain (PD) consisting of PAI (N) and RED(C) subdomains, each of which is composed of three helices in a helix-turn-helix motif. The third helix of each subdomain is shown in contact with the target DNA. The Pax3 protein also contains an octapeptide (OP) followed by a homeodomain (HD) containing an additional helix-turn-helix DNA binding domain. Finally, the transactivation domain (TD) is indicated.

Structural analysis has revealed that the PD consists of two independent helix-turn-helix subdomains, an N-terminal (PAI) and a C-terminal (RED) (Xu *et al.,* 1995). Mutations in the PAI subdomain result in a loss of both PD and HD binding (Underhill *et al.,* 1995; Fortin *et al.,* 1997; Underhill & Gros, 1997) perhaps due to loss of crucial major and minor groove DNA contacts (Xu *et al.,* 1995). The RED subdomain has been shown to be dispensable for binding in deletion studies (Wilson *et al.,* 1993; Miskiewicz *et al.,* 1996); however, more recent studies detailing distinct PD C-terminal subdomain sequence preferences amongst Pax family members suggests that this subdomain may be used for discrimination of DNA targets (Vogan & Gros, 1997).

The 61 amino acid HD conforms to a helix-turn-helix motif (Wilson *et al.,* 1995) and is able to bind DNA both monomerically recognising an ATTA motif and as a dimer utilising a palindromic motif of 5' TAAT$(N)_{2-3}$ATTA 3' (Wilson *et al.,* 1993). It is suggested that binding of the initial HD cause DNA distortions thus preparing a template for further binding by the second HD. Because the binding affinity of the HD as a monomer is considered weak, homodimerisation of the HD is thought to enable recognition of target sequences long enough to ensure further binding specificity and affinity (Wilson *et al.,* 1995).

Alone, the 128 amino acid PD recognises a GTCAC binding motif (Epstein *et al.,* 1993; Chalepakis & Gruss, 1995). However, when binding in conjunction with the homeodomain, the paired domain recognises either a GTTCC motif (Chalepakis *et al.,* 1994) or a GTTAT motif (Phelan & Loeken, 1998) located downstream of the consensus homeodomain motif of ATTA.

Paired and homeo- DNA binding domains have been seen expressed separately in *Caenorhabditis elegans*, suggesting functional independence (Chisholm & Horvitz, 1995; Zhang & Emmons, 1995). However, mutations of the PD in the human PAX3 protein such as those seen in Waardenburg

syndrome have been shown to affect or abrogate DNA binding by the HD, signifying that the two domains function interdependently (Baldwin *et al.*, 1995; Fortin *et al.,* 1997). Moreover, *in vitro* binding studies have illustrated cooperative interactions between the PD and the HD of PAX3 (Jun & Desplan, 1996; Vogan & Gros, 1997; Underhill & Gros, 1997; Fortin & Gros, 1998).

To further illustrate the complexity involved in PAX3 target gene selection and binding, recent studies have demonstrated that PAX3 interacts with other factors to activate promotor and enhancer regions of downstream target genes. For example, Sox10 and Pax3 synergise to activate the *c-RET* gene enhancer (Lang *et al.,* 2000). Pax3 and Sox10 physically interact with each other through contacts mediated by the PD while at the same time Pax3 binds the *c-RET* enhancer via a PD-DNA protein interaction (Lang & Epstein, 2003). In contrast, SOX10 and PAX3 must bind DNA recognition elements independently in order to synergistically upregulate the *MITF* gene promotor (Bondurand *et al.,* 2000). In this interaction, PAX3 binds DNA utilising the HD (Lang & Epstein, 2003). In summary, it is notable that PAX3 interacts with the *c-RET* enhancer via PD-DNA interactions, while it binds the *MITF* promotor via HD-DNA interactions. This illustrates how alternate PAX3/Pax3 proteins may play different roles to activate different downstream gene targets during development and CMM.

2.4.10 PAX3 Transactivation Domains

It is now generally accepted that transcription factors function through the transactivating region of the protein by interaction with proteins of the basal transcriptional machinery including RNA polymerase II (Ptashe & Gann, 2002). There is strong evidence that the mechanism by which trans-activators function is via "recruitment". The recruitment model of transcriptional activation states that the trans-activation regions of the

transcription factor serve to attract the basal transcription complex to the vicinity of the promotor region of the gene leading to a signal for polymerase II to initiate transcription (Barberis *et al.,* 1995; Gaudreau *et al.,* 1998; Keaveney & Struhl, 1998).

The transactivation domain of PAX3/Pax3 is located within the last 78 COOH-terminal amino acids and is classified as a proline-serine-threonine (PST) activation domain due to the amino acid composition (Chalepakis *et al.,* 1993). COOH-terminal deletion studies of PAX3/Pax3 further support the recruitment model; these studies have shown that deletion of part or the entire COOH transactivation domain of PAX3/Pax3 results in the failure of mutant proteins to tran-sactivate reporter genes (Chalepakis *et al.,* 1994; Bondurand *et al.,* 2000; Cao & Wang, 2000; Pritchard *et al.,* 2002). Similar results were obtained in a study in which the transcriptional competence of Pax2, Pax5 and Pax8 were eliminated via a frameshift mutation in the transactivating region of the protein (Dorfler & Busslinger, 1996).

2.4.11 PAX3 and the Basal Transcriptional Complex

To date there are no studies demonstrating a direct interaction between the transactivating region of PAX3/Pax3 and the basal transcriptional complex. However, Smit *et al* (2000) demonstrated an interaction of Pax3, Sox10 and Brn-2 cofactors with TATA-box-binding protein and p300, two components of the basal transcriptional complex. Cvekl *et al* (1999) also demonstrated protein-protein interactions of the C-terminal-activation domain of Pax6 with the TATA-binding-protein.

2.5 MELANOCYTIC SURVIVAL FACTORS

Since *PAX3* is over-expressed in CMM, an investigation of possible candidate downstream target genes was undertaken. Review of key developmental genes involved in melanogenetic events as well as evidence suggesting *c-KIT* and *MITF* may be probable cofactors or downstream targets of *PAX3* in melanoblast proliferation, migration or differentiation prompted further investigation of their co-expression in this study.

2.5.1 The *c-KIT* Gene

The *c-KIT* gene encodes a receptor tyrosine kinase which, along with its ligand, stem cell factor (SCF), has been shown to play a crucial role in the survival and migration of melanoblasts. Expression patterns of SCF have suggested that c-Kit/SCF mediates migratory or chemotactic processes for *c-Kit* expressing cells.

In the embryo, neural crest cells initially produce SCF, which functions in an autocrine fashion to induce melanogenesis in adjacent *c-Kit* expressing crest cells. Werhle-Haller & Weston (1995) demonstrated soluble SCF functions to disperse *c-Kit*$^+$ melanoblasts along a dorsolateral pathway, whereas membrane bound SCF induces migration from the neural crest to the dermis. Subsequently, SCF is expressed in the mesenchyme of embryonic skin during the period in which *c-Kit*$^+$ melanoblasts migrate from the neural crest toward the dermis (Matsui *et al.*, 1990; Manova & Bachvarova, 1991; Werle-haller & Weston, 1995).

Nishikawa *et al* (1991) and Yoshida *et al* (1996) demonstrated that stages of melanoblast migration and proliferation require *c-Kit* expression. Specifically, entry into and proliferation within the epidermis is dependent upon *c-Kit* expression; this is in contrast to a period just prior to epidermal invasion, when melanoblasts are dormant in the dermis and *c-Kit* negative.

SCF/c-Kit signalling is also required in the development of the hair

follicle pigmentary unit. Before the onset of hair follicle morphogenesis, in perinatal mice, *c-Kit* expressing melanoblasts are seen migrating into the developing hair placode where widespread epithelial SCF expression exists (Peters *et al.*, 2002). Thus it is apparent that *c-Kit* expression plays an important role in the temporal regulation of melanoblast proliferation and migration.

2.5.2 Alterations of c-Kit Signaling Pathways

Murine transgenic studies and mutational analyses of *c-Kit* have shown that this gene is crucial for melanocyte development since this gene affects the functional role of the encoded tyrosine receptor (Nishikawa, 1991; Galli *et al.*, 1993; Grabbe *et al.*, 1994; Broudy, 1997). In humans, mutations in *c-KIT* result in piebaldism, a syndrome in which affected individuals possess a white forelock and absence of pigmentation of the medial portion of the forehead, eyebrows and chin, chest, abdomen, and extremities. This mutation in *c-KIT* leads to substitution of leucine for phenylalanine at codon 584 within the tyrosine kinase domain of the c-KIT receptor (Giebel & Spritz, 1991).

2.5.3 *c-KIT* and CMM

Progression of CMM has been correlated to a loss of *c-KIT* gene expression. Increasing loss of the c-KIT receptor has been demonstrated during the invasive and metastatic phases of CMM and a majority of CMM cell lines lack detectable levels of *c-KIT* expression (Lassam *et al.,* 1992; Natali *et al.,* 1992; Zakut *et al.,* 1993). In a study by Huang *et al* (1996) transfection of the *c-Kit* gene into c-Kit negative CMM cells was shown to inhibit tumour growth and metastasis in nude mice.

There are several grounds to investigate influence of *PAX3* on *c-KIT* expression, the most notable being that the promotor region of the *c-KIT* gene possesses several potential DNA binding sites for the paired and

homeodomain regions of PAX3 (Figure 2.21). No investigation of *Pax3* interactions with *c-Kit* have been undertaken (to date) to discern repercussions of aberrant *Pax3d* expression on *c-Kit* expression in CMM.

```
1     gagggatgtcttattagtttatcagaatgcatagggaaagctcatctttcttggagtagg
61    tcttccaataagtgttcaagccctgggtcttccctcactacaataataaacatacctgct
121   ctaccctcctcacaaagctgttatcgtgagcatgaaaagacgagtcgctgtggggaagaa
181   ctattaacccctatacagatactgttgttgctttccgttcaaggatccaccatgagactg
241   tgggtaaggcactttctgggcagtgaaatcgggcttaagagaatcattgtacttttattt
301   tgctcctgggaccggcaagggcagttaagagccctagccctaaaactgtcgtctgttaca
361   gaggcagagaaatcattactggggttggcagcgttgggggagggggaaaacgtgtatg
421   aaaacctgggctcccagagcaaacttcgccacgcgccctccatcgcccctgtctccacac
481   aagtcccggcaggggcttcttgggcggaggccacgccgaccaataggaacccactgtgtt
541   cctacaggttacgaagcaggtggagaaattgagcagaaacaattagcgaaaccgggctca
601   gcctttaccgcggtgccaggagctcctaacaggcctggaggggaatgtcggggctcaatt
661   tcctaacgctcccctccccatccccatgccacctccacgagcagcggcgtccagcctcct
721   cccgcccgaacgtgctcgaggggcgggcagtcgacctttattgtctggggagcacctggc
781   aggtggcgggcccgtgccctaacgtgtgcgtggtgcccagcttcacaaagcgagcgggca
841   gcacctccttggtccgggaacgcctcagcctggccgtccacatcccaggggtggaaaggt
901   ggagagagaaaggggctccggagtcaagagcggggagagagggcgcgcgccctcctcctc
961   ccggcgggcacagccccccggcattaacacgtcgaaagagcaggggccagacgccgccgg
1021  gaagaagcgagacccgggcgggcgcgagggaggggaggcgaggaggggcgtggccggcgc
1081  gcagagggagggcgctgggaggaggggctgctgctcgccgctcgcggctctgggggctcg
1141  gctttgccgcgctcgctgcacttgggcgagagctggaacgtggaccagagctcggatccc
1201  atcgcagctaccgcgatgagaggcgctcgcggcgcctgggattttctctgcgttctgctc
1261  ctactgcttcgcgtccagacaggtgggacacgcggctggcaccccg
```

Figure 2.21. **Promotor region of *c-KIT*.**
Potential PAX3 binding motifs indicated in red.

Potential PAX3 binding sites, as well as lack of previous co-expression studies, overlapping temporal expression in embryogenesis and similarity of functional roles in melanocytic development prompted investigation into possible co-relations between *c-Kit* and *Pax3* expression in this study. Furthermore, *c-Kit* expression is downregulated in CMM (Huang *et al.*, 1996 and 1998) while Pax3 is a known gene repressor (Chalepakis *et al.*, 1994). Therefore, we hypothesised that overexpression of *PAX3* in CMM may inhibit *c-KIT* expression, therefore a negative correlation between these genes was assessed in melanogenesis.

2.5.4 The *MITF* Gene

Micropthalmia-associated transcription factor (MITF) is a basic helix-loop-helix transcription factor known to function both in the early survival of melanoblasts (Hornyak *et al.,* 2001) and subsequently in regulation of genes required for synthesis of enzymes involved in melanogenesis (Bentley *et al.,* 1994; Ganss *et al.,* 1994; Yasumoto *et al.,* 1994; Tachibana *et al.,* 1996). Furthermore, MITF regulates expression of a melanocortin-1 receptor, a receptor involved in determining relative proportions of pheomelanin and eumelanin production (Aoki & Moro, 2002).

MITF expression is one of the earliest markers of melanocyte differentiation and crucial for melanoblast survival during migration from the neural crest (Opdecamp *et al.,* 1997). Studies of strict temporal regulation of MITF activity and expression levels during melanocytic development suggest that *MITF* expression cooperates with many factors working coordinately to regulate differentiation of the neural crest cell through melanoblast stages on through further differentiation until capable of melanin production (Beerman *et al.,* 1992; Ferguuson & Kidson, 1997; Nakayama *et al.,* 1997; Opdecamp *et al.,* 1997).

2.5.5 *MITF* Mutations

Mutations in the *MITF* gene result in Waardenburg Syndrome type IIa (Tassabehji *et al.*, 1994), Tietz Syndrome (a hypopigmentation albinism with sensorineural deafness) (Smith *et al.,* 2000) or ocular albinism with sensorineural deafness (Morell *et al.,* 1997). Phenotypes of persons in these affected families reveal severe congenital sensorineural hearing loss, hypopigmentation of follicular melanocytes causing blonde hair to turn grey during adolescence, pale skin with numerous orange freckles and blue eyes lacking retinal pigmentation. Similarly, in mice, mutations in *Mitf* lead to loss of pigmentation in the eye, inner ear, and skin, and to reduced eye size and

early-onset deafness (Hodgkinson *et al.,* 1993; Nakayama *et al.,* 1998).

MITF, like *PAX3*, produces alternate isoforms which are constitutively expressed in various tissues. The neural crest-derived melanocyte specific isoform is MITF-M (Yajima *et al.,* 1999), the predominant isoform in heart and kidney is MITF-H (Steingrimsson *et al.,* 1994) and in retinal pigmented epithelial cells it is MITF-A (Amae *et al.,* 1998). Both the antibodies used for immunohistochemical staining and primers designed to amplify RT-PCR products in this study were specific for the melanocyte-specific isoform of protein or transcript, respectively.

2.5.6 *MITF* and *PAX3*

Pax3 has been shown to bind to the promoter and transactivate the *Mitf-m* gene (Watanabe *et al.,* 1998). As stated previously, Pax3, along with Sox10 have been implicated as having important synergistic effects on upregulation of *Mitf-m* expression levels (Bondurand *et al.,* 2000; Potterf *et al.,* 2000). Mutations in *PAX3* result in generation of protein transcription factors unable to regulate transcription of *MITF-M*; the phenotype of Waardenburg Syndrome type I, characterised by pigmentary disorders and hearing loss, reflects this. Similarly, *Splotch* mice bearing *Pax3* mutations (leading to a nonfunctional Pax3 protein unable to bind to *Mitf-m*) demonstrates the dependence of *Mitf-m* on functional Pax3 transcription factors for normal expression. The activation of *Mitf* by Pax3 initiates a cascade of genes within a genetic hierarchy that brings about differentiation of the melanocytic cell.

2.5.7 *MITF* and *c-KIT*

There is some controversy over the rank of both *c-KIT* and *MITF* in the genetic hierarchy of melanocytic specific genes. Evidence supports a feedback loop in which *MITF* regulates *c-KIT* expression/activity and *c-KIT* signaling regulates *MITF* expression/activity. The *c-KIT* promoter contains an E-box

motif for MITF binding and *in vitro* analysis has shown that MITF is able to activate *c-KIT* transcription in cultured cells (Tsujimura *et al.*, 1996). Moreover, Opdecamp (1997) has demonstrated that MITF is required for upregulation of *c-KIT* expression.

Further studies confirm a feedback loop since c-KIT signaling increases MITF phosphorylation leading to stimulation of MITF transcriptional activity (Hemesath *et al.*, 1998; Price *et al.*, 1998; Wu *et al.*, 2000; Xu *et al.*, 2000). Finally, mice doubly heterozygous for mutations in both *c-Kit* and *Mitf* have a more severe phenotype than mice heterozygous for either mutation alone (Beechey & Harrison, 1994). These and previously mentioned studies suggest an interesting interplay between *Pax3*, *c-Kit* and *Mitf* expression and experiments in this study aim to confirm whether co-relations in their gene expression do exist in murine embryogenesis and melanogenesis.

2.6 CONCLUSION OF LITERATURE REVIEW

It is not unlikely that developmental genetic programs regulating cell properties may be reactivated in the neoplastic cell. The ability of the melanoblast to migrate, proliferate and differentiate is vital, whether in embryogenesis or postnatal re-pigmentation processes. We hypothesise that the particular properties of the melanoblastic cell that enable it to undergo these events in both embryonic and postnatal tissue may be conferred through expression of *PAX3*, a gene strongly associated with development of melanocytic precursor cells. Thus the high, aberrant expression levels of *PAX3*, consistently observed in CMM, may be directly linked to the progression of CMM.

Clinical research and animal studies have shown that tumourigenesis is an event reflecting the properties of both host tissues and the neoplastic cell itself. The ability of a cancer cell to take advantage of genetic programs set in place specifically for normal cellular events such as cell proliferation,

migration and signaling could give the neoplastic cell a tremendous selective advantage and therefore enhance both its chance of survival and its ability to evade body defenses. In this study, experimentation sought to provide information regarding a possible role for *PAX3* in the tumourigenesis of CMM, in light of important genetic events its encoded transcription factors regulate during normal melanocyte development.

3

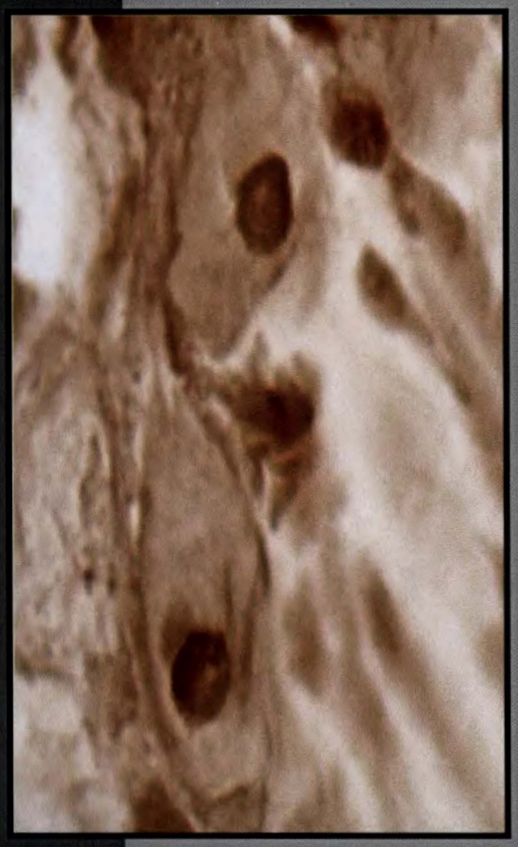

HYPOTHESES & RESEARCH AIMS

3.1 HYPOTHESES

- The *PAX3D* transcription factor (predominantly expressed in CMM) is not a cryptic splice form, but rather, is utilised during the development of normal melanocytes.
- Aberrant expression of *PAX3D* contributes to the progression of CMM through transactivation of *MITF-M* and/or repression of *c-KIT* genes.

3.2 RESEARCH AIMS

- Compare relative mRNA expression of *PAX3C/PAX3D* in cutaneous melanoma biopsies using mRNA isolation, RT-PCR and nucleic acid sequencing.
- Investigate and compare relative mRNA expression of *Pax3c/Pax3d* at key stages of murine embryonic development using mRNA isolation, RT-PCR and nucleic acid sequencing.
- Investigate and compare relative mRNA expression of *Pax3c/Pax3d* in an *in vivo* model of murine melanogenesis using mRNA isolation, RT-PCR and nucleic acid sequencing.
- Assess spatial and temporal Pax3c/Pax3d protein expression in developing murine embryos at key stages of melanocytic development by immunohistochemistry.

4

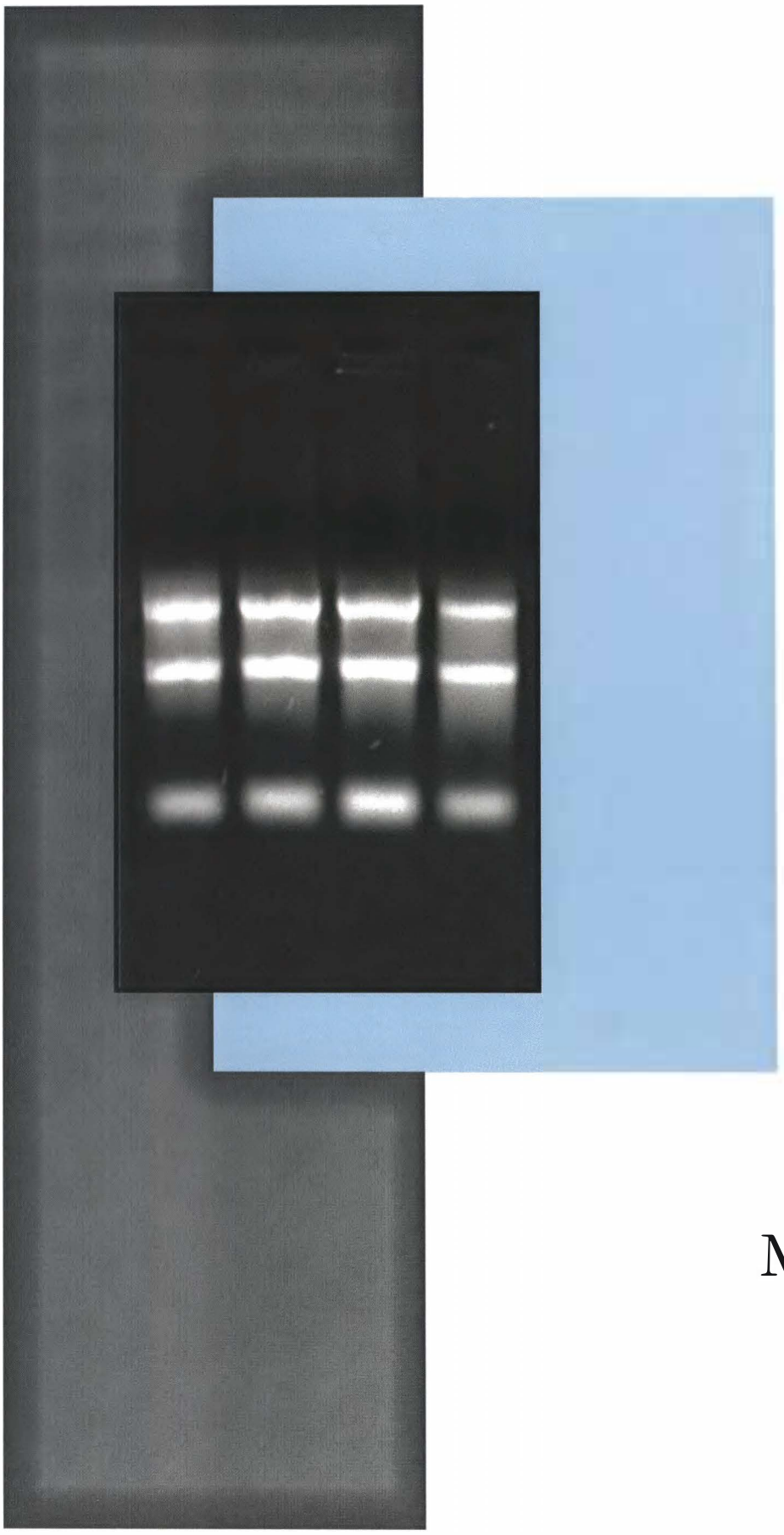

METHODS

4.1 *PAX3* TRANSCRIPT ANALYSIS IN CMM

4.1.1 Human Tissue Collection

Five metastatic CMM excised from regional lymph nodes were acquired through Clinical Professor Dominic Spagnolo of PathCentre (Perth, WA). Following patient consent, samples were snap-frozen in liquid nitrogen immediately following surgical excision and stored at -70° until use, according to PathCentre protocol for acquisition and storage of tissue samples for research use. Subsequent collaboration with surgeons allowed samples to be retrieved from tissue archives; ethical clearance for use of the human tissues was acquired through the Human Ethics Committee of Edith Cowan University (project #02-68).

4.1.2 Isolation of Total RNA

Total RNA was isolated from samples using TriZol Reagent (Invitrogen). Tissues were homogenised in 1mL of TriZol per 50-100 mg of tissue using a glass-col homogeniser. Homogenised samples were incubated at 15°-30° for 5 minutes. 0.2mL of chloroform was added followed by 3 minutes incubation at 15°-30°. Samples were centrifuged at 12000rpm for 15 minutes at 2°-8° to isolate the RNA into the aqueous phase of the solution. RNA was precipitated from the aqueous phase by addition of 0.5 mL of isopropyl alcohol, incubation for 10 minutes at 15°-30° and centrifuged at 12000rpm at 2°-8° for 10 minutes. RNA precipitates were washed with 1 mL 75% ethanol, centrifuged at 7500rpm at 2°-8° for 5 minutes and briefly air-dried for 10 minutes. RNA was redissolved in 0.4 mL RNase free water and incubated at 60° for 10 minutes. Integrity of the total RNA extracted from the samples was assessed by 1% agarose-gel electrophoresis and ethidium bromide stained visualisation of the gel under UV light..

4.1.3 PolyA$^+$ mRNA Purification

An Oligotex mRNA kit (Qiagen) was utilised according to the manufacturer's instructions. Briefly, mRNA, containing polyadenylated tails was isolated from total RNA by hybridisation of the polyA$^+$ tail to a dT oligomer coupled to a solid-phase matrix. Following separation of the mRNA:Oligotex complex, poly A$^+$ mRNA was eluted from the matrix using 120μL 5mM Tris-Cl (pH 7.5) and stored at -70°C until further use.

4.1.4 RT-PCR Analysis of *PAX3C/PAX3D* Transcripts

Negative controls for each polyA$^+$ sample were performed by elimination of the reverse transcription portion of reverse transcription-polymerase chain reaction (RT-PCR). RT-PCR products were assessed by 2% agarose-gel electrophoresis and ethidium bromide staining. PolyA$^+$ mRNA was converted to cDNA using the One-Step RT-PCR Kit (Qiagen) according to the following protocols:

Component	Volume
RNase free water	7.0μL
5x Qiagen OneStep RT-PCR Buffer	5.0μL
dNTP Mix (containing 10mM of each dNTP)	1.0μL
5x Q solution (Qiagen)	5.0μL
Forward Primer (0.6μM)	1.5μL
Reverse Primer (0.6μM)	1.5μL
Qiagen One-Step RT-PCR Enzyme Mix	1.0μL
Template mRNA (1 pg-2μg/reaction)	3.0μL

The following primers were designed prior to manufacture by Geneworks Pty Ltd. for RT-PCR of *PAX3C* and *PAX3D* from CMM samples:

- *PAX3C* (FWD) 5' gcaatttctcctggaaggga 3'
- *PAX3C* (REV) 5' attgataccggcatgtgtgg 3'
- *PAX3D* (FWD) 5' tgggcagtatggacaaagtg 3'
- *PAX3D* (REV) 5' ggctgcgaagaccagaaac 3'

RT-PCR cycling conditions were as follows:

Cycle	Time	Temperature
Reverse transcription	30 min	50°C
Initial PCR activation step	15min	95°C
3-step cycling:		
Denaturation	30 sec	94°C
Annealing	15 sec	56°C
Extension	15 sec	72°C
Number of cycles: 40		
Final extension	10min	72°C

Negative controls eliminating template mRNA were included in each RT-PCR assay. RT-PCR products were analysed by 2% agarose-gel electrophoresis and ethidium bromide staining relative to pUC19 DNA ladder. Gels were run at 110 mV for 30 minutes in TAE buffer.

4.1.5 Sequencing Reactions

Using the MinElute PCR Purification Kit (Qiagen) according to manufacturer's instructions, 200mL Buffer PB was added to 40μL of PCR sample and loaded into a MinElute spin-column prior to centrifugation at 13000 rpm for 1 minute. Following DNA binding to the spin-column matrix, flow-through was discarded prior to addition of 750 mL Buffer PE to the spin-column and further centrifugation at 13000 rpm for 1 minute. Flow-through was again discarded prior to centrifugation for an additional 1 minute. DNA was eluted by addition of 10 mL Buffer EB to centre of MinElute membrane, stood at room temperature for 1 minute prior to centrifugation at 13000 rpm for 1 minute. This purification method removed all PCR reagents and DNA fragments under 70 base-pairs long. The ABI PRISM BigDye Terminator Cycle Sequencing Ready Reaction Kit (PE Biosystems) was used to prepare and analyse sequence amplicons by the dideoxy sequencing method. Sequencing reactions were run using the following protocol:

DNA (approx. 100bp)	4μL (10ng)
Primer (Fwd or Rev)	1μL (50 ng)
Big Dye Terminator Mix	4μL
ddH_20	1μL

Sequencing cycling conditions were as follows:

96° C------ 10 sec.

50° C------ 5 sec.

60° C------ 4 min. Repeat for 25 cycles.

For removal of excess dye terminators prior to sequencing, ethanol/sodium acetate precipitation of DNA was done by addition of 2.0 mL 3M sodium acetate (pH 4.6) and 50mL 95% ethanol to each completed sequencing reaction. Tubes were shaken, left at room temperature for 5 minutes then centrifuged at 13000 rpm for 45 minutes. Supernatant was discarded before addition of 150mL 70% ethanol and centrifugation at 13000 rpm for 10 minutes. Supernatant was again discarded and 150 µL of 70% ethanol added to each pellet prior to centrifugation at 13000 rpm for 10 minutes. Supernatants were discarded and pellets dried at 65°C. Products were sequenced by the DNA sequencing services at Royal Perth Hospital (Perth) using an ABI Prism 3730 48 capillary sequencer; sequences were aligned with known sequences in GenBank using the multialign tool in the Angis computer program, available on GenBank.

4.2 MURINE EMBRYO TRANSCRIPT ANALYSIS

4.2.1 Collection of murine embryonic samples

Wild-type ARC outbred mice were housed in community cages at Edith Cowan University, fed water and murine chow *ad libitum* and kept in 12 hour light and dark cycles. Pregnant female mice and embryos were euthanised by CO_2 overdose in a sealed container. Pregnancies and embryonic ages were timed by sight of the vaginal plug and embryos were surgically removed at embryonic day 11 (E11), E12.5, E15 and E20.

Whole embryos were used to analyse *Pax3* transcripts at E11, the time of migration of melanoblasts from neural crest to the dermis. At E12.5, there is synchronous migration of melanoblasts from the dermis to the epidermis. Skin could not be dissected from the embryo at this time, however, to analyse Pax3 transcripts, segregation of head from body of E12.5 embryos was used to analyse *Pax3* transcripts of the developing limb, trunk and diaphragm musculature as compared to *Pax3* transcripts of the brain. Tissues isolated

from E15 and E20 embryos included whole skin, body (less skin) and head (less skin). Skin was segregated, in particular, to examine *Pax3* transcripts during the E15 stage of melanoblast migration into the developing hair placode and the E20 stage of differentiation of the melanoblast toward the melanin producing melanocyte. All murine embryonic tissue specimens for mRNA analyses were immediately snap-frozen in liquid nitrogen following excision and kept frozen at -70° until use. Ethical clearance for use of the animals was acquired through the Animal Ethics Committee of Edith Cowan University (project # 03-A8).

4.2.2 Total RNA and polyA$^+$ mRNA Isolation

Total RNA isolation and polyA$^+$ mRNA purification from murine embryonic samples was performed as detailed in sections 4.1.2 and 4.1.3.

4.2.3 RT-PCR Analysis of *Pax3c/3d* Transcripts

Protocols for RT-PCR assays were as detailed in section 4.1.4. The following primers were designed for RT-PCR of *Pax3c/3d* from murine embryonic samples:

- *Pax3c* (FWD) 5' gggggtagttcctcctgg 3'
- *Pax3c* (REV) 5' caatcagctgtctttgccac 3'
- *Pax3d* (FWD) 5' tgggcagtatggacaaagtg 3'
- *Pax3d* (REV) 5' gtggaggccggaaacagg 3'

These primers were manufactured by Geneworks Pty Ltd., Australia.

4.2.4 RT-PCR Analysis of *c-Kit* Transcripts

PolyA$^+$ mRNA was converted to cDNA using the protocol described in 4.1.4. The following primers were designed for RT-PCR of *c-Kit* from murine embryonic samples:

- *mcKitF* (FWD) 5' agacagacaagaggagatc 3'

- *mcKit*R (REV) 5' aatacaattcttggaggcga 3'

These primers were manufactured by Geneworks Pty Ltd., Australia.

RT-PCR cycling conditions were as follows:

Cycle	Time	Temperature
Reverse transcription	30 min	50°C
Initial PCR activation step	15min	95°C
3-step cycling:		
Denaturation	30 sec	94°C
Annealing	15 sec	52°C
Extension	15 sec	72°C
Number of cycles: 40		
Final extension	10min	72°C

Negative controls eliminating template mRNA were included in each RT-PCR assay. RT-PCR products were analysed by 2% agarose-gel electrophoresis and ethidium bromide staining relative to pUC19 DNA ladder; gels were run at 110 mV for 30 minutes in TAE buffer.

4.2.5 RT-PCR Analysis of *Mitf-m* Transcripts

PolyA$^+$ mRNA was converted to cDNA using the protocol described in 4.1.4. The following primers were designed for RT-PCR of *Mitf-m* from murine embryonic samples:

- m*MITF*F (FWD) 5' taagtggtctgcggtgtc 3'
- m*MITF*R (REV) 5' atgcctctttttcacagttg 3'

These primers were manufactured by Geneworks Pty Ltd., Australia.

RT-PCR cycling conditions were as follows:

Cycle	Time	Temperature
Reverse transcription	30 min	50°C
Initial PCR activation step	15min	95°C
3-step cycling:		
Denaturation	30 sec	94°C
Annealing	15 sec	54°C
Extension	15 sec	72°C
Number of cycles: 40		
Final extension	10min	72°C

Negative controls eliminating template mRNA were included in each RT-PCR assay. RT-PCR products were analysed by 2% agarose-gel electrophoresis and ethidium bromide staining relative to pUC19 DNA ladder; gels were run at 110 mV for 30 minutes in TAE buffer.

4.3 MURINE FOLLICULAR TRANSCRIPT ANALYSIS

To assess the expression of *Pax3c* and *Pax3d* in murine melanoblastic cells during proliferation and migration throughout normal hair follicle re-pigmentation, active synchronised hair growth (anagen) was induced in mice by depilation. Methods were based on those previously described by Paus *et al.* (1999) as these are recognised methods used to assess gene expression during murine hair regrowth.

4.3.1 Collection of Murine Skin Samples

Wild-type C57BL/6 inbred mice were housed in community cages at Edith Cowan University, fed water and murine chow *ad libitum* and kept in 12 hr light/dark cycles. Mice were sedated with midazolam (Hyponovel, Roche) via intramuscular injection at a dosage of 0.1mg/kg. Using a wax/rosin mixture warmed to 38°, a 15x15mm area of skin was depilated at the cervical region of the back. At 12, 24, 36, 48 and 60 hours post depilation, mice were euthanised by CO_2 overdose and skin samples harvested. Skin was thoroughly cleansed with 100% ethanol prior to being immediately snap-frozen in liquid nitrogen and kept at -70° until use. Ethical clearance for depilation and use of the animals was acquired through the Animal Ethics Committee of Edith Cowan University (project # 03-A8).

4.3.2 Isolation of Total RNA-Murine Skin Samples

Frozen skin samples were crushed with liquid nitrogen in a mortar and pestle prior to addition to TriZol Reagent (Invitrogen). Crushed tissues were homogenised in 1mL of TriZol per 50-100 mg of tissue using a glass-col homogeniser. Homogenised samples were passed several times through a 19 gauge needle with syringe prior to addition of 10μL proteinase K solution (10mg/mL ddH_20). Solution sat at room temperature for 10 minutes prior to continuation of isolation procedure as described in section 4.1.2.

4.3.3 PolyA$^+$ mRNA Purification

PolyA$^+$ mRNA purification of 10 murine skin samples was performed using protocol detailed in section 4.1.3.

4.3.4 RT-PCR Analysis of *Pax3c/3d* Transcripts

RT-PCR of 10 murine skin samples for *Pax3c/3d* was performed using protocol detailed in section 4.2.3.

4.3.5 RT-PCR Analysis of *c-Kit* Transcripts

RT-PCR of 10 murine skin samples for *c-Kit* was performed using protocol detailed in section 4.2.4.

4.3.6 RT-PCR Analysis of *Mitf-m* Transcripts

RT-PCR of 10 murine skin samples for *Mitf-m* was performed using protocol detailed in section 4.2.5.

4.4 IMMUNOHISTOCHEMISTRY ANALYSES

4.4.1 Pax3 Protein Analysis in Murine Embryogenesis

Following surgical excision, embryos were immersed in OCT and frozen immediately in thawing isopentene. These were stored at -70 °C until further use. Frozen murine embryos were cryosectioned into 6 μm tissue sections at –20°C onto Superfrost Plus slides and immediately taken through the staining protocol as follows.

Sections were air-dried for six hours prior to immersion in acetone at 4 °C for 1 minute and allowed to stand at room temperature for 1 minute. Sections were rehydrated in Tris buffered saline for 5 minutes prior to incubation in phosphate buffered saline (PBS) and Triton-X100 (0.2%) for 10 minutes. Sections were then incubated in PBS containing 3% H_2O_2 for 10 minutes. Sections were rinsed in fresh PBS 2 times for 7.5 minutes prior to incubation for 30 minutes with PBS and 10% fetal calf serum. PBS/10%fetal calf serum was poured off sections prior to incubation with Pax3c or Pax3d antibodies. These rabbit polyclonal antibodies were manufactured and kindly donated by Tom Barber and Johns Hopkins University; sequences of C-terminus amino acids used for their manufacture are kpwtf for Pax3c and afhylkpdia for Pax3d. These primary antibodies were applied at a 1:10 working dilution prior to standing overnight at 4°C.

Sections were washed in fresh PBS 2 times for 15 minutes followed by incubation of secondary antibody consisting of biotinylated anti-rabbit IgG (DAKO LSAB2 System) for 10 minutes at room temperature. Sections were washed in PBS for 15 minutes prior to application of tertiary antibody consisting of horseradish peroxidase (HRP) linked streptavidin (DAKO LSAB2 System) for 10 minutes at room temperature. Following a wash in PBS for 15 minutes, the staining reactions were completed using 3, 3-diaminobenzidine (DAB) substrate (Sigma Chemicals) as chromogen. Sections

were incubated with DAB for 2 minutes, placed in ddH_2O to stop reaction and taken through an ethanol and xylene series (70/95/100/100/100/3X xylene) prior to coverslipping with DEPEX mounting medium (EMS). Negative controls consisted of sections processed at the same time and in the same manner, however primary antibodies were eliminated.

5

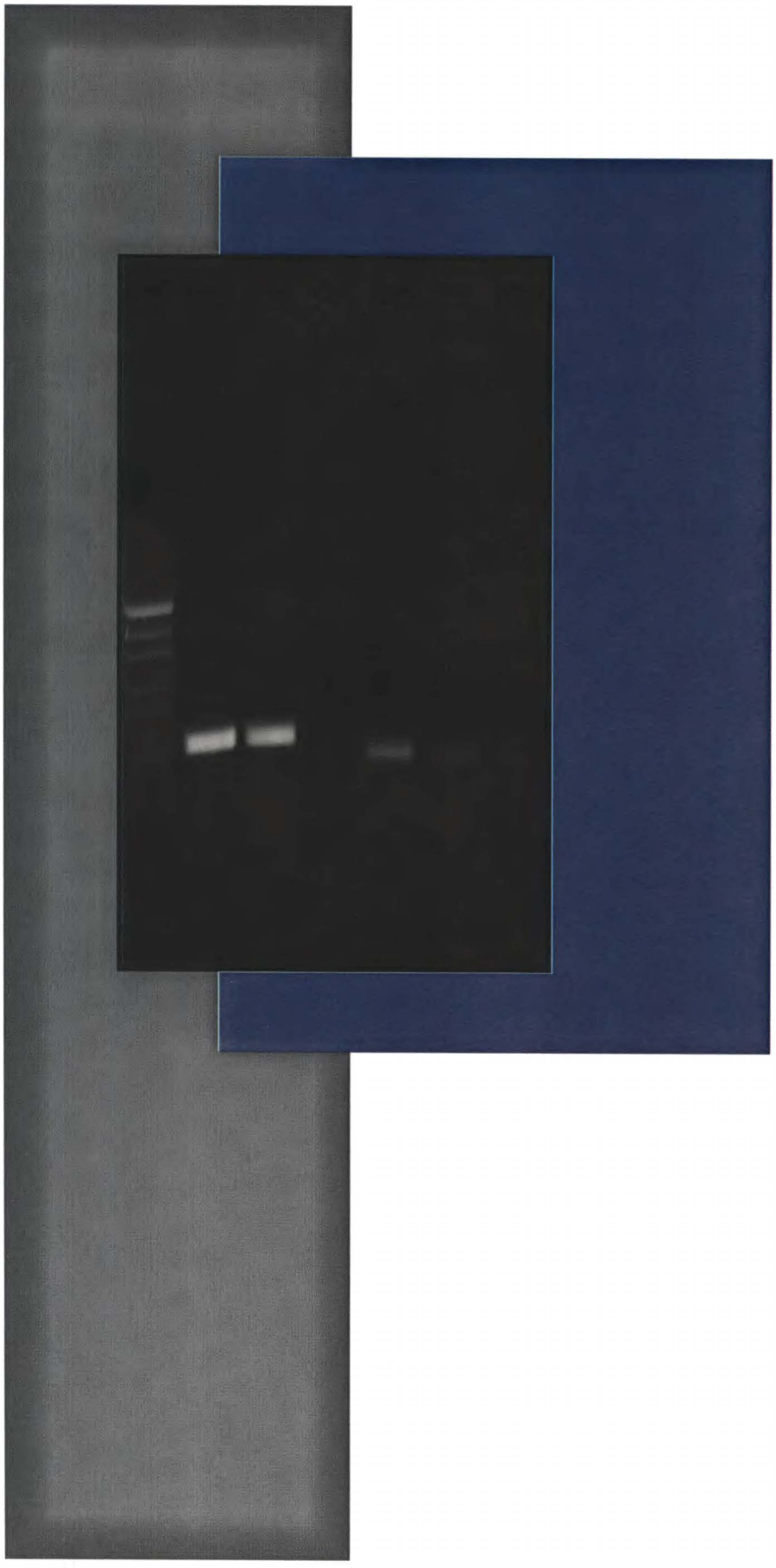

RESULTS

"Science knows of instances where an investigator was in possession of all the important facts yet failed to ask the right questions."

Ernst Mayr

5.1 mRNA ANALYSES

5.1.1 *PAX3* mRNA in CMM

Aberrant expression of *PAX3* in CMM was first detected by Barr *et al.* (1999), who found that expression levels were "notably high"; moreover, they described the predominant *PAX3d* transcript as a novel transcript. In a similar study, Scholl *et al.* (2001) reported that 77% of melanomas tested showed *PAX3* expression while all normal perilesional skin, melanocytes and benign lesions tested showed no *PAX3* expression. In order to analyse the relative expression profiles of *PAX3* in CMM, metastatic CMM samples (cytologic diagnosis following excision confirmed using Giemsa staining and immunohistochemistry) were assayed for *PAX3C* and *PAX3D* mRNA.

Total RNA was isolated from each sample, prior to isolation of polyadenylated (polyA$^+$) mRNA. PolyA$^+$ isolation of mRNA was necessary to ensure that products generated by RT-PCR were from mRNA rather than from genomic DNA as differential amplification of *PAX3C* from *PAX3D* utilises a 3' primer corresponding to a retained intronic sequence within the *PAX3C* sequence. Negative controls for each sample were performed by elimination of the reverse transcription portion of the RT-PCR reaction. Each sample was then analysed for both *PAX3C* and *PAX3D* transcripts by RT-PCR to provide a relative expression profile of these transcripts within each sample. Controls and RT-PCR products were then analysed and visualised by 2% agarose gel electrophoresis.

In the CMM biopsies tested, 100% (5/5) showed both *PAX3C* and *PAX3D* expression, as was expected (Figure 5.1).

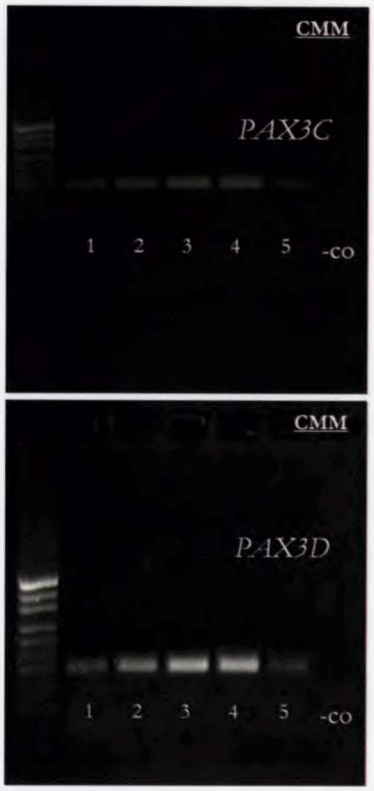

Figure 5.1. **Detection of *PAX3C*, *PAX3D* Transcripts in Human Skin Biopsies.**
RT-PCR products generated from mRNA of human skin biopsies, using exon 8 (*PAX3C*) and exon 9 (*PAX3D*) primers, visualised on 2% ethidium bromide-stained agarose gels. ***PAX3C***= *PAX3C* transcript amplified (expected product length- 89 bp); ***PAX3D***= *PAX3D* transcript amplified (expected product length- 104 bp); **1-5=** specimen identification number; **-co=** negative control for primers without template mRNA; **pUC=** DNA ladder (pUC19 digested with HpaII).

5.1.2 *Pax3* mRNA in Murine Embryogenesis

To date, no published studies have identified expression of *PAX3D/Pax3d* in normal human or mouse melanocytic tissues. Consequently, a primary aim of the study was to investigate whether the *Pax3d* transcript is expressed during normal melanocytic development. *Pax3* is known to alter transactivational function through alternative splicing of the 3' end, so it was queried whether *Pax3d* may be primarily utilised by muscle or brain cells with expression in CMM being uncharacteristic for melanocytic cells. Therefore, murine embryonic tissues were separately analysed as brain, trunk and limb skeletal muscle (herein referred to as *body* samples) and skin samples (where possible) to identify specific localisation of *Pax3* mRNA

expression within brain, limb bud and skin cells; embryonic age was chosen to reflect key stages of melanocytic development. Samples are outlined in Table 6.

Table 4. **Sample selection for investigation of *Pax3c* and *Pax3d* transcript expression in murine embryogenesis.**

Stage	Number of samples	Tissue sections
Embryonic day 11 (E11): Melanoblasts migrate from neural crest to dermis (Mayer, 1973)	**one**	**whole**
E12.5: Melanoblasts synchronously migrate from dermis into epidermis (Yoshida *et al.*, 1996)	**six**	**head, body**
E15: Melanoblasts migrate into hair follicles (Hirobe, 1984)	**nine**	**head, body, skin**
E20: Visible melanin formation indicates melanocytic differentiation (Müller-Röver *et al.*, 2001)	**nine**	**head, body, skin**

Thus, a total of 25 murine embryonic samples were assayed for *Pax3c* and *Pax3d* expression. Total RNA was isolated from samples prior to isolation of polyA$^+$ mRNA. Again, polyA$^+$ isolation of mRNA was necessary as differential amplification of *Pax3c* from *Pax3d* utilises a 3' primer corresponding to a retained intronic sequence. Negative controls for each sample were performed by elimination of the reverse transcription portion of a RT-PCR prior to visualisation by 2% agarose gel electrophoresis. Each sample was then analysed for both *Pax3c* and *Pax3d* transcripts by RT-PCR and visualised by 2% agarose gel electrophoresis (this method of analysis provides a relative expression profile of these transcripts within each sample).

At E11, both *Pax3c* and *Pax3d* transcripts are expressed (Figure 5.2). At this stage, whole embryos were used because it was merely necessary to show the presence or absence of *Pax3c* or *Pax3d*; consequently, while the *Pax3d* transcript is expressed, lineage (s) activity at this developmental stage remains undetermined.

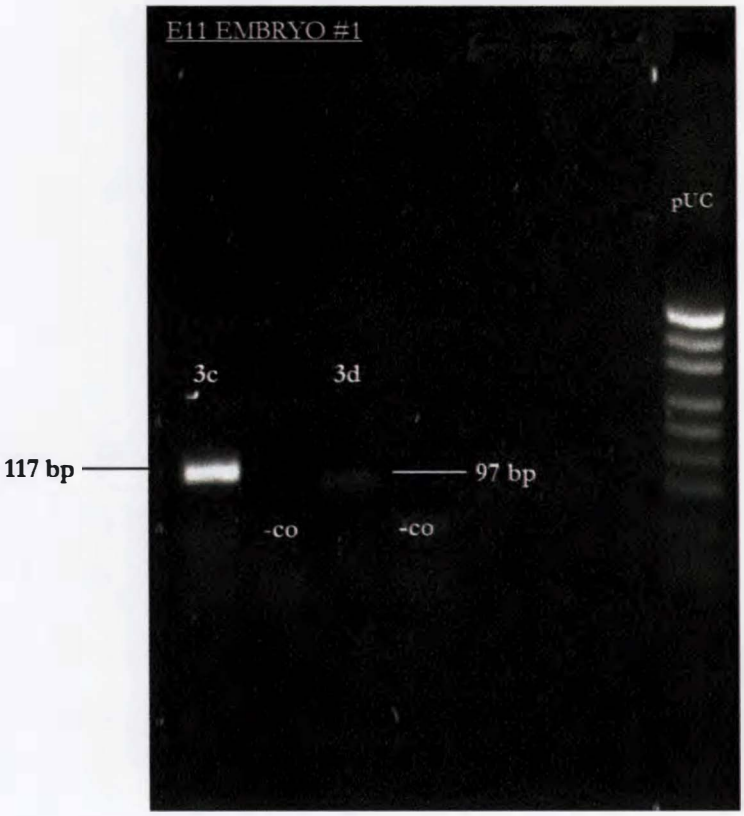

Figure 5.2. **Detection of *Pax3c*, *Pax3d* Transcripts in E11 Murine Embryo.**
RT-PCR products generated from whole E11 mRNA, using exon 8 (*Pax3c*) and exon 9 (*Pax3d*) primers, visualised on 2% ethidium bromide-stained agarose gel. **3c**= *Pax3c* transcript amplified (expected product length- 117 bp); **3d**= *Pax3d* transcript amplified (expected product length- 97 bp); **-co**= negative control for primers without template mRNA; **pUC**= DNA ladder (pUC 19 digested with HpaII).

At E12.5, both *Pax3c* and *Pax3d* transcripts are expressed in the head and body (Figure 5.3). Segregation of the skin from these embryos was unsuccessful as it was fragile and thin; therefore, *Pax3c* and *Pax3d* expression may be indicative of transcriptional activity in neural, muscle and/or melanocytic lineages at this stage. It suffices to say that both transcripts are expressed at this stage of murine embryogenesis and that *Pax3d* is a functioning transcript.

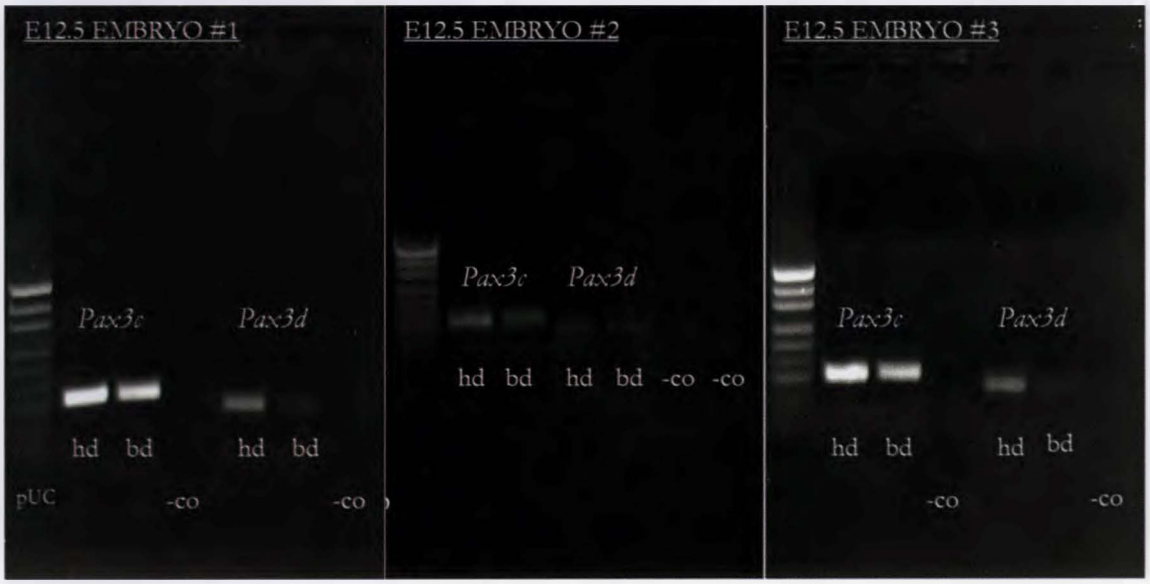

Figure 5.3. **Detection of *Pax3c*, *Pax3d* Transcripts in E12.5 Murine Embryos.**
RT-PCR products generated from E12.5 mRNA, using exon 8 (*Pax3c*) and exon 9 (*Pax3d*) primers, visualised on 2% ethidium bromide-stained agarose gels. ***Pax3c*= *Pax3c*** transcript amplified (expected product length- 117 bp); ***Pax3d*= *Pax3d*** transcript amplified (expected product length- 97 bp); **hd=** head; **bd=** body; **-co=** negative control for primers without template mRNA; **pUC=** DNA ladder (pUC 19 digested with HpaII).

At E15, all tissue samples showed *Pax3c* and *Pax3d* transcript expression (with the exception of the skin of embryo #2) thus indicating a role for both transcripts in neural, muscle and melanocytic cells at this stage of development (Figure 5.4).

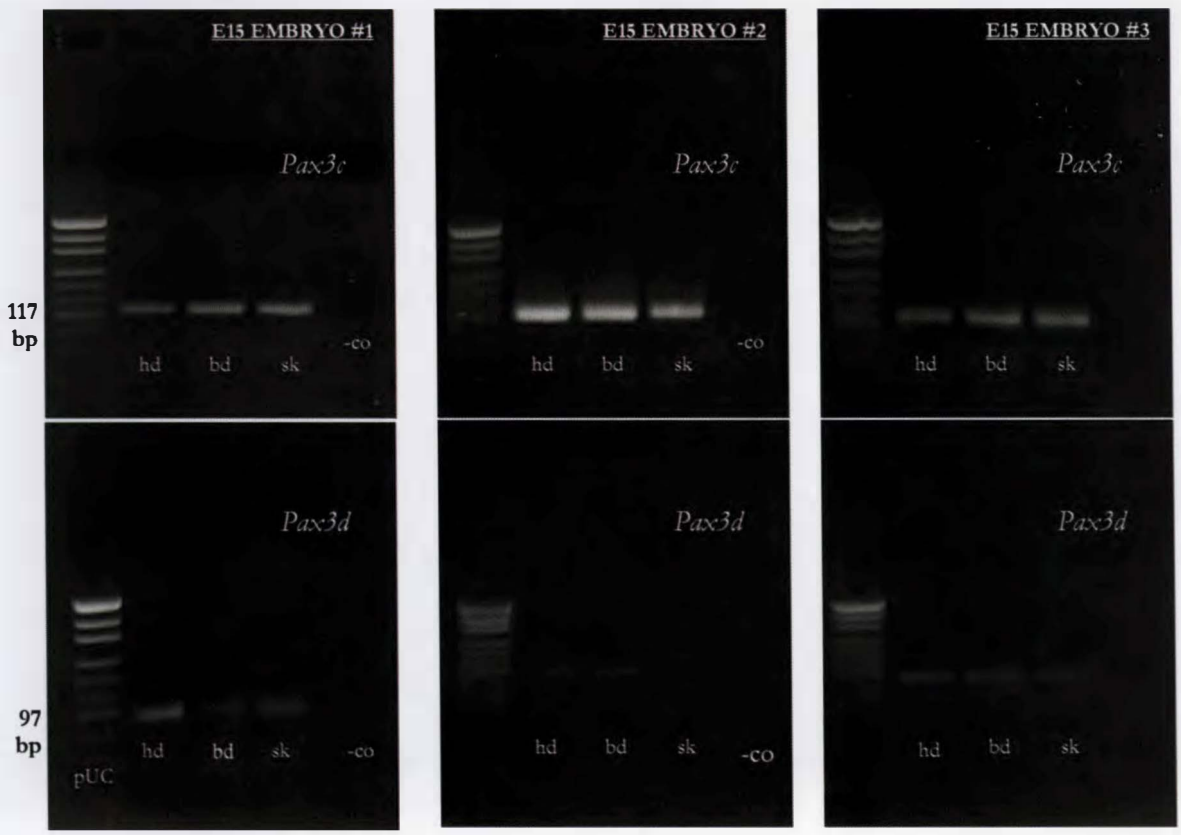

Figure 5.4. **Detection of *Pax3c*, *Pax3d* Transcripts in E15 Murine Embryos.**
RT-PCR products generated from E15 mRNA, using exon 8 (*Pax3c*) and exon 9 (*Pax3d*) primers, visualised on 2% ethidium bromide-stained agarose gels. ***Pax3c***= *Pax3c* transcript amplified (expected product length- 117 bp); ***Pax3d***= *Pax3d* transcript amplified (expected product length- 97 bp); **hd**=head; **bd**=body; **sk**=skin; **-co**= negative control for primers without template mRNA; **pUC**=DNA ladder (pUC 19 digested with HpaII).

By E20, *Pax3c* transcript expression is evident in all, while skin primarily lacks *Pax3d* expression (Figure 5.5).

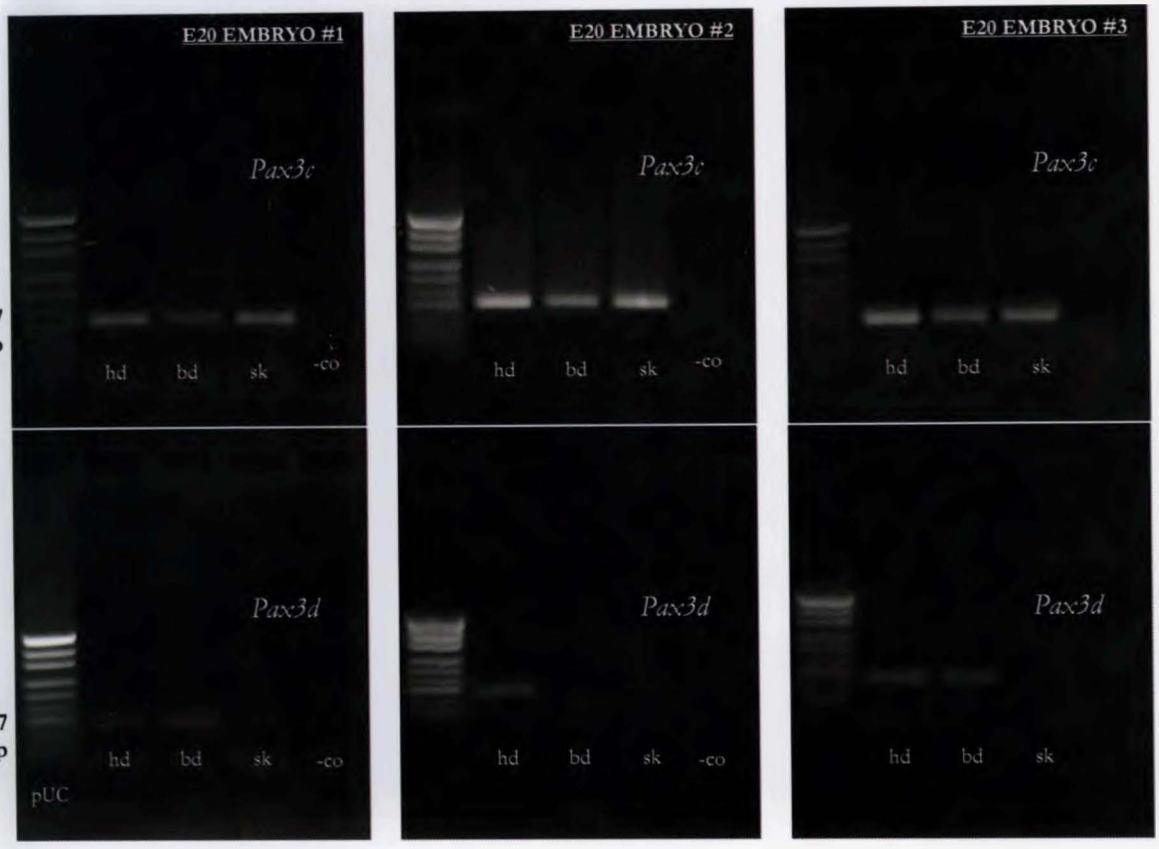

Figure 5.5. **Detection of *Pax3c*, *Pax3d* Transcripts in E20 Murine Embryos.**
RT-PCR products generated from E20 mRNA, using exon 8 (*Pax3c*) and exon 9 (*Pax3d*) primers, visualised on 2% ethidium bromide-stained agarose gels. ***Pax3c***= *Pax3c* transcript amplified (expected product length- 117 bp); ***Pax3d***= *Pax3d* transcript amplified (expected product length- 97 bp); **hd**=head; **bd**=body; **sk**=skin; **-co**= negative control for primers without template mRNA; **pUC**=DNA ladder (pUC 19 digested with HpaII).

In summary, the *Pax3d* transcript is found expressed in normal murine embryogenesis at key stages of melanocytic development. Moreover, both *Pax3c* and *Pax3d* transcripts are expressed in various segregated tissue samples chosen to reflect brain, muscle and skin lineages.

5.1.3 *Pax3* mRNA in Follicular Regrowth

As the hair follicle cycles through stages of growth, regression, resting and shedding, pigment cells also cycle through periods of proliferation, migration, differentiation and apoptosis (Müller-Röver *et al.*, 2001). Histologic and ultrastructural studies have demonstrated that when the hair follicle undergoes active growth (anagen), melanoblasts migrate out of a stem cell niche, proliferate, localise in the hair matrix before further proliferation and differentiation into mature melanocytes (Nishimura *et al.*, 2002).

In order to induce spontaneous anagen, depilation of C57/BL6 pigmented mice was carried out according to standard methods (Paus *et al.*, 1999). Subsequent hair growth was exploited to analyse *Pax3* expression, in particular, to investigate generation of *Pax3d* transcripts in an additional "normal" melanocytic proliferation, migration and differentiation model. Skin samples were taken every 12 hours up to 60 hours post depilation, corresponding to proliferation and migration of melanoblasts into the regenerating hair placode during anagen. Two separate depilation experiments were performed using one mouse for each stage of 12 hour analysis, therefore providing a total of 10 skin samples for analysis of *Pax3c* and *Pax3d* expression. Prior to isolation of mRNA from the depilated skin samples, haematoxylin and eosin staining was performed on adjacent sections of depilated skin to ensure complete removal of hair sheath and associated melanocytes of the inner root sheath.

Total RNA was isolated from each sample, prior to isolation of polyA$^+$ mRNA. To ensure genomic DNA was not present in the isolated mRNA samples, negative controls for each sample were performed by elimination of the reverse transcription portion of a RT-PCR reaction. RT-PCR products were assessed by 2% agarose gel electrophoresis. Each sample was analysed for both *Pax3c* and *Pax3d* transcripts by RT-PCR, providing a relative expression profile of these transcripts within each sample.

In depilation experiment #1, individual samples were taken at 12-hour intervals up to 60 hours post depilation. In this trial, *Pax3c* expression was seen at 24, 36, 48 and 60 hours post depilation. By contrast, *Pax3d* expression was only observed at 12 hours and then at 48 hours post depilation (Figure 5.6).

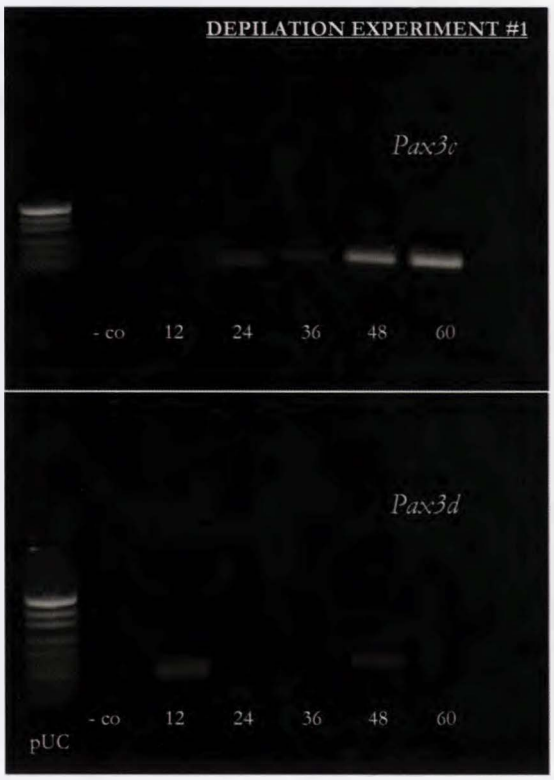

Figure 5.6. **Detection of *Pax3c*, *Pax3d* Transcripts in Depilation Experiment #1.**
RT-PCR products generated from depilated skin mRNA samples, using exon 8 (*Pax3c*) and exon 9 (*Pax3d*) primers, visualised on 2% ethidium bromide-stained agarose gels. ***Pax3c***= *Pax3c* transcript amplified (expected product length- 117 bp); ***Pax3d***= *Pax3d* transcript amplified (expected product length- 97 bp); **12, 24, 36, 48, 60** indicates 12 hour time interval from depilation; **-co**= negative control for primers without template mRNA; **pUC**=DNA ladder (pUC 19 digested with HpaII).

Depilation experiment #2 confirmed findings of experiment #1. Again, individual samples were again taken every 12 hours up until 60 hours post depilation. As for trial #1, in trial #2 *Pax3c* expression was seen at 24, 36, 48 and 60 hours post depilation and *Pax3d* expression was seen first at 12 hours and then at 48 hours post depilation (Figure 5.7).

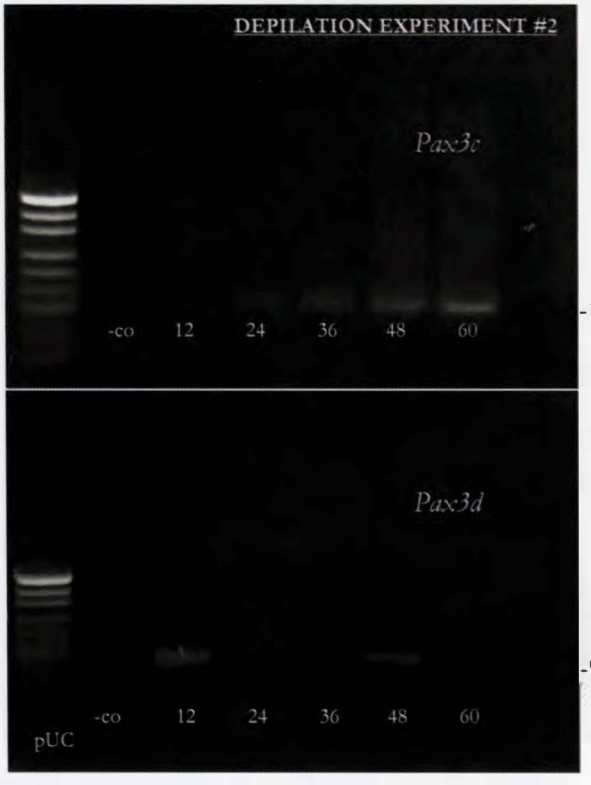

Figure 5.7. **Detection of *Pax3c*, *Pax3d* Transcripts in Depilation Experiment #2.**
RT-PCR products generated from depilated skin mRNA samples, using exon 8 (*Pax3c*) and exon 9 (*Pax3d*) primers, visualised on 2% ethidium bromide-stained agarose gels. ***Pax3c***= *Pax3c* transcript amplified (expected product length- 117 bp); ***Pax3d***= *Pax3d* transcript amplified (expected product length- 97 bp); **12, 24, 36, 48, 60** indicates 12 hour time interval from depilation; **-co**= negative control for primers without template mRNA; **pUC**=DNA ladder (pUC 19 digested with HpaII).

In summary, the depilation experiments reiterated a role for *Pax3d* in normal melanocytic development, in this instance when coupled to hair follicle cycling. The *Pax3c* transcript was expressed in 8:10 samples assayed; the *Pax3d* transcript was expressed in 4:10 samples. As melanin granules appear above the dermal papilla at approximately 96 hours post depilation

(Müller-Röver *et al.*, 2001), *Pax3c* and *Pax3d* expression seen in these experiments is indicative of an early role in proliferation, migration and/or differentiation of melanoblasts during anagen hair growth. Furthermore, *Pax3d* expression is seen within 12 hours post depilation, prior to *Pax3c* expression in these experiments.

5.1.4 *c-Kit* mRNA in Follicular Regrowth

Both *Pax3* and *c-Kit* are important in melanocytic development, therefore, we tested the hypothesis that *Pax3* may regulate *c-Kit*. Overlapping spatial and temporal expression of *Pax3* and *c-Kit* in murine melanogenesis prompted investigation into possible concurrent expression patterns in hair follicle cycling. The expression pattern of *c-Kit* in the early stages of hair follicle melanogenesis was therefore assessed for correlation with the observed expression patterns of *Pax3* in skin samples from depilation experiments.

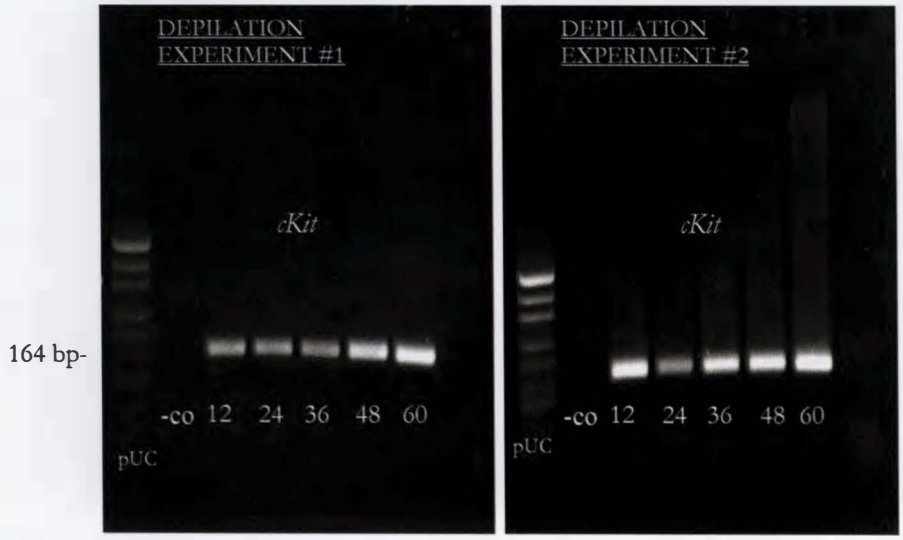

Figure 5.8. **Detection of *cKit* Transcripts in Depilation Experiments.**
RT-PCR products generated from depilated skin mRNA samples, using *cKit* primers, visualised on 2% ethidium bromide-stained agarose gels. ***cKit***= *cKit* transcript amplified (expected product length-164 bp); **12, 24, 36, 48, 60** indicates 12 hour time intervals for depilation; **-co**= negative control for primers without template mRNA; **pUC**=DNA ladder (pUC 19 digested with HpaII).

c-Kit expression was seen in 100% (10/10) of depilated skin samples, ranging from 12 to 60 hours post-depilation (Figure 5.8). In both depilation trials, *c-Kit* expression is seen at 12 hours post depilation, preceding *Pax3c* expression therefore indicating that *c-Kit* expression is not related to *Pax3c* expression. Consistency of *c-Kit* expression throughout anagen, as compared to varied temporal expression of *Pax3d*, also indicates that *c-Kit* expression may not be related to *Pax3d* expression.

5.1.5 *Mitf-m* mRNA in Embryogenesis

Another candidate gene thought linked to *Pax3(d)* transactivation was micropthalmia-associated transcription factor (*Mitf*). *Mitf* is one of the earliest genes expressed in the melanocytic lineage (Opdecamp *et al.*, 1997). Like *Pax3*, *Mitf* produces alternative isoforms that are constitutively expressed in various tissues, the melanocyte specific isoform being *Mitf-m* (Yajima *et al.*, 1999). Pax3 has been shown to bind and transactivate the promoter region of *Mitf-m* (Watanabe *et al.*, 1998), therefore, co-expression studies were undertaken to investigate a possible association between *Pax3* and *Mitf-m* expression in embryogenesis. Using primers specific for the *Mitf-m* isoform, RT-PCR of murine embryonic mRNA samples (previously tested for *Pax3* mRNA) was performed to analyse *Mitf-m* mRNA expression.

The results indicate that *Mitf-m* is initially expressed in the E11 embryo, but is not seen in tissues of the E12.5 embryo. Expression is again apparent in the skin of E15 and E20 embryos (Figures 5.9 and 5.10); like Pax3c and Pax3d, Mitf-m is observed at most stages of melanocyte development (bar E12.5).

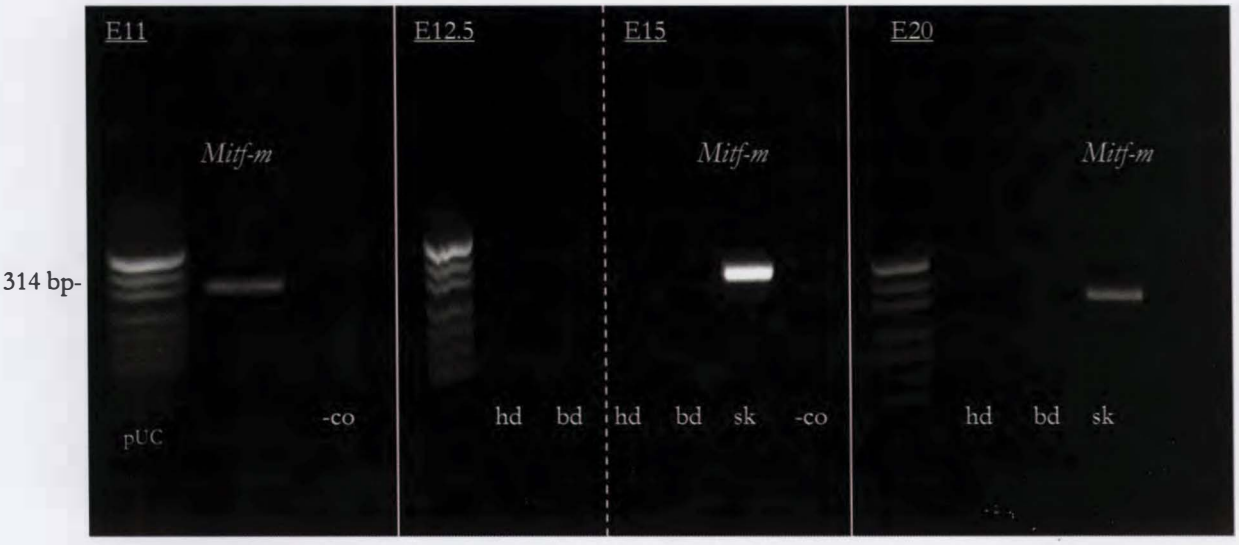

Figure 5.9. **Detection of *Mitf-m* Transcripts in Murine Embryos.**

RT-PCR products generated from E11, E12.5, E15 and E20 mRNA, using *Mitf-m* primers for melanocytic specific isoform, visualised on 2% ethidium bromide-stained agarose gels. ***Mitf-m***= *Mitf-m* transcript amplified (expected product length- 314 bp); **hd**=head; **bd**=body; **sk**=skin; **-co**= negative control for primers without template mRNA; **pUC**=DNA ladder (pUC 19 digested with HpaII).

Figure 5.10. **Detection of *Mitf-m* Transcripts in Murine Embryos.**

RT-PCR products generated from E11, E12.5, E15 and E20 mRNA, using *Mitf-m* primers for melanocytic specific isoform, visualised on 2% ethidium bromide-stained agarose gels. ***Mitf-m***= *Mitf-m* transcript amplified (expected product length- 314 bp); **hd**=head; **bd**=body; **sk**=skin; **-co**= negative control for primers without template mRNA; **pUC**=DNA ladder (pUC 19 digested with HpaII).

5.1.6 *Mitf-m* mRNA in Follicular Regrowth

Investigation of potential *Pax3* and *Mitf-m* co-expression patterns was also undertaken with skin samples from depilation experiments. Using primers specific for the *Mitf-m* isoform, RT-PCR of depilated skin mRNA samples (previously tested for *Pax3* mRNA) was performed to analyse *Mitf-m* mRNA expression. Results indicate varied expression of *Mitf-m* in depilation experiments with expression seen in 50% (5/10) of skin samples assayed. In both experiments, no *Mitf-m* is observed at 12 hours past depilation and varied expression is observed at 24, 36, and 48, hours past depilation (Figure 5.11). Furthermore, *Mitf-m* is observed at 60 hours in both experiments confirming a role for *Mitf-m* in the maintenance of the melanocytic lineage.

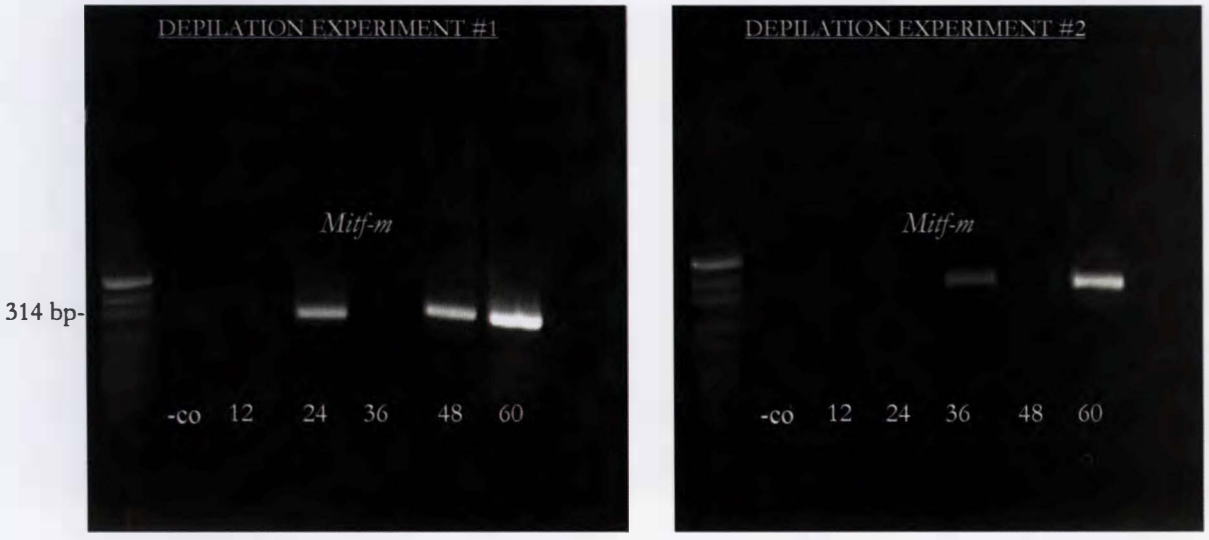

Figure 5.11. **Detection of *Mitf-m* Transcripts in Depilation Experiments.**
RT-PCR products generated from depilated skin mRNA samples, using *Mitf-m* primers for melanocytic specific isoform, visualised on 2% ethidium bromide-stained agarose gels. ***Mitf-m***= *Mitf-m* transcript amplified (expected product length-314 bp); **12, 24, 36, 48, 60** indicates 12 hour time intervals for depilation; **-co**= negative control for primers without template mRNA; **pUC**=DNA ladder (pUC 19 digested with HpaII).

In summary, RNA expression analyses of *Pax3c*, *Pax3d*, *c-Kit* and *Mitf-m* revealed no obvious relationship between *c-Kit* and *Pax3* expression. *Mitf-m* expression patterns within murine embryogenesis may be linked to *Pax3c*

expression, however further immunohistochemical co-localisation studies are required to investigate this possibility. The following table summarises *Pax3c*, *Pax3d*, *cKit* and *Mitf-m* RNA expression patterns observed throughout murine stages of embryogenesis and hair follicle cycling (Table 7).

***Table 5.* Overview of *Pax3c*, *Pax3d*, *cKit* and *Mitf-m* Expression in Stages of Murine Embryogenesis.**

	Pax3c	*Pax3d*	*Mitf-m*
E11- Melanoblasts migrate from neural crest to dermis (Mayer, 1973)	Expressed	Expressed	Expressed
E12.5- Melanoblasts synchronously migrate from dermis into epidermis (Yoshida *et al.*, 1996)	Expressed in head, body	Expressed in head, body	Not expressed
E15- Melanoblasts migrate into hair follicles (Hirobe, 1984)	Expressed in head, body, skin	Expressed in head, body, skin	Expressed in skin
E20- Visible melanin formation indicates melanocytic differentiation (Müller-Röver *et al.*, 2001)	Expressed in head, body, skin	Expressed in head, body	Expressed in skin

Table 6. **Overview of *Pax3c*, *Pax3d*, *cKit* and *Mitf-m* Expression in Depilation Experiments. PD=** post depilation.

	Pax3c	*Pax3d*	*c-Kit*	*Mitf-m*
12 hr PD	Not expressed	Expressed in all samples	Expressed in all samples	Not expressed
24 hr PD	Expressed in all samples	Not expressed	Expressed in all samples	Expressed in 50% of samples
36 hr PD	Expressed in all samples	Not expressed	Expressed in all samples	Expressed in 50% of samples
48 hr PD	Expressed in all samples	Expressed in all samples	Expressed in all samples	Expressed in 50% of samples
60 hr PD	Expressed in all samples	Not expressed	Expressed in all samples	Expressed in all samples

5.2.1 Analysis of E12.5 Pax3 Localisation

Yoshida *et al.* (1996) demonstrated that around E12.5-13.5, melanoblasts enter the epidermis synchronously and proliferate extensively. In order to examine the location of Pax3+ cells in the embryo at this stage, immunohistochemical staining of E12.5 frozen sections was undertaken using Pax3c and Pax3d specific antibodies. At the periphery of many sections, throughout the dermis, positive staining could be seen for Pax3c and Pax3d proteins, in a pattern typifying migration of melanoblasts from the dermis toward the epidermis during this window of time (Figure 5.12).

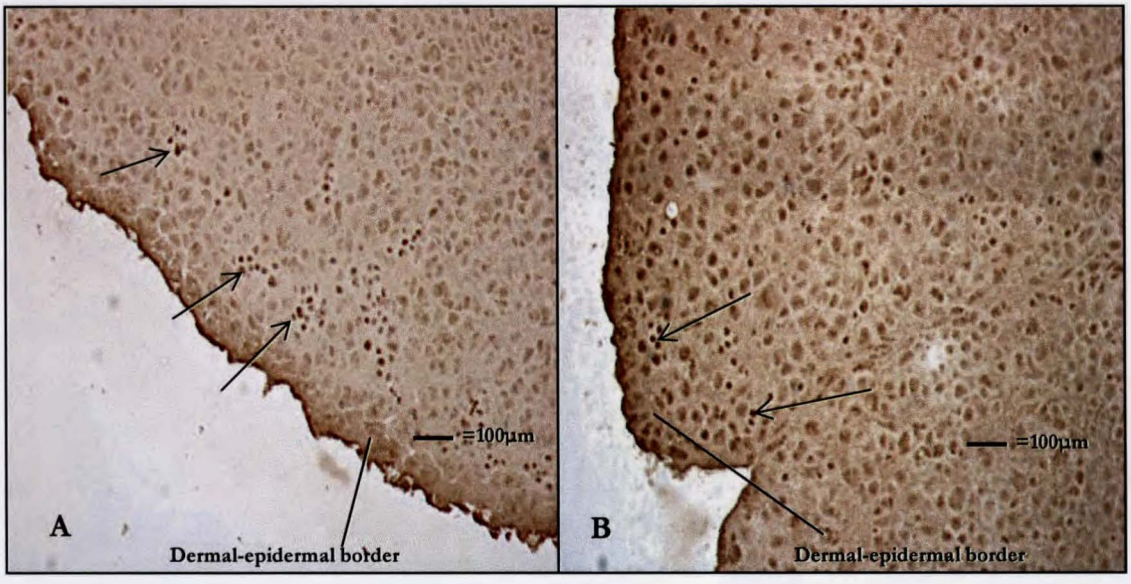

Figure 5.12. **Immunohistochemical Staining of Pax3+ Cells in E12.5 Skin.**
Immunohistochemical staining of E12.5 sections using Pax3 primary antibodies, and a biotin-streptavidin-peroxidase system visualised with diaminobenzidine chromogen (DAB). Populations of (**A**) Pax3c+ (**B**) Pax3d+ cells, such as those indicated by arrows, are seen scattered throughout the dermis, in particular, proximal to the dermal/epidermal border.

Both Pax3c+ and Pax3d+ cells are most evident in the buccal region, vibrassal region and dorsal tail regions of the skin at E12.5, differing slightly in number (Figure 5.13). While Pax3c+ staining was uniform throughout the entire dermis of the E12.5 sections, Pax3d+ staining was confined to regions

of buccal and caudal dermis. Staining results of E12.5 embryos confirm that *Pax3c* and *Pax3d* expression demonstrated in RT-PCR analyses of head and body samples is linked to a role in melanocytic development at this stage.

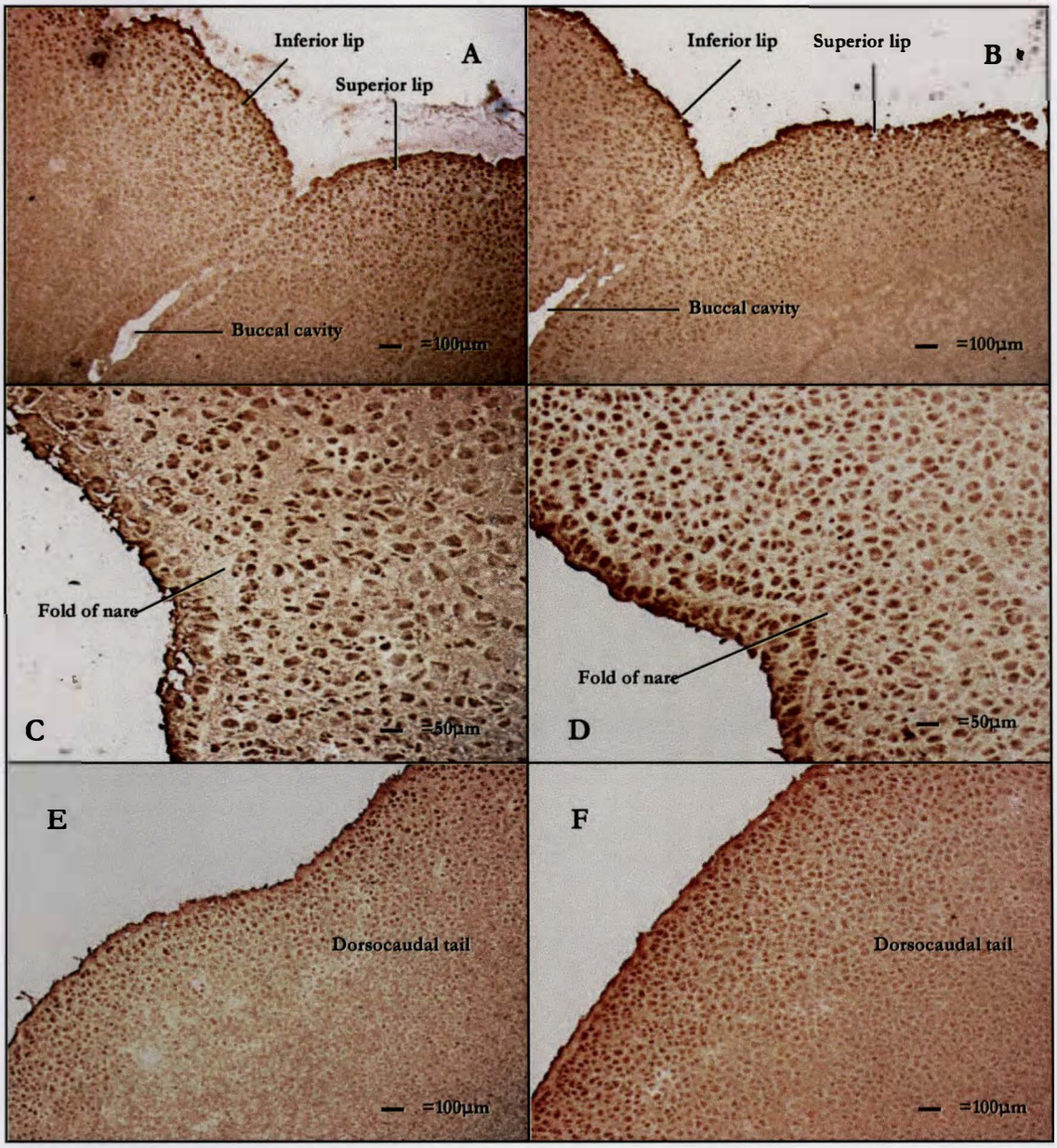

Figure 5.13. **Immunohistochemical Staining of Pax3+ Cells in E12.5 Regions of Skin.**
Immunohistochemical staining of E12.5 sections using Pax3 primary antibodies and a biotin-streptavidin-peroxidase system visualised with DAB. Dark brown Pax3c+ (**A,C,E**) and Pax3d+ (**B,D,F**) cells are seen in the buccal region (**A,B**), vibrassal region (**C,D**) and dorsalcaudal region of the tail (**E,F**). In these sections, most Pax3+cells are scattered within the dermis.

5.2.2 Analysis of Pax3 E15 Localisation

In order to examine the location of Pax3+ cells in the embryo at this stage, immunohistochemical staining of E15 frozen sections was undertaken using Pax3c and Pax3d specific antibodies. At around E15, a subpopulation of melanoblasts migrates toward the developing hair germs where they localise in hair follicle pigmentary units (Hirobe, 1984). Analysis of staining within E15 skin sections revealed positive staining for Pax3c and Pax3d proteins at the periphery of all sections, throughout the epidermis (Figure 5.14). In the skin, there is a notable variance between Pax3c and Pax3d staining; many Pax3c+ cells are seen within developing hair follicles while few Pax3d+ cells are seen here. Moreover, Pax3d+ cells are distributed profusely throughout the epidermis where Pax3c+ cells are sparse. These results confirm RT-PCR analyses of samples demonstrating both *Pax3c* and *Pax3d* expression in embryos at E15; immunohistochemistry, however, highlights different expression patterns.

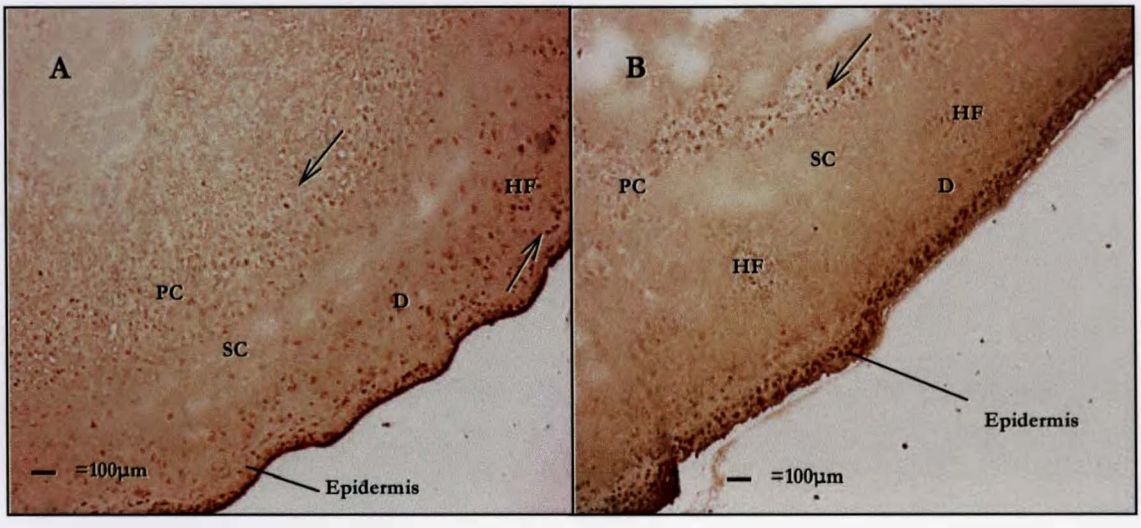

Figure 5.14. **Immunohistochemistry for Pax3c and Pax3d Proteins in E15 Embryo.**
Immunohistochemical staining of E15 sections using Pax3 primary antibodies and a biotin-streptavidin-peroxidase system visualised with DAB. Dark brown Pax3c+ cells (**A**) and Pax3d+cells (**B**) are seen in the epidermis, hair follicles (**HF**) and panniculus carnosus muscle (**PC**) as indicated by arrows. **D**) dermis; **SC**) subcutis.

Furthermore, Pax3c+ and Pax3d+ cell staining is seen within the midbrain of the E15 embryonic sections (Figure 5.15); this is significant in that ours is the first evidence for a role for the *Pax3d* transcription factor within the developing brain.

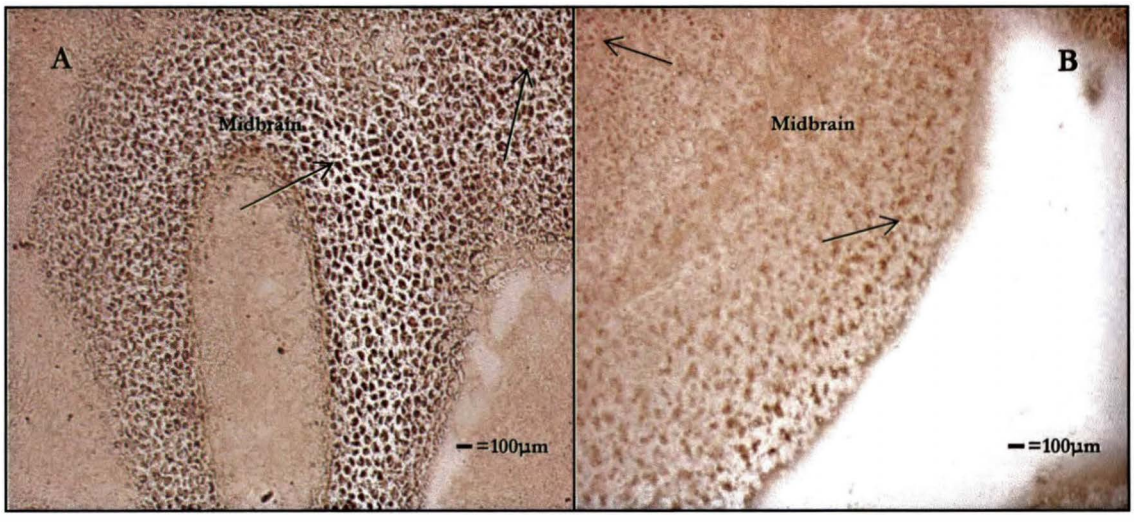

Figure 5.15. **Immunhistchemical Staining of Pax3+ Cells in E15 Midbrain.**
Immunohistochemical staining of E15 sections using Pax3 primary antibodies and a biotin-streptavidin-peroxidase system visualised with DAB. Dark brown Pax3c+ (**A**) and Pax3d+ (**B**) cells are seen in the dorsal layers of the superior colliculus as indicated by arrows.

Positive staining is also seen for both Pax3c and Pax3d in the panniculus carnosus muscle located beneath the subcutis (Figure 5.14) explaining evidence for *Pax3c* and *Pax3d* expression seen within head and body samples (less skin) in the RT-PCR analyses.

5.2.3 Analysis of Pax3 E20 Localisation

Murine epidermal melanoblasts begin to terminally differentiate at around E14, with subsequent pigmentation activity induced 2 days later (Hirobe, 1984). Perinatally, at E20, hair follicles are characterised by initial melanin formation thus indicating an advanced stage of melanocytic differentiation. Furthermore, after birth most epidermal melanocytes, except those of hairless areas such as the ears and tail, undergo apoptosis (Hirobe,

1984) leaving only melanoblasts and melanocytes of the hair follicles to produce pigmentation of the murine coat. Therefore, immunohistochemical staining of E20 frozen sections was undertaken using Pax3c and Pax3d specific antibodies in order to compare Pax3 distribution just prior to birth.

In E20 skin, Pax3c$^+$ positive staining is greatly diminished (as compared to the E15 embryonic skin) with only few positive cells along the entire periphery of the skin. Positive Pax3c staining is primarily seen within the hair follicle above the dermal papilla and amongst the distal hair follicle epithelium (Figure 5.16) while no Pax3d$^+$ staining is observed in the skin (Figure 5.17).

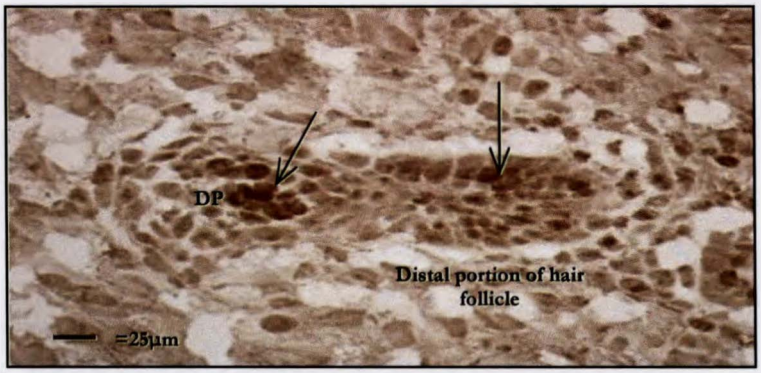

Figure 5.16. **Immunohistochemical Staining of Pax3c$^+$ Cells in the E20 Hair Follicle.**

Immunohistochemical staining of an E20 section using Pax3c primary antibody and a biotin-streptavidin-peroxidase system visualised with DAB. Dark brown Pax3c+ cells are seen above the oval shaped dermal papilla (**DP**) and in the midst of the distal hair follicle epithelium (located closest to the epidermis) as indicated by arrows.

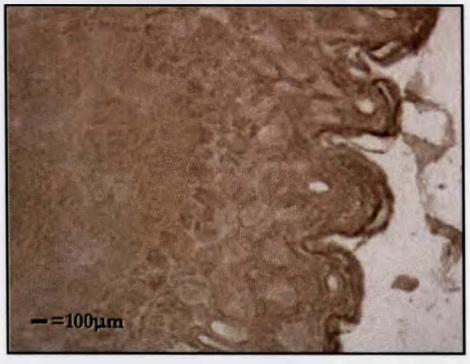

Figure 5.17. **Immunohistochemical Staining of E20 Embryo.**

Immunohistochemical staining of an E20 section using Pax3d primary antibody and a biotin-streptavidin-peroxidase system visualised with DAB. No positive staining observed.

Moreover, in the E20 head, the midbrain shows positive staining for both Pax3c and Pax3d further supporting a role for Pax3d in development of the brain (Figure 5.18).

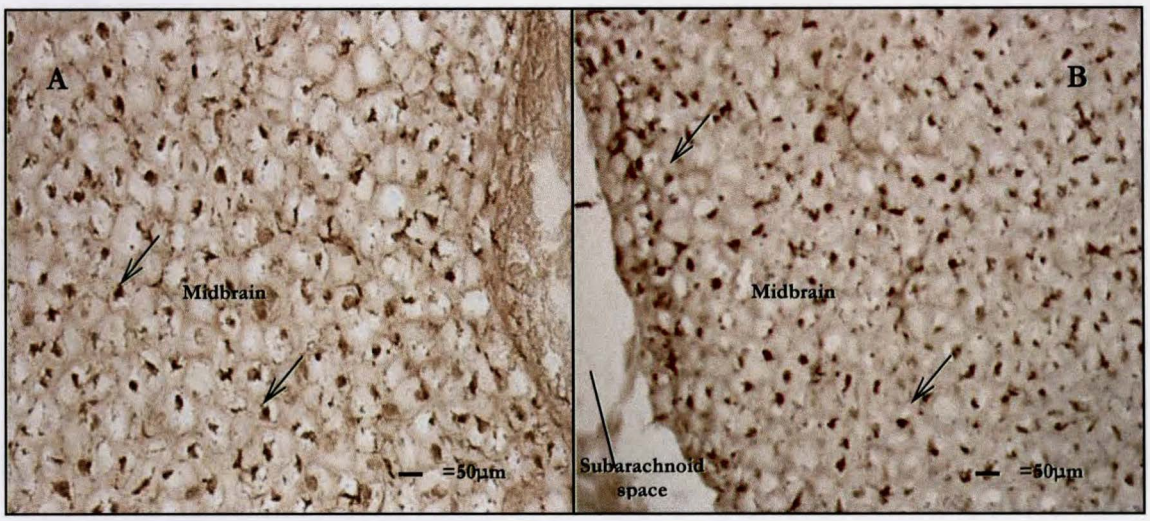

Figure 5.18. **Immunohistochemical Staining of Pax3$^+$ Cells in E20 Midbrain.**
Immunohistochemical staining of E20 section using Pax3 primary antibodies and a biotin-streptavidin-peroxidase system visualised with DAB. Dark brown Pax3c+ (**A**) and Pax3d+ (**B**) cells are throughout the midbrain as indicated by arrows.

In the E20 body, sparse Pax3d$^+$ cells are seen within the peritoneal cavity in the region of the ileum while no Pax3c$^+$ cells are seen (results not shown). Pax3c$^+$ staining is also detected in the nuclei of trunk skeletal muscle (Figure 5.19) and within the panniculus carnosus muscle located directly beneath the skin (Figure 5.20) while Pax3d$^+$ cells are not observed in these regions. The presence of positive cells in the midbrain and within the body confirms E20 embryonic RT-PCR assays demonstrating *Pax3c* and *Pax3d* expression in head and body (less skin) while immunohistochemical staining results of the skin highlight differential expression of Pax3c and Pax3d in the skin and support RT-PCR findings that *Pax3c* is expressed in murine E20 skin while *Pax3d* is not expressed.

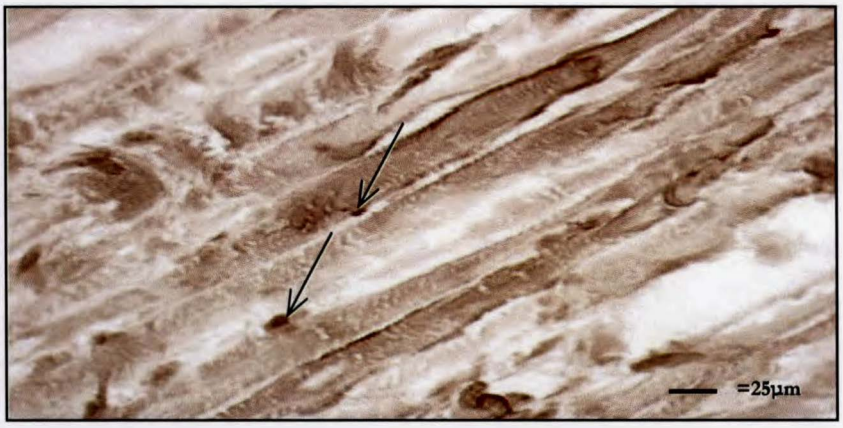

Figure 5.19. **Immunohistchemical Staining of Pax3c+ Cells in E20 Skeletal Muscle.**

Immunohistochemical staining of E20 section using Pax3c primary antibody and a biotin-streptavidin-peroxidase system visualised with DAB. Dark brown Pax3c+ nuclei are seen at the periphery of the sarcolemma.

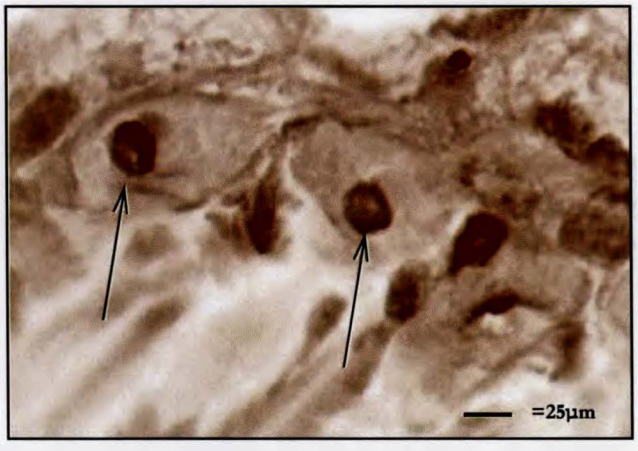

Figure 5.20. **Nuclear Pax3c Proteins in Panniculus Carnosus Cells.**

Immunohistochemical staining of E20 section using Pax3c primary antibody and a biotin-streptavidin-peroxidase system visualised with DAB. Dark brown Pax3c+ cells are seen in the panniculus carnosus muscle as indicated by arrows.

In summary, Pax3 immunohistochemical staining of frozen sections throughout stages of murine embryogenesis reveals that Pax3d is constitutively expressed and appears to have distinct spatial and temporal expression patterns relative to Pax3c. Differences in Pax3c and Pax3d protein expression seen in our experiments are summarised in Table 9.

Table 7. **Overview of Pax3 Protein Expression in Stages of Murine Embryogenesis.**

	Pax3c^{+} *cells...*	*Pax3d*$^{+}$ *cells...*
E12.5	distributed evenly throughout the entire dermis with concentrated staining in the buccal, vibrassal and tail regions of the embryo.	sparsely distributed solely in buccal, vibrassal, and tail regions of the dermis.
E15	sparsely located in the epidermis, with few scattered cells in the dermis. observed in the panniculus carnosus. located in the midbrain.	concentrated in the epidermis with almost no cells within the dermis. observed in the panniculus carnosus. located in the midbrain.
E20	located in developing hair follicles, few cells seen in the epidermis. distributed in thoracic body wall skeletal muscle and panniculus carnosus muscle. observed throughout the midbrain.	not apparent in the skin. sparsely distributed within the peritoneal cavity in the region of the ileum. observed throughout the midbrain.

6

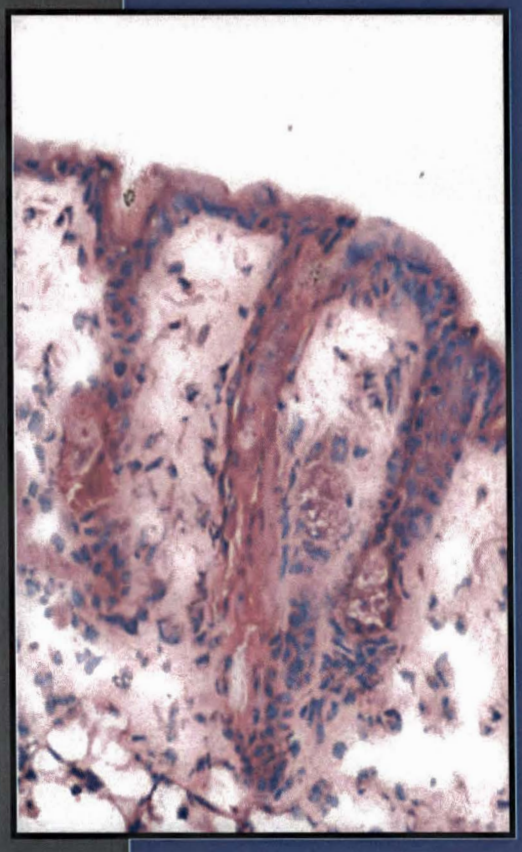

DISCUSSION

6.1 *Pax3* Expression in Embryogenesis

The impetus for this research originated due to two studies reporting aberrant *PAX3* expression in CMM. In 1999, Scholl *et al.* reported that *PAX3* expression in CMM was "unambiguously confined to tumour cells and not detected in surrounding normal tissue, normal skin sections, or sections of benign lesions." Barr *et al.* (1999) demonstrated that the predominant *PAX3* transcript in CMM splices the eighth exon to a "previously uncharacterised ninth exon" thus sparking a particular interest in the possible relationship of this alternative transcript to tumourigenesis in CMM.

The first objective became to assess whether the alternative PAX3D/*Pax3d* transcript is a cryptic splice form observed only in tumour cells or a functional transcript utilised in cell development or specification. In a GenBank search for *PAX3* transcripts with alternative 3' ends, two published expressed sequence tags from a human melanocyte cDNA library (GenBank H82467 and H97691) were found, implying that two alternate transcripts are expressed in melanocytic cells. Moreover, a sequence encoding an identical COOH-terminal to the Pax3d transcript was found in a cloned quail *Pax3* cDNA (GenBank AF000673). The finding of an identical COOH-terminal region encoded by the quail *Pax3* gene suggested that the Pax3d 3' region is conserved. Therefore, a central aim of this research became to determine the *Pax3* transcripts expressed during normal murine melanocytic development and ascertain evidence of the expression of the alternative *Pax3d* transcript during normal murine embryogenesis.

Murine embryos were assayed for both *Pax3c* and *Pax3d* mRNA and protein expression during embryogenesis; in particular, key stages of melanocytic development were analysed. Embryonic day 11 was chosen to reflect the stage when melanoblasts are known to migrate from the neural crest. It was not possible to isolate neural crest cells at this stage , however at E11, *Pax3c* and *Pax3d* transcripts are expressed in whole embryo extracts,

indicating an early role for both transcripts in murine embryogenesis. Immunohistochemical analysis of Pax3 in embryos at this stage remains to be analysed.

Embryonic day 12.5 was chosen to investigate *Pax3* expression at a point in murine development when synchronous migration of melanoblasts from the dermis into the epidermis is known to occur. Segregation of skin from these embryos was unsuccessful; therefore, mRNA *Pax3c* and *Pax3d* expression noted in the RT-PCR assays of head and body samples alluded to transcriptional activity in either neural, muscle or melanocytic lineages at this stage. The immunohistochemical staining for Pax3c and Pax3d proteins, however, showed clear evidence of their expression within the E12.5 skin; furthermore, no visible staining was apparent in skeletal muscle and brain. In the E12.5 sections, Pax3c and Pax3d positive cells are noted in the dermis patterned in a way resembling streams of cells "migrating" from the dermis toward the dermal-epidermal border. This pattern of staining was evident throughout the entire dermis for Pax3c+ cells, while primarily regions of the mouth, nose and tail showed Pax3d+ cells in the dermis. The results of these assays are original evidence for the conserved role of the Pax3d transcription factor as early as embryonic day 11 with explicit, yet not exclusive, roles in murine melanocytic development.

At embryonic day 15 melanoblasts are known to migrate from the epidermis into developing hair follicles. At E15, all segregated tissue samples (head, body and skin) show *Pax3c* and *Pax3d* transcript expression (with the exception of one sample) thus suggesting a role for both transcripts in neural, muscle and melanocytic cells at this stage of murine development. Immunohistochemical staining for Pax3c and Pax3d proteins reveal positive cells located within the midbrain and panniculus carnosus muscle. These combined assays are original evidence for the conserved role of the Pax3d

transcription factor in the development of the brain and panniculus carnosus muscle in murine development.

In the E15 skin, Pax3c+ cells are sparsely distributed in the epidermis with heavy staining evident within the developing hair follicles. This is in contrast to Pax3d positive staining which is heavily distributed in the epidermis with few positive cells seen within developing hair follicles. This pattern of staining may indicate that Pax3c+ cells localise in the developing hair follicles prior to Pax3d+ cells, or that cells which successfully migrate to the developing hair placode subsequently express Pax3c at this stage, while cells that remain within the epidermis continue to express Pax3d prior to their migration to the hair follicle. In either case, this seemingly spatial demarcation between protein expression in melanoblasts at this stage is possibly related to functional diversity for the two transcription factors.

Perinatally, at embryonic day 20, melanogenesis in the hair bulb has commenced and melanin synthesis indicates an advanced stage of melanocytic differentiation. In the E20 mRNA assays, *Pax3c* expression is again evident in skin as well as in all the segregated tissue samples indicating a continued role for the transcription factor in the development of skin, brain and skeletal muscle at this stage of murine development. Pax*3d* expression is evident within the head and body samples, while skin samples lack mRNA expression at this stage. Immunohistochemical staining for Pax3c and Pax3d proteins confirm positive cells located in midbrain, thus reconfirming a role for both isoforms in development of the brain. While Pax3c proteins are evident in skeletal muscle and panniculus carnosus, Pax3d positive cells are evident in the region of the ileum again supporting a spatial demarcation of protein expression that may be related to functional diversity. Finally, Pax3c positive cells are observed in developing hair follicles proximal to the dermal papilla; whereas, Pax3d positive cells are not stained within the epidermis or hair follicles. This difference in protein expression between Pax3c and Pax3d

within the E20 skin further supports the notion of a complex regulaton of melanocytic development through use of temporally expressed *Pax3* alternative transcripts.

Finally, it may be significant that *Pax3d* expression is not detected within normal murine melanocytes at and from E20 onwards (unpublished observations). These results clearly demonstrate a conserved role for the *Pax3d* transcription factor in the *early* development of the melanoblast, prior to differentiation and the cellular capability for synthesis of melanin.

6.2 *Pax3* Expression in Melanogenesis

Demonstration of a conserved role for *Pax3d* in the early stages of murine embryonal development prompted further investigation into specific expression of the isoform during the processes of melanoblast proliferation and migration during induced hair regrowth. In adult skin, following depilation, melanocytic stem cells of the hair follicle are known to proliferate, migrate to a region proximal to the dermal papilla and differentiate in order to produce melanin for the new hair (Nishimura *et al.,* 2002). Using a reliable time-scale for the strict coupling of melanogenesis to active hair regrowth (anagen), depilation experiments investigated *Pax3c* and *Pax3d* expression as melanoblasts undergo anagen induced proliferation, migration and differentiation within the hair follicle.

Following depilation, the first melanin pigments are visible within 96 hours. Knowing that *Pax3d* has an early role in the melanoblast, prior to melanin production, skin assays were conducted every 12 hours past induction of regrowth to focus on early events of anagen. It should be reiterated that, in murine skin following successful depilation, the only melanocytic cells remaining in the skin are those of the follicular stem cell niche; therefore, analyses of *Pax3* expression within the samples gives an indication of mitotic and post-mitotic melanocytic events in the early stages of melanogenesis.

In the depilation experiments, *Pax3* transcripts exhibit differential expression patterns during anagen lending further insight into their possible roles in melanogenesis. For example, *Pax3c* is initially expressed at 24 hours and is continuously expressed thereafter (up to 60 hours) while *Pax3d* is expressed solely in the period up to 12 hours past depilation and within the 36-48 hour post depilation period. Using the time-scale of Müller-Röver *et al.* (2001), follicular transition from resting state (telogen) to anagen occurs around 24 hours following depilation. Therefore, expression of *Pax3d* within the 12-hour period, much earlier than anagen induction, may indicate a role for this transcript in the proliferation of stem cells (Nishimura *et al.*, 2002) within the follicle. It should be noted that depilation induces a short healing response immediately thereafter; however, mRNA assays of wounded and healing murine skin do not demonstrate *Pax3d* expression (unpublished observations). Furthermore, *Pax3d* is also expressed within the 36 to 48 hour post depilation period as the follicle continues through the early stages of anagen. Again, this controlled temporal expression may be related to a secondary wave of melanoblast proliferation as progeny cells of the stem cell population undergo further mitosis (Nishimura *et al.*, 2002) prior to differentiation into pigmented melanocytes. If *Pax3d* expression seen in these experiments *is* linked to melanoblast proliferation, this could be an important link to the retention of proliferative capacity in CMM as compared to benign naevi (which lack *Pax3d* expression).

An alternate hypothesis may be that observed *Pax3d* expression is linked to migration of melanoblasts, initially in the 12 hours post depilation period as stem cells migrate from the niche prior to mitosis and then again between 36 to 48 hours post depilation as post mitotic cells migrate from the bulge area toward the dermal papilla. In our murine embryonic mRNA assays, *Pax3d* expression is demonstrated at all times of melanoblast migration; therefore, supporting this hypothesis. If then, *Pax3d* expression has a role in

melanoblast migration, this could be an important link to the highly metastatic capabilities of CMM.

Conversely, in the 12-hour period past depilation, *Pax3c* expression is not demonstrated. This lack of expression indicates that *Pax3c* may not have a role in the events prior to anagen induction. Moreover, *Pax3c* expression directly correlates to the onset of anagen at 24 hours and continues through anagen until the onset of melanin production. This is not unexpected, however, as *Pax3* is known to regulate genes involved in melanin synthesis, such as Mitf-m and tyrosinase-related protein-1 (Galibert *et al.,* 1999). Finally, it should be noted that in the 36 to 48 hour period post depilation, both *Pax3c* and *Pax3d* transcripts are concurrently expressed within the samples. Further studies are required to investigate concurrent intracellular *Pax3c* and *Pax3d* expression in order to gain insight into possible dosage effects for the two transcription factors and their individual and specific roles. Such experiments would include *in situ* hybridisation with transcript specific probes followed by CHIP (Chromosomal Hybridisation Immunoprecipitation) assays to determine transcript specific target gene sequences.

6.3 Correlation Studies of *Pax3* and *c-Kit* Expression

Another objective of the research was to link aberrant *Pax3c* and *Pax3d* transcript expression in CMM to regulation of downstream target genes. *c-Kit* and *Mitf-m* were chosen as potential targets regulated by Pax3c and Pax3d (in particular) as *c-Kit* and *Mitf-m* have key roles in melanocytic cell development. *c-Kit* became an important candidate for investigation as *c-Kit* expression is downregulated in CMM and Pax3 is a known gene repressor. Furthermore, analysis of the *c-Kit* promotor element sequence revealed potential binding sites for *Pax3* transcription factors. Finally, mutations in the *c-Kit* locus of the mouse result in failure of stem cell populations to migrate and/or proliferate effectively due to loss of the tyrosine kinase receptor (Geissler *et al.,* 1988). As

our previous experiments had shown an early role for *Pax3d* in melanogenesis, possibly in proliferation and/or migration of melanocytic stem cells, the possibility of aberrant *Pax3d* downregulation of *c-Kit* in CMM was proposed and expression therefore investigated.

mRNA analyses of *c-Kit* expression in murine embryogenesis was not undertaken, however, as the *c-Kit* encoded transmembrane tyrosine kinase receptor for stem cell factor (SCF) is required for normal hematopoiesis, melanogenesis, gametogenesis (Geissler *et al.,* 1988) and development of the smooth musculature of the gastrointestinal tract (Huizinga *et al.*,1995). Thus detection of *c-Kit* mRNA would be expected in *all* embryonic mRNA assays and be inconclusive. It was decided, rather, that investigation of *c-Kit* expression in the depilation model would provide a more conclusive model for study of melanogenesis. In the depilation experiments, *c-Kit* expression is seen in all time periods, immediately following depilation and throughout anagen hair regrowth. These results allow us to conclude that *c-Kit* expression is not linked to *Pax3c* expression; its expression both precedes and continues together with that of *Pax3c.* Furthermore, *c-Kit* expression is concurrent with *Pax3d* expression early in anagen while loss of *Pax3d* expression during a 36 hour period in which *c-Kit* continues to be expressed certainly negates evidence of *c-Kit* downregulation by *Pax3d.* These results clearly indicate a lack of direct correlation between the *Pax3* and *c-Kit* genes in our murine melanogenesis model and allow us to conclude that aberrant *PAX3D* expression does not contribute to the progression of CMM through repression of the *c-KIT* gene.

6.4 Correlation Studies of *Pax3* and *Mitf-m* Expression

It was important to correlate the expression of *Pax3* and *Mitf-m* in melanogenesis as *Pax3* is known to synergistically up-regulate *Mitf-m* together with *Sox10* (Potterf *et al.,* 2000). In the embryonic mRNA assays and depilated

skin samples tested, where *Mitf-m* expression is demonstrated, *Pax3c* expression is seen as well (18/19 samples). However, in the E12.5 embryo *Mitf-m* expression is *not* detected while *Pax3c* expression is. In the least, this result indicates that while *Mitf-m* expression may be reliant on *Pax3c* to initiate expression, *Pax3c* expression is not solely required for maintenance of *Mitf-m* expression. Finally, no apparent correlation is evident between *Mitf-m* and *Pax3d* expression in our experiments as both inverse and overlapping expression is randomly seen in embryogenesis and early anagen hair re-growth. While a double dosage effect due to concurrent *PAX3C* and *PAX3D* expression such as is seen in CMM *may* effect MITF-M upregulation, these results allow us to conclude that aberrant *PAX3D* expression does not solely contribute to the progression of CMM through transactivation of *MITF-M.*

6.5 *PAX3* Expression in CMM

The hypotheses that aberrant *PAX3* expression is linked to disruption of normal *c-Kit* or *Mitf-m* expression in CMM are null; however, our study has clarified significant aspects of *PAX3/Pax3* expression in normal melanocytic cells therefore providing a greater framework for investigations of the role of *PAX3* in the tumouricity of melanocytes seen in CMM. To begin with, the *PAX3/Pax3* gene is known to play a role in the early morphogenesis of the embryo being informally referred to as a "developmental control gene"; it is currently thought that terminal cellular differentiation follows downregulation of the *PAX3/Pax3* gene. Our study has supported this notion as we saw *Pax3* mRNA expression in murine skin ceasing at embryonic day 20. Therefore, the *re*-expression of this developmental control gene in metastatic CMM biopsies, primary CMM tumours and melanoma cell lines (page 74, Scholl *et al.;* 1999; Barr *et al.;* 1999) may be theorised as a consequence of three cellular circumstances.

Firstly, re-expression of *PAX3* in CMM may be a consequence of aberrant transcriptional regulation by *its* upstream genes. A known regulator of *PAX3* transcription, N-Myc is found expressed in CMM (Harris *et al.*, 2002; Bauer *et al.*, 1990; Shin *et al.*, 1987). Another *PAX3* regulator, Tead2, is not found expressed in CMM (Milewski *et al.*, 2004), therefore, future experiments are required to examine correlations between *N-Myc* and *PAX3* in CMM to determine whether *PAX3* upregulation is a consequence of upstream gene targeting.

Secondly, *PAX3* re-expression may be a consequence of the neoplastic melanocyte, once perturbed by a mutagenic event, undergoing a series of de-differentiation steps, taking it back to a stem cell state. Indeed, Mark Keating and his colleagues at Harvard Medical School in Boston, Massachusetts, have previously described a way to induce the de-differentiation of cells through genetic manipulation (Odelburg *et al.*, 2000). Many CMM pathologists theorise that de-differentiation occurs within one or several melanocytes located in a nest of atypical naevi which ultimately results in malignancy. This being the case, however, it would seem that the probability of finding some *PAX3* expression within benign biopsies would exist (and in fact increase with an increase in naevi numbers) as random naevi cells progressively de-differentiate through devlopmntal stages and re-express *PAX3*. However, Scholl *et al.* (1999) saw *PAX3* expression strictly limited to cancerous melanocytes; they saw no *PAX3* expression in normal perilesional skin or benign naevi samples. This leads to the possibility that a third oncogenic event causes the re-expression of *PAX3* in CMM. In our depilation experiments, *Pax3* re-expression in adult murine skin is seen with the induction of anagen hair regrowth (almost certainly) related to proliferation or migration of melanoblasts or quiescent melanocytic precursor cells as they repopulate hair follicles. If induced melanocytic apoptosis, such as is seen with excessive UV exposure, leads to cell replacement from a stem cell population, perhaps

subsequent mutagenesis of mitotic or post-mitotic replacement cells occurs in CMM resulting in cell "suspension" at a stage in which *PAX3* expression is typical.

In any case, several significant points have been raised that require further investigation. For example, is the clinical finding of *PAX3* mRNA expression in skin (the *PAX3D* isoform in particular) valid as a tumour marker for CMM malignancy? Does the expression of *PAX3* occur in serological studies of CMM patients and if so, does this clinically indicate CMM metastates? Finally, if *PAX3* expression tightly correlates with the undifferentiated melanoblast cell state as we saw in our study, would inactivation of the gene be sufficient to induce sustained regression of CMM due to ensuing differentiation of tumour cells into melanocytes?

In conclusion, future studies of the CMM phenotype would benefit from continued investigation of gene expression patterns, particularly those involved in cell proliferation and migration (such as *PAX3*) during embryonal patterning and development. As we continue to uncover the cellular events that take place during the transformation of the undifferentiated stem cell to the terminally differentiated adult cell, we may discover key players responsible for the propagation of neoplastic cell properties.

7

REFERENCES

REFERENCES

Abdel-Malek, Z.A., Swope,V.B. & Suzuki, I. (1995). Mitogenic and melanogenic stimulation of normal human melanocytes by melanotropic peptides. *Proc. Natl. Acad. Sci. U S A 92,* 1789-1793.

Albino, A.P., Reed, J.A. & McNutt, N.S. (1997). Molecular Biology of Cutaneous Malignant Melanoma. *Cancer: Principles and Practice of Oncology.* (DeVita, Hellman & Rosenberg, Editors). New York, Lippencott-Raven, pp 1935-1946.

Allsopp, T.E., Wyatt, S., Paterson, H.F. & Davies, A.M. (1993). The proto-oncogene Bcl-2 can selectively rescue neurotrophic factor-depenedent neurons from apoptosis. *Cell 73*: 295-307.

Alvino, E., Marra, G., Pagani, E., Falcinelli, S., Pepponi, R., Perrera, C., Haider, R., Castiglia, D., Ferranti, G., Bonmassar, E., Jiricny, J., Zambruno, G. & D'Atri, S. (2002). High-frequency microsatellite instability is associated with defective DNA mismatch repair in human melanoma. *J Invest Dermatol. 118*(1):79-86.

Amae, S., Fuse, N., Yasumoto, K., Sato, S., Yajima, I., Yamumoto, H., Udono, T., Durlu, Y.K., Tamai, M., Takahashi, K., Shibahara, S. (1998). Identification of a novel isoform of micropthalmia-associated transcription factor that is enriched in retinal pigment epithelium. *Biochem. Biophys. Res. Commun. 247*: 710-715.

Aoki, H. & Moro, O. (2002).n Involvement of micropthalmia-associated transcription factorn(MITF) in expression of human melanocortin -1 receptor (MCIR). *Life Sci:71*(18): 2171-9.

Asher, J.H. Jr, Harrison, R.W., Morell, R., Carey, M.L. & Friedman, T.B. (1996). Effects of Pax3 modifier genes on craniofacial morphology, pigmentation, and viability: a murine model of Waardenburg syndrome variation. *Genomics 34*(3):285-98.

Bacharach-Buhles, M., Lubowietzki, M. & Altmeyer, P. (1999). Dose-dependent shift of apoptotic and unaltered melanocytes into the dermis after irradiation with UVA 1. *Dermatology 198*(1), 5-10.

Baker CV, Stark MR, Bronner-Fraser M. (2002). Pax3-expressing trigeminal placode cells can localize to trunk neural crest sites but are committed to a cutaneous sensory neuron fate. *Dev Biol. 249*(2):219-36.

Baldi A, Santini D, Battista T, Dragonetti E, Ferranti G, Petitti T, Groeger AM, Angelini A, Rossiello R, Baldi F, Natali PG, Paggi MG. (2001). Expression of AP-2 transcription factor and of its downstream target genes c-kit, E-cadherin and p21 in human cutaneous melanoma. *J Cell Biochem. 83*(3):364-72.

Baldwin CT, Hoth CF, Amos JA, da-Silva EO, Milunsky A. (1992). An exonic mutation in the HuP2 paired domain gene causes Waardenburg's syndrome. *Nature 355*(6361):637-8.

Bale, S.J., Chakravarti, A. & Greene, M.H. (1986). Cutaneous malignant melanoma and familial dysplastic nevi: evidence for autosomal dominance and pleiotropy. *Am. J. Hum. Genet. 38*, 188-196.

Bale, S.J., Dracopoli, N.C., Tucker, M.A., Clark, W.H., Fraser, M.C., Stanger, B.Z., Green, P., Donis-Keller, H., Housman, D.E. & Greene, M.H. (1989). Mapping the gene for hereditary cutaneous malignant melanoma-dysplastic nevus to chromosome 1p. *New Eng. J. Med. 320*, 1367-1372.

Barber, T.D., Barber, M.C., Cloutier, T.E. & Friedman, T.B. (1999). PAX3 gene structure, alternative splicing and evolution. *Gene 237*, 311-319.

Barberis A, Pearlberg J, Simkovich N, Farrell S, Reinagel P, Bamdad C, Sigal G, Ptashne M. (1995). Contact with a component of the polymerase II holoenzyme suffices for gene activation. *Cell 81*(3):359-68.

Barker, D., Dixom, K., Medrano, E. E., Smalara, D., Im, S., Mitchell, D., Bab, G. & Abdel-Malek Z. A. (1995). Comparison of the responses of human melanocytes with different melanin contents to ultraviolet B irradiation. *Cancer Res. 15*(18), 4041-6.

Barnhill, R.L. & Mihm, M.C. (1993). The histopathology of cutaneous malignant melanoma. *Semin. Diagn. Pathol. 10*:47-75.

Barr, F.G., Fitzgerald, J.C., Ginsberg J.P., Vanella, M.L., Davis, R.J. & Bennicelli, J.L. (1999). Predominant expression of *PAX3* and *PAX7* forms in myogenic and neural tumor cell lines. *Cancer Res. 59*, 5443-5448.

Beermann, F., Schmid, E., and Schütz, G. (1992). Expression of the mouse tyrosinase gene during embryonic development: Recapitulation of the temporal regulation in transgenic mice. *Proc. Natl. Acad. Sci. 89:* 2809-2813

Bennicelli, J.L., Edwards, R.H. & Barr, F.G. (1996). Mechanism for transcriptional gain of function resulting from chromosomal translocation in alveolar rhabdomyosarcoma. *Proc. Natl. Acad. Sci. U S A 93*, 5455-9.

Bentley, N.J., Eisen, T. & Goding, C.R. (1994). Melanocyte-specific expression of the human tyrosinase promoter: activation by the microphthalmia gene product and role of the initiator. *Mol. Cell Biol. 14*, 7996-8006.

Bittner, M., Meltzer, P., Chen, Y., Jiang, Y., Seftor, E., Hendrix, M., Radmacher, M., Simon, R., Yakhini, Z., Ben-Dor, A., Sampas, N., Dougherty, E., Wang, E., Marincola, F., Gooden, C., Lueders, J., Glatfelter, A., Pollock, P., Carpten, J., Gillanders, E., Leja, D., Dietrich, K., Beaudry, C., Berens, M., Alberts, D. and Sondak, V. (2000). Molecular classification of cutaneous malignant melanoma by gene expression profiling. *Nature 406*, 536-540.

Black DL, Chabot B, Steitz JA. (1985). U2 as well as U1 small nuclear ribonucleoproteins are involved in premessenger RNA splicing. *Cell 42*(3):737-50.

Bladt, F., Riethmacher, D., Isenmann, S., Aguzzi, A., Birchmeier, C. (1995). Essential role for the c-met receptor in the migration of myogenic precursor cells into the limb bud. *Nature 376*, 768-71.

Blake J, Ziman MR. (2003). Aberrant PAX3 and PAX7 expression. A link to the metastatic potential of embryonal rhabdomyosarcoma and cutaneous malignant melanoma? *Histol Histopathol. 18*(2):529-39.

Bauer J, Sokol L, Stribrna J, Kremen M, Krajsova I, Hausner P, Hejnar P. (1990). Amplification of N-myc oncogene in human melanoma cells. *Neoplasia 37*(3):233-8.

Bober E, Franz T, Arnold HH, Gruss P, Tremblay P. (1994). Pax-3 is required for the development of limb muscles: a possible role for the migration of dermomyotomal muscle progenitor cells. *Development 120*(3):603-12.

Bopp, D., Burri, M., Baumgartner, S., Frigerio, G. & Noll, M. (1986). Conservation of a large protein domain in the segmentation gene paired and in functionally related genes of Drosophila. *Cell 47*, 1033-1040.

Botchkareva NV, Khlgatian M, Longley BJ, Botchkarev VA, Gilchrest BA. (2001). SCF/c-kit signaling is required for cyclic regeneration of the hair pigmentation unit. *FASEB J. 15*(3):645-58.

Bottaro, D.P., Rubin, J.S., Faletto, D.L., Chan, A.M., Kmiecik, T.E., Vande Woude, G.F. & Aaronson, SA. (1991). Identification of the hepatocyte growth factor receptor as the c-met proto-oncogene product. *Science 251*, 802-4.

Breslow, A. (1975). Tumour thickness, level of invasion and node dissection in stage I cutaneous melanoma. *Annals of Surgery 182:* 572.

Broudy VC. (1997). Stem cell factor and hematopoiesis. *Blood 90*(4):1345-64.

Burri, M., Tromvoukis, Y., Bopp, D., Frigerio, G. & Noll, M. (1989). Conservation of the paired domain in metazoans and its structure in three isolated human genes. *EMBO J. 4*, 1183-1190.

Chalepakis G, Gruss P. (1995). Identification of DNA recognition sequences for the Pax3 paired domain. *Gene 162*(2):267-70.

Chalepakis, G., Jones, F.S., Edelman, G.M. & Gruss, P. (1994). *Pax-3* contains domains for transcription activation and transcription inhibition. *Proc. Natl. Acad. Sci. USA. 91*, 12745-12749.

Chalepakis, G., Stoykova, A., Wijnholds, J., Tremblay, P. & Gruss, P. (1993). Pax: gene regulators in the developing nervous system. *J. Neurobiol. 24*, 1367-1384.

Cheng SC, Abelson J. (1987). Spliceosome assembly in yeast. *Genes Dev 1*(9):1014-27

Chisholm AD, Horvitz HR. (1995). Patterning of the Caenorhabditis elegans head region by the Pax-6 family member vab-3. *Nature 377*(6544):52-5.

Cillo, C., Faiella, A., Cantile, M. & Boncinelli, E. (1999). Homeobox genes and cancer. *Exp Cell Research 248*, 1-9.

Clark, W.H., Ainsworth, A.M., Bernardino, E.A., Yang, C.H., Mihm, M.C. and Reed, R.J. (1975). The developmental biology of primary human

malignant melanomas. *Seminars in Oncology 2:* 83.

Cvekl A, Kashanchi F, Brady JN, Piatigorsky J. (1999). Pax-6 interactions with TATA-box-binding protein and retinoblastoma protein. *Invest Ophthalmol Vis Sci. 40*(7):1343-50.

Dracopoli, N.C., Bale, S.J & Housman, D.E. (1989). Assignment of the familial melanoma gene to chromosome 1p36: frequent loss of heterozygosity of this region occurs late in tumor progression. *Am. J. Hum. Genet. 45*, A19.

Davis, N.C. (1982). Malignant Melanoma: Clinical Presentation and Differential Diagnosis. In: Emmett, A.J. and O'Rourke, M.G. (eds) *Malignant Skin Tumours* (2nd Ed). Churchill Livingstone, Melbourne.

Dellon AL, Edelson RL, Chretien PB. (1976). Defining the malignant potential of the giant pigmented nevus. *Plast Reconstr Surg. 57*(5):611-8.

Dorfler P, Busslinger M. (1996). C-terminal activating and inhibitory domains determine the transactivation potential of BSAP (Pax-5), Pax-2 and Pax-8. *EMBO J. 15*(8):1971-82.

Elder, D.E., Green, M.H., Guerry, D.I., Kraemer, K.H. and Clark, W.H. Jr. (1982). The dysplastic naevus syndrome. Our definition. *American Journal of Dermapathology 4:* 455.

Eller MS, YaarM, Gilcrest BA. (1994). DNA damage and melanogenesis. *Nature 372:* 413-414.

Epstein, D.J., Malo, D., Vekemans, M. & Gros, P. (1991). Molecular characterization of a deletion encompassing the splotch mutation on mouse chromosome 1. *Genomics 10*, 89-93.

Epstein, J.A., Lam, P., Jepeal, L., Maas, R.L. & Shapiro, D.N. (1995). Pax3 inhibits myogenic differentiation of cultured myoblast cells. *J. Biol. Chem. 270* ,11719-22.

Epstein JA, Shapiro DN, Cheng J, Lam PY, Maas RL. (1996). Pax3 modulates expression of the c-Met receptor during limb muscle development. *Proc Natl Acad Sci U S A. 93*(9):4213-8.

Ferguson, C.A. and Kidson, S.H. (1997). The regulation of tyrosinase gene transcription. *Pigment Cell. Res. 10:* 127-138.

Fidler, I.J. (1970). Metastasis: Quantitative analysis of distribution and fate of tumor emboli labelled with 125I-5-iodo-2'-deoxyuridine. *J. Natl. Cancer I. 45*, 775.

Fitzpatrick, T. B., Elsen, A. Z. & Wolff, K. Vitiligo. *Dermatology in General Medicine.* 3rd ed. (ed. Fitzpatrick, T. B.) p 810. McGraw Hill, New York, 1987.

Fortin, A.S., Underhill, D.A. & Gros, P. (1998). Helix 2 of the paired domain plays a key role in the regulation of DNA-binding by the Pax-3 homeodomain. *Nucl Acids Res*: 4574-4581.

Fortin AS, Underhill DA, Gros P. (1997). Reciprocal effect of Waardenburg syndrome mutations on DNA binding by the Pax-3 paired domain and homeodomain. *Hum Mol Genet. 6*(11):1781-90.

Fountain, J.W., Bale, S.J., Housman, D.E. & Dracopoli, N.C. (1990). Genetics of melanoma. *Cancer Surv. 9*, 645-671.

Franz, T. (1990). Defective ensheathment of motoric nerves in the splotch mutant mouse. *Acta Anat. 138*, 246- 252.

Galibert, MD., Yavuzer, U., Dexter T.J. & Goding C.R. (1999). Pax3 and regulation of the -specific tyrosinase-related protein-1 promoter. *J. Biol. Chem. 274*, 26894-26900.

Galli SJ, Zsebo KM, Geissler EN. (1994). The kit ligand, stem cell factor. *Adv Immunol. 55*:1-96.

Ganss, R., Montoliu, L., Monaghan, A.P., and Schutz, G. 1994a. A cell-specific enhancer far upstream of the mouse tyrosinase gene confers high level and copy number-related expression in transgenic mice. *EMBO J. 13:* 3083-3093

Gaudreau L, Adam M, Ptashne M. (1998). Activation of transcription in vitro by recruitment of the yeast RNA polymerase II holoenzyme. *Mol Cell 1*(6):913-6.

Geissler, E. N.; Ryan, M. A.; Housman, D. E. (1988). The dominant-white spotting (W) locus of the mouse encodes the c-kit proto-oncogene. *Cell 55*: 185-192.

Giebel LB, Spritz RA. (1991). Mutation of the KIT (mast/stem cell growth factor receptor) protooncogene in human piebaldism. *Proc Natl Acad Sci U S A; 88*(19): 8696-9.

Goodman RM, Caren J, Ziprkowski M, Padeh B, Ziprkowski L, Cohen BE. (1971). Genetic considerations in giant pigmented hairy naevus. *Br J Dermatol. 85*(2):150-7.

Goulding, M.D., Chalepakis, G., Deutsch, U., Erselius, J.R. & Gruss, P. (1991). Pax-3, a novel murine DNA binding protein expressed during early neurogenesis. *EMBO J. 10*, 1135-1147.

Green MR. (1991). Biochemical mechanisms of constitutive and regulated pre-mRNA splicing. *Annu Rev Cell Biol.7*:559-99.

Greene, M.H., Clark, W.H., Tucker, M.A., Elder, D.E., Kraemer, K.H., Guerry, D., Witmer, W.K., Thompson, J., Matozzo, I. & Fraser, M.C. (1985). Acquired precursors of cutaneous malignant melanoma. The familial dysplastic nevus syndrome. *N. Engl. J. Med. 312*, 91-97.

Grichnik, J. M., Burch, J. A., Burchette, J. & Shea, C. R. (1998). The SCF/KIT pathway plays a critical role in the control of normal human melanocyte homeostasis. *J. Invest. Dermatol. 111,* 233-238.

Halaban, R., Langdon, R., Birchall, N. (1988). Basic fibroblast growth factor from human keratinocytes is a natural mitogen for melanocytes. *J. Cell Biol. 107,* 1611-1619.

Haley JC, Hood AF, Chuang TY, Rasmussen J. (2000). The frequency of histologically dysplastic nevi in 199 pediatric patients. *Pediatr Dermatol. 17*(4): 266-9.

Harris RG, White E, Phillips ES, Lillycrop KA. (2002). The expression of the developmentally regulated proto-oncogene Pax-3 is modulated by N-*Myc. J Biol Chem. 277*(38):34815-25.

Hashimoto, K. (1970). The ultrastructure of the skin of human embryos. V. The hair germ and perifollicular mesenchymal cells, hair germ-mesemchymal interaction. *Br. J. Dermatol. 83*, 167.

Hashimoto, K. (1971). The ultrastruscture of human embryos. VIII. Melanoblast and interfollicular melanocyte. *J. Anat.108,* 99.

Heanue, T.A., Reshef, R., Davis, R.J., Mardon, G., Oliver, G., Tomarev, S., Lassar, A.B. & Tabin, C.J. (1999). Synergistic regulation of vertebrate muscle development by Dach2, Eya2, and Six1, homologs of genes required for Drosophila eye formation. *Genes Dev.13*, 3231-43.

Hemesath, T.J., Price, E.R., Takemoto, C., Badalian, T., and Fisher, D.E. (1998). MAP kinase links the transcription factor Microphthalmia to c-Kit signalling in melanocytes. *Nature 391:* 298-301.

Henderson, D.J., Conwan, S.J. & Copp, A.J. (1999). Rib truncations and fusions in the Sp2H mouse reveal a role for Pax3 in specification of the ventro-lateral and posterior parts of the somite. *Dev. Biol. 209*, 143-158.

Hirobe, T. (1984). Histochemical survey of the distribution of the epidermal melanoblasts and melanocytes in the mouse during fetal and postnatal periods. *Anat. Rec. 208,* 589-594.

Hodgkinson, C.A., Moore, K.J., Nakayama, A., Steingrimsson, E., Copeland, N.G., Jenkins, N.A., and Arnheiter, H. (1993). Mutations at the mouse *microphthalmia* locus are associated with defects in a gene encoding a novel basic-helix-loop-helix-zipper protein. *Cell 74:* 395-404.

Hornyak, T.J., Hayes, D.J., Chiu, L.Y. & Ziff, E.B. (2001). Transcription factors in melanocyte development: distinct roles for Pax-3 and Mitf. *Mech. Dev.101*, 47-59.

Hu DN, Savage HE, Roberts JE. (2002). Uveal melanocytes, ocular pigment epithelium, and Muller cells in culture: in vitro toxicology. *Int J Toxicol* (6): 465-72.

Huizinga, J. D.; Thuneberg, L.; Kluppel, M.; Malysz, J.; Mikkelsen, H. B.; Bernstein, A. (1995). W/kit gene required for interstitial cells of Cajal and for intestinal pacemaker activity. *Nature 373*: 347-349.

Huang S, Jean D, Luca M, Tainsky MA, Bar-Eli M. (1998). Loss of AP-2 results in downregulation of c-KIT and enhancement of melanoma tumorigenicity and metastasis. *EMBO J. 17*(15):4358-69.

Huang S, Luca M, Gutman M, McConkey DJ, Langley KE, Lyman SD, Bar-Eli M. (1996). Enforced c-KIT expression renders highly metastatic human melanoma cells susceptible to stem cell factor-induced apoptosis and inhibits their tumorigenic and metastatic potential. *Oncogene 13*(11):2339-47.

Hussein MR, Wood GS. (2003). hMLH1 and hMSH2 gene mutations are present in radial growth-phase cutaneous malignant melanoma cell lines and can be induced further by ultraviolet-B irradiation. *Exp Dermatol; 12*(6):872-5.

Hussein MR, Sun M, Roggero E, Sudilovsky EC, Tuthill RJ, Wood GS, Sudilovsky O. (2002). Loss of heterozygosity, microsatellite instability, and mismatch repair protein alterations in the radial growth phase of cutaneous malignant melanomas. *Mol Carcinog; 34*(1):35-44.

Iida, S., Rao, P.H., Nallasivam, P., Hibshoosh, H., Butler, M., Louie, D.C., Dyomin, V., Ohno, H., Chaganti, R.S. & Dalla-Favera, R. (1996). The t(9; 14)(p13; q32) chromosomal translocation associated with lymphoplasmacytoid lymphoma involves the PAX-5 gene. *Blood 88*, 4110-4117.

Imokawa, G., Yada, Y. &Kimura, M. (1996). Signalling mechanisms of endothelian-induced mitogenesis in human melanocytes. *Biochem. J. 314,* 305-312.

Imber, M.J. & Mihm, M.C. (1990). Benign melanocytic tumors. (Farmer & Hood, Editors). *Pathology of the Skin.* Norwalk, CT, Appleton & Lange pp 663-683.

Ishikiriyama, S. (1993). Gene for Waardenburg syndrome type I is located at 2q35, not at 2q37.3. *Am. J. Med. Genet. 46*, 608.

Ito M, Kawa Y, Ono H, Okura M, Baba T, Kubota Y, Nishikawa SI, Mizoguchi M. (1999). Removal of stem cell factor or addition of monoclonal anti-c-KIT antibody induces apoptosis in murine melanocyte precursors. *J Invest Dermatol. 112*(5):796-801.

Jun, S. and Desplan, C. (1996). Cooperative Interactions between paired domain and homeodomain. *Development 122:* 2639-2650.

Kamaraju AK, Adjalley S, Zhang P, Chebath J, Revel M. (2004). C/EBP-delta induction by gp130 signaling. Role in transition to myelin gene expressing phenotype in a melanoma cell line model. *J Biol Chem. 279*(5):3852-61.

Kamb A, Gruis NA, Weaver-Feldhaus J, Liu Q, Harshman K, Tavtigian SV, Stockert E, Day RS 3rd, Johnson BE, Skolnick MH. (1994). A cell cycle regulator potentially involved in genesis of many tumor types. *Science; 264*(5157): 436-40.

Kawaguchi, Y., Mori, N. & Nakayama, A. (2001). Kit^+ melanocytes seem to contribute to melanocyte proliferation after UV exposure to precursor cells. *J. .Invest. Dermatol. 116* (6), 920-925.

Keaveney M, Struhl K. (1998). Activator-mediated recruitment of the RNA polymerase II machinery is the predominant mechanism for transcriptional activation in yeast. *Mol Cell;1*(6):917-24.

Kioussi, C., Gross, M.K. & Gruss P. (1995). Pax3: a paired domain gene as a regulator in PNS myelination. *Neuron 15*, 553-562.

Konarska MM, Sharp PA. Interactions between small nuclear ribonucleoprotein particles in formation of spliceosomes. *Cell; 49*(6):763-74.

Kraemer KH, Greene MH. (1985). Dysplastic nevus syndrome. Familial and sporadic precursors of cutaneous melanoma. *Dermatol Clin; 3* (2):225-37.

Kroll, T.G., Sarraf, P., Pecciarini, L., Chen, C.J., Mueller, E., Spiegelman, B.M. & Fletcher, J.A. (2000). PAX8-PPARgamma1 fusion oncogene in human thyroid carcinoma. *Science 9*, 1357-1360.

Krull, C.E. (1998). Inhibitory Interactions in the Patterning of Trunk Neural Crest Migration. *Annal. N.Y. Acad. Sci. 857*, 13-22.

Kunisada T, Lu SZ, Yoshida H, Nishikawa S, Nishikawa S, Mizoguchi M, Hayashi S, Tyrrell L, Williams DA, Wang X, Longley BJ. (1998). Murine cutaneous mastocytosis and epidermal melanocytosis induced by keratinocyte expression of transgenic stem cell factor. *J Exp Med. 187*(10):1565-73.

Lam BJ, Hertel KJ. (2002). A general role for splicing enhancers in exon definition. *RNA* (10):1233-41.

Lamey TM, Koenders A, Ziman M. (2004). Pax genes in myogenesis: alternate transcripts add complexity. *Histol Histopathol; 19*(4):1289-300.

Landi MT, Baccarelli A, Tarone RE, Pesatori A, Tucker MA, Hedayati M, Grossman L. (2002). DNA repair, dysplastic nevi, and sunlight sensitivity in the development of cutaneous malignant melanoma. *J Natl Cancer Inst. 94*(2): 94-101.

Lang D, Epstein JA. (2003). Sox10 and Pax3 physically interact to mediate activation of a conserved c-RET enhancer. *Hum Mol Genet; 12*(8):937-45.

Lang D, Chen F, Milewski R, Li J, Lu MM, Epstein JA. (2000). Pax3 is required for enteric ganglia formation and functions with Sox10 to modulate expression of c-ret. *J Clin Invest; 106*(8):963-71.

Lassam N, Bickford S. (1992). Loss of c-kit expression in cultured melanoma cells. *Oncogene 7*(1):51-6.

Lei, T. C., Vieira, W. D. & Hearing, V.J. (2002). In Vitro Migration of Melanoblasts Requires Matrix Metalloproteinase-2: Implications to Vitiligo Therapy by Photochemotherapy *Pigment Cell Research 15* (6):426.

Li J, Liu KC, Jin F, Lu MM, Epstein JA. (1999). Transgenic rescue of congenital heart disease and spina bifida in Splotch mice. *Development 126* (11):2495-503

Loo JC, Liu L, Hao A, Gao L, Agatep R, Shennan M, Summers A, Goldstein AM, Tucker MA, Deters C, Fusaro R, Blazer K, Weitzel J, Lassam N, Lynch H, Hogg D. (2003). Germline splicing mutations of CDKN2A predispose to melanoma. *Oncogene 25*; 22(41): 6387-94.

Lopansri, S. & Mihm, M.C. (1979). Clinical and pathological correlation of malignant melanoma. *J Cutan Pathol. 6*: 180-194.

Lund, H.Z. & Stobbe, G.D. (1949). The natural history of the pigmented nevus; factors of age and anatomic location. *Am J Pathol. 25*(6):1117-55, incl 4 pl.

Mackintosh, J. A. (2001). The antimicrobial properties of melanocytes, melanosomes and melanin and the evolution of black skin. *J. Theor. Biol. 211*(2), 101-103.

Manova K, Bachvarova RF. (1991). Expression of c-kit encoded at the W locus of mice in developing embryonic germ cells and presumptive melanoblasts. *Dev Biol.146*(2):312-24.

Maroto, M., Reshef, R., Munsterberg, A.E., Koester, S., Goulding, M. & Lassar, A.B. (1997). Ectopic Pax-3 activates MyoD and Myf-5 expression in embryonic mesoderm and neural tissue. *Cell 89*, 139-48.

Martin BL, Harland RM. (2001). Hypaxial muscle migration during primary myogenesis in Xenopus laevis. *Dev Biol. 239*(2):270-80.

Masuda M, Yamazaki K, Kanzaki J, Hosoda Y. (1994). Ultrastructure of melanocytes in the dark cell area of human vestibular organs: functional implications of gap junctions, isolated cilia, and annulate lamellae. *Anat Rec. 240*(4):481-91

Matsui Y, Zsebo KM, Hogan BL. (1990). Embryonic expression of a haematopoietic growth factor encoded by the Sl locus and the ligand for c-kit. *Nature 347*(6294):667-9.

Mayer, T.C. (1973). The migratory pathway of neural crest cells into the skin of mouse embryos. *Dev. Biol. 34*, 39-46.

McArdle, L., Rafferty, M., Maelandsmo, G., Bergin, O., Farr, C.J., Dervan, P.A., O'Loughlin, S., Herlyn, M. & Easty, DJ. (2001). Protein Tyrosine Phosphotase Genes Downregulated in Melanoma. *J. Invest. Dermatol. 117*, 1255-1260.

McGovern, V.J. and Murad, T. (1985). Pathology of melanoma: an overview. In: Balch C.M. and Milton, G.W. (eds) *Cutaneous melanoma.* Lipponcott, Philadelphia.

Milewski RC, Chi NC, Li J, Brown C, Lu MM, Epstein JA. (2004). Identification of minimal enhancer elements sufficient for Pax3 expression in neural crest and implication of Tead2 as a regulator of Pax3. *Development 131*(4):829-37.

Miskiewicz P, Morrissey D, Lan Y, Raj L, Kessler S, Fujioka M, Goto T, Weir M. (1996). Both the paired domain and homeodomain are required for in vivo function of Drosophila Paired. *Development 122*(9):2709-18.

Mitchell PJ, Tjian R. (1989). Transcriptional regulation in mammalian cells by sequence-specific DNA binding proteins. *Science 245*(4916):371-8.

Morelli JG, Kincannon J, Yohn JJ, Zekman T, Weston WL, Norris DA. (1991). Leukotriene C4 and TGF-alpha are stimulators of human melanocyte migration *in vitro. J Invest Dermatol 98:* 290-295.

Morell, R.; Spritz, R. A.; Ho, L.; Pierpont, J.; Guo, W.; Friedman, T. B.; Asher, J. H., Jr. (1997). Apparent digenic inheritance of Waardenburg syndrome type 2 (WS2) and autosomal recessive ocular albinism (AROA). *Hum. Molec. Genet.* 6: 659-664.

Mou K, Adamson CL, Davis RL. (1997). Stria vascularis morphogenesis in vitro. *Hear Res. 103*(1-2):47-62.

Mount SM, Pettersson I, Hinterberger M, Karmas A, Steitz JA. (1983). The U1 small nuclear RNA-protein complex selectively binds a 5' splice site in vitro. *Cell 33*(2):509-18.

Nakayama, A., Nguyen, M.T., Chen, C.C., Opdecamp, K., Hodgkinson, C.A., and Arnheiter, H. (1998). Mutations in microphthalmia, the mouse homolog of the human deafness gene MITF, affect neuroepithelial and neural crest-derived melanocytes differently. *Mech. Dev.* 70: 155-166.

Natali PG, Nicotra MR, Winkler AB, Cavaliere R, Bigotti A, Ullrich A. (1992). Progression of human cutaneous melanoma is associated with loss of expression of c-kit proto-oncogene receptor. *Int J Cancer 52*(2):197-201.

Nelson, K.K. & Green, M.R. (1988). Splice site selection and ribonucleoprotein complex assembly during in vitro pre-mRNA splicing. *Genes & Dev. 4*:89-97.

Nishikawa S, Kusakabe M, Yoshinaga K, Ogawa M, Hayashi S, Kunisada T, Era T, Sakakura T, Nishikawa S. (1991). In utero manipulation of coat color formation by a monoclonal anti-c-kit antibody: two distinct waves of c-kit-dependency during melanocyte development. *EMBO J. 10*(8):2111-8.

Nishimura, E.K., Jordan, S.A., Oshima, H., Yoshida, H., Osawa, M., Moriyama, M., Jackson, I.J., Barrandon, Y., Miyachi, Y. & Nishikawa, S. (2002). Dominant role of the niche in melanocyte stem-cell fate determination. *Nature 416*, 854-860.

Oakley, R.A. & Tosney, K.W. (1993). Contact-mediated mechanisms of motor axon segmentation. *J. Neurosci. 13*, 3773-3792.

Odelberg, SJ, Kollhoff, A, Keating, MT (2000). Dedifferentiation of mammalian myotubes induced by msx1. *Cell 103*, 1099-1109.

Opdecamp, K., Nakayama, A., Nguyen, M.T., Hodgkinson, C.A., Pavan, W.J., and Arnheiter, H. (1997). Melanocyte development in vivo and in neural crest cell cultures: Crucial dependence on the Mitf basic-helix-loop-helix-zipper transcription factor. *Development 124:* 2377-2386.

Ortonne JP, Prota G. (1993). Hair melanins and hair color: ultrastructural and biochemical aspects. *J Invest Dermatol. 101*(1 Suppl):82S-89S.

Padgett RA, Konarska MM, Grabowski PJ, Hardy SF, Sharp PA. (1984). Lariat RNA's as intermediates and products in the splicing of messenger RNA precursors. *Science 225*(4665):898-903.

Parker CJ, Shawcross SG, Li H, Wang QY, Herrington CS, Kumar S, MacKie RM, Prime W, Rennie IG, Sisley K, Kumar P. (2004). Expression of PAX 3 alternatively spliced transcripts and identification of two new isoforms in human tumors of neural crest origin. *Int J Cancer 108*(2):314-20.

Parker R, Siliciano PG, Guthrie C. (1987). Recognition of the TACTAAC box during mRNA splicing in yeast involves base pairing to the U2-like snRNA. *Cell 49*(2):229-39

Phelan, S.A. and Loeken, M.R. (1998). Identification of a New Binding Motif for the Paired domain of Pax-3 and Unusual Characteristics of Spacing of Bipartite Recognition Elements on Binding and Transcription Activation. *J. Biol. Chem. 273* (30), 19153-19159.

Peters EM, Tobin DJ, Botchkareva N, Maurer M, Paus R. (2002). Migration of melanoblasts into the developing murine hair follicle is accompanied by transient c-Kit expression. *J Histochem Cytochem. 50*(6):751-66.

Pikielny CW, Rymond BC, Rosbash M. (1986). Electrophoresis of ribonucleoproteins reveals an ordered assembly pathway of yeast splicing complexes. *Nature 324*(6095): 341-5.

Potterf SB, Furumura M, Dunn KJ, Arnheiter H, Pavan WJ. (2000). Transcription factor hierarchy in Waardenburg syndrome: regulation of MITF expression by SOX10 and PAX3. *Hum Genet. 107*(1):1-6.

Price, E.R., Ding, H.-F., Badalian, T., Bhattacharya, S., Takemoto, C., Yao, T.-P., Hemesath, T.J., and Fisher, D.E. (1998). Lineage-specific signalling in melanocytes: c-Kit stimulation recruits p300/CBP to Microphthalmia. *J. Biol. Chem. 273:* 17983-17986.

Pritchard C, Grosveld G, Hollenbach AD. (2003). Alternative splicing of Pax3 produces a transcriptionally inactive protein. *Gene 13*; 305(1):61-9.

Ptashne M. (1988). How eukaryotic transcriptional activators work. *Nature 335*(6192):683-9.

Puig, S., Ruiz, A., Lazaro, C., Castel, T., Lynch, M., Palou, J., Vilalta, A., Weissenbach, J., Mascaro, J.M. & Estivill, X. (1995). Chromosome 9p

deletions in cutaneous malignant melanoma tumors: the minimal deleted region involves markers outside the p16 (CDKN2) gene. *Am. J. Hum. Genet. 57*, 395-402.

Quaba, A.A. and Wallace, A.F. (1986). The incidence of malignant melanoma arising in large congenital nevocellular naevi. *Plastic and Reconstructive Surgery 27:* 305-307.

Query CC, Moore MJ, Sharp PA. (1994). Branch nucleophile selection in pre-mRNA splicing: evidence for the bulged duplex model. *Genes Dev. 8*(5):587-97.

Rawles, M. E. (1947). Origin of pigment cells from the neural crest in the mouse embryo. *Phys. Zool. 20,* 248-266.

Reed, J.A., Finnerty, B. & Albino, A.P. (1999). Divergent Cellular Differentiation Pathways during the Invasive Stage of Cutaneous Malignant Melanoma Progression. *Am. J. Pathol. 155*, 549-555.

Ruddon, RW. (1987). *Cancer Biology.* (2nd Ed.). Oxford University Press: Oxford, pp. 1987.

Rudolph, P., Schubert, C., Tamm, S., Heidorn, K., Hauschild, A., Michalska, I., Majewski, S., Krupp, G., Jablonska S. and Parwaresch R. (2000). Telomerase Activity in Melanocytic Lesions: A Potential Marker of Tumor Biology. *American Journal of Pathology; 156*:1425-1432.

Ptashe, M. and Gann, A. (2002). *Genes and Signals.* Cold Spring Harbor, NY: Cold Spring Harbor Laboratory Press.

Ruskin B, Krainer AR, Maniatis T, Green MR. (1984). Excision of an intact intron as a novel lariat structure during pre-mRNA splicing in vitro. *Cell 38*(1): 317-31.

Scholl, F.A., Kamarashev, J., Murmann, O.V., Geertsen, R., Dummer, R & Schafer, B.W. (2001). *PAX3* is expressed in human melanomas and contributes to tumor cell survival. *Cancer Res. 61*, 823-826.

Seo, H., Saetre, B.O., Havik, B., Ellingsen, S. & Fjose, A. (1998). The zebrafish Pax3 and Pax7 homologues are highly conserved, encode multiple isoforms and show dynamic segment- like expression in the developing brain. *Mech. Devel. 70*, 49-63.

Serrano M, Hannon GJ, Beach D. (1993). A new regulatory motif in cell-cycle control causing specific inhibition of cyclin D/CDK4. *Nature; 366*(6456): 704-7.

Sharp PA. (1994). Split genes and RNA splicing. *Cell 77*(6):805-15.

Shin DM, Gupta V, Donner L, Chawla S, Benjamin R, Gutterman J, Blick M. (1987). Aberrant oncogene expression in uncultured human sarcoma and melanoma. *Anticancer Res. 7*(6):1117-23.

Slominski A, Paus R, Costantino R. (1991). Differential expression and activity of melanogenesis-related proteins during induced hair growth in mice. *J Invest Dermatol; 96*(2):172-9.

Smit DJ, Smith AG, Parsons PG, Muscat GE, Sturm RA. (2000). Domains of Brn-2 that mediate homodimerization and interaction with general and melanocytic transcription factors. *Eur J Biochem. 267*(21):6413-22.

Smith, S. D.; Kelley, P. M.; Kenyon, J. B.; Hoover, D. (2000). Tietz syndrome (hypopigmentation/deafness) caused by mutation of MITF. *J. Med. Genet. 37*: 446-448.

Smith, C.W.; Chu, T.T.; Bernardo, N. (1993). Scanning and Competition between AGs are Involved in 3' Splice Site Selection in Mammalian Introns. *Molecular and Cellular Biology 13*(8):4939-4952.

Sonnenberg, E., Meyer,D., Weidner, K.M. & Birchmeier, C. (1993). Scatter factor/hepatocyte growth factor and its receptor, the c-met tyrosine kinase, can mediate a signal exchange between mesenchyme and epithelia during mouse development. *J. Cell Biol. 123*, 223-35.

Staricco RG. (1962). Activation of amelanotic melanocytes in the outer root sheath of the hair follicle following ultraviolet exposure. *J. Invest. Dermotol.: 39*: 163-164.

Steingrímsson, E., Moore, K.J., Lamoreaux, M.L., Ferré-D'Amaré, A.R., Burley, S.K., Sanders Zimring, D.C., Skow, L.C., Hodgkinson, C.A., Arnheiter, H., Copeland, N.G. (1994). Molecular basis of mouse *microphthalmia* (*mi*) mutations helps explain their developmental and phenotypic consequences. *Nat. Genet. 8*: 256-263.

Tachibana, M., Takeda, K., Nobukuni, Y., Urabe, K., Long, J. E., Meyers, K. A., Aaronson, S. A. & Miki, T. (1996). Ectopic expression of MITF, a

gene for Waardenburg syndrome type 2, converts fibroblasts to cells with melanocytes characteristics. *Nature Genet. 14*: 50-54.

Takeuchi S, Ando M. (1998). Dye-coupling of melanocytes with endothelial cells and pericytes in the cochlea of gerbils. *Cell Tissue Res. 293*(2):271-5.

Tassabehji, M., Read, AP., Newton, VE., Patton, M., Gruss, P., Harris, R. & Strachan, T. (1993). Mutations in the PAX3 gene causing Waardenburg syndrome type 1 and type 2. *Nat. Genet. 3*: 26-30.

Tjian R, Maniatis T. (1994). Transcriptional activation: a complex puzzle with few easy pieces. *Cell 77*(1):5-8.

Tobin DJ, Colen SR, Bystryn JC. (1995). Isolation and long-term culture of human hair-follicle melanocytes. *J Invest Dermatol 104*(1):86-9.

Tobin DJ, Bystryn JC. (1996). Different populations of melanocytes are present in hair follicles and epidermis. *Pigment Cell Res 9*(6):304-10.

Tobin,D.J., Hagen, E., Botchkarev A.A., & Paus, R. (1998). Do Hair Bulb Melanocytes Undergo Apotosis During Hair Follicle Regression (Catagen)? *Journal of Investigative Dermatology 111* (6): 941.

Tremblay, P., Dietrich, S., Mericskay, M., Schubert, F.R., Li, Z. & Paulin, D. (1998). A crucial role for Pax3 in the development of the hypaxial musculature and the long-range migration of muscle precursors. *Dev. Biol. 203*: 49-61.

Tsukamoto, K., Nakamura, Y. & Niikawa, N. (1994). Isolation of two isoforms of the *PAX3* gene transcripts and their tissue- specific alternative expression in human adult tissues. *Hum. Genet. 93*: 270-274.

Underhill, D.A. & Gros, P. (1997). The paired-domain regulates DNA binding by the homeodomain within the intact Pax-3 protein. *J. Biol. Chem. 272*: 14175-14182.

Underhill DA, Vogan KJ, Gros P. (1995). Analysis of the mouse Splotch-delayed mutation indicates that the Pax-3 paired domain can influence homeodomain DNA-binding activity. *Proc Natl Acad Sci U S A; 92*(9):3692-6.

Valverde, P.; Healy, E.; Jackson, I.; Rees, J. L.; Thody, A. J. (1995).Variants of the melanocyte-stimulating hormone receptor gene are associated with red hair and fair skin in humans. *Nature Genet. 11*: 328-330.

Vogan, K.J. & Gros, P. (1997). The C-terminal subdomain makes an important contribution to the DNA binding activity of the Pax-3 paired domain. *J. Biol. Chem. 272*: 28289-28295.

Walton, R.G., Jacobs, A. H. & Cox A.J. (1976). Pigmented lesions in newborn infants. *Br J Dermatol 95*: 389-396.

Wang, H.U. & Anderson, D.J. (1997). Eph family transmembrane ligands can mediate repulsive guidance of trunk neural crest migration and motor axon outgrowth. *Neuron 18*: 383-96.

Watakabe A, Tanaka K, Shimura Y. (1993). The role of exon sequences in splice site selection. Genes Dev; 7(3):407-18.

Watanabe, A., Takeda, K., Ploplis, B., and Tachibana, M. (1998). Epistatic relationship between Waardenburg syndrome genes *MITF* and *PAX3*. *Nat. Genet. 18:* 283-286.

Wehrle-Haller B, Weston JA. (1995). Soluble and cell-bound forms of steel factor activity play distinct roles in melanocyte precursor dispersal and survival on the lateral neural crest migration pathway. *Development 121*(3):731-42.

Williams, B.A. & Ordahl, C.P. (1994). Pax-3 expression in segmental mesoderm marks early stages in myogenic cell specification. *Development 120*: 785-796.

Wilson, D.S., Guenther, B., Desplan, C., and Kuriyan, J. (1995). High resolution crystal structure of a paired (Pax) class cooperative homeodimer on DNA. *Cell 82* (5): 709-19.

Wilson D, Sheng G, Lecuit T, Dostatni N, Desplan C. (1993). Cooperative dimerization of paired class homeo domains on DNA. *Genes Dev. 7*(11):2120-34.

De Winter S, Vink AA, Roza L, Pavel S. (2001). Solar_Stimulated Adaptation and its Effect on Subsequent UV–Induced Epidermal DNA Damage. *J Invest Dermatol. 117*: 678.

Wu, M., Hemesath, T.J., Takemoto, C.M., Horstmann, C.A., Wells, A.G., Price, E.R., Fisher, D.Z., and Fisher, D.E. (2000). c-Kit triggers dual

phosphorylations, which couple activation and degradation of the essential melanocyte factor Mi. *Genes & Dev. 14:* 301-312.

Wu J & Manley JL. (1989). Mammalian pre-mRNA branch site selection by U2 snRNP involves base pairing. *Genes Dev. 3*(10): 1553-61.

Xu W, Rould MA, Jun S, Desplan C, Pabo CO. (1995). Crystal structure of a paired domain-DNA complex at 2.5 A resolution reveals structural basis for Pax developmental mutations. *Cell 80*(4): 639-50.

Xu, W., Gong, L., Haddad, M.M., Bischof, O., Campisi, J., Yeh, E.T., and Medrano, E.E. (2000). Regulation of microphthalmia-asociated transcription factor Mitf protein levels by association with the ubiquitin-conjugating enzyme hUBC9. *Exp. Cell Res. 255:* 135-143.

Yajima, I., Sato, S., Kimura, T., Yasumoto, K., Shibahara, S., Goding, C.R., and Yamamoto, H. (1999). An L1 element intronic insertion in the black-eyed white (*Mitf$^{mi\text{-}bw}$*) gene: The loss of a single Mitf isoform responsible for the pigmentary defect and inner ear deafness. *Hum. Mol. Genet. 8:* 1431-1441.

Yasumoto, K., Yokoyama, K., Shibata, K., Tomita, Y., and Shibahara, S. (1994). Microphthalmia-associated transcription factor as a regulator for melanocyte-specific transcription of the human tyrosinase gene. *Mol. Cell. Biol. 14:* 8058-8070.

Yasumoto, K., Yokoyama, K., Takahashi, K., Tomita, Y. & Shibahara, S. (1997). Functional analysis of microphthalmia-associated transcription factor in pigment cell-specific transcription of the human tyrosinase family genes. *J Biol Chem. 272*, 503-509.

Yoshida,H.(1996). Neural and skin-cell specific expression pattern conferred by steel factor regulatory sequence in transgenic mice. *Dev Dyn. 207*: 222-232.

Zamore, P.D.; Patton, J.G. & Green, M.R. (1992). Cloning and domain structure of the mammalian splicing factor U2AF. *Science 355*: 609-614.

Zenzie-Gregory, B., O'Shea-Greenfield, A. & Smale, S.T. (1992). Similar mechanisms for transcription initiation mediated through a TATA box or an initiator element. *J. Biol. Chem. 267*: 2823-30.

Zhang Y, Emmons SW. (1995). Specification of sense-organ identity by a Caenorhabditis elegans Pax-6 homologue. *Nature 377*(6544):55-9.

Zhuang Y & Weiner AM. (1989). A compensatory base change in human U2 snRNA can suppress a branch site mutation. *Genes Dev. 3*(10):1545-52.

Zhuang YA, Goldstein AM & Weiner AM. (1989). UACUAAC is the preferred branch site for mammalian mRNA splicing. *Proc Natl Acad Sci U S A 86*(8): 2752-6.

Ziman, M. & Kay, P. (1998). Differential expression of four alternate *Pax7* paired box transcripts is influenced by organ- and strain- specific factors in adult mice. *Gene 217*: 77-81.

FIGURE REFERENCES

Page/Figure	Hyperlink
11	http://users.rcn.com/jkimball.ma.ultranet/BiologyPages/M/MSH.html
2.1	http://www.mun.ca/biology/desmid/brian/BIOL3530_W2003/DB_Ch08/DBNMorph.html
2.2	http://pathology.mc.duke.edu/research/PTH225.html
2.3	http://www.cell.ucr.edu/index1.php?content=research/gallery/index.html#fish
2.4	http://images.google.com/images?q=tbn:q4xOSV7D7C8J:http://cal.vet.upenn.edu/histo
2.5	www.nanogen.co.uk/ nanoguard.htm
2.6	http://biology.clc.uc.edu/fankhauser/Labs/Anatomy_&_Physiology/A&P201/Integumentary/Integument.htm
2.7	http://www.ratbehavior.org/CoatTypes.htm
2.8 a	http://nevus.org/
2.8b	http://www.mja.com.au/public/bookroom/1998/cooper/cooper.html
2.8c	http://www.skincancerinfo.com/sectionf/10c.html
2.9	www.daklex.com/jpeg/library/Dysplasticnevi.JPG

2.10 http://forlag.fadl.dk/sample/derma/images/1811.htm

2.11 http://cybermed.ucsd.edu/derm2/Case4/case4a13.html

2.12a,b http://www.uaq.mx/medicina/mediuaq/Especialidades/dermatologia/

2.12c http://www.skincancerinfo.com/sectionf/5e.html

2.13 http://eduserv.hscer.washington.edu/dermUW/mela/typed.htm

2.15 http://eatworms.swmed.edu/~leon/med_neuro/neurogenesis_files/v3_slide0049.htm

2.16 http://www.emedicine.com/derm/topic690.htm